ENERGY LABORATORY

MASSACHUSETTS INSTITUTE
OF TECHNOLOGY

CONTROL OF NO_x BY COMBUSTION PROCESS MODIFICATIONS

by

Janos Bèer, Malcolm Jacques
and W. F. Farmayan

MIT Energy Laboratory Report No. MIT-EL 81-001

April 1981

CONTROL OF NO_x BY COMBUSTION PROCESS MODIFICATIONS

by

Prof. J. M. Béer
Dr. M. T. Jacques
Mr. W. F. Farmayan

Energy Laboratory
and
Department of Chemical Engineering

Massachusetts Institute of Technology
Cambridge, Massachusetts 02139

sponsored by

Northeast Utilities Service Company
New England Power Service Company
Consolidated Edison Company of New York
Southern California Edison Company

under the

MIT Energy Laboratory Electric Utility Program

MIT Energy Laboratory Report No. MIT-EL 81-001

January 1981

TABLE OF CONTENTS

List of Tables

Table of Contents
Continued

page

List of Figures

List of Figures
Continued

List of Figures
Continued

page

List of Figures
Continued

page

List of Figures
Continued

List of Figures
Continued

List of Figures
Continued

List of Tables

List of Tables
Continued

page

List of Tables
Continued

page

Executive Summary

A theoretical and experimental study was carried out to determine lower bounds of NO_x emission from staged combustion of a 0.7% N #6 fuel oil. Thermodynamic and chemical kinetic calculations have shown minimum NO_x emissions at fuel rich stage equivalence ratios between 1.6 and 1.8 and fuel rich stage temperatures in the range of 1900 to 2100 K (2960 to 3812°F).

In the experimental investigations the use of the MIT Combustion Research Facility permitted the detailed study of aerodynamically complex industrial-type turbulent flames in thermal and chemical environments similar to those in utility boiler furnaces. The primary stage fuel equivalence ratio, the flow and mixing pattern in the flame, the level of air preheat and the mode and quality of fuel atomization, were varied to determine their effect upon the NO_x and combustibles emission.

Unstaged flame studies were carried out to establish baseline data for comparison with those obtained in fuel rich-lean staged flames in which a fuel rich stage was formed near the burner and the lean stage was established by the admixing of the rest of the combustion air at a distance farther downstream.

Results of the computational modeling studies have shown that in the fuel rich zone of the flame the fuel bound nitrogen compounds (FBN) can be converted to molecular nitrogen, N_2, which renders the FBN innocuous for forming NO_x in the lean stage of the flame.

Care has to be taken however to ensure that the mixing of the secondary air with the products from the fuel rich stage does not produce high flame temperatures, in excess of 1800K (2780°K) and hence "thermal NO_x."

The modeling studies have shown also that the FBN conversion to N_2 goes through a minimum as the fuel equivalence ratio is varied and that this minimum is lower, and shifts more towards the fuel rich as the fuel rich stage temperature is raised.

The experiments guided by the modeling have led to significant reduction in NO_x emission; NO_x was reduced from a level of 0.51 $lb/10^6$ Btu (400 ppm @ 3% O_2) in a single stage flame to 0.10 $lb/10^6$ Btu (80 ppm @ 3% O_2) in staged combustion when the fuel equivalence ratio in the fuel rich stage was maintained in the range of ϕ=1.5 to 1.7 (50 to 70% fuel rich), very close to that predicted from the model. The overall excess air was maintained in all experiments at EA=10%, and the combustibles (soot) emission was generally low, always well below the emission standard of 0.1 $lb/10^6$ Btu.

It is considered that an important factor in the very low NO_x emission levels obtained in this study is the favorable mode of secondary air admixing with the fuel rich flame gases which ensure complete combustion without any additional "thermal" NO_x formation.

It is emphasized that the conditions for these experiments were carefully selected to approach optimum values for the concentration and temperature history of the fuel. The tight controls of combustion aerodynamics and of the heat extraction along the flame available in the MIT Combustion Research Facility were highly favorable for the physical realization and experimental study of these flames.

Due to the practical difficulties in controlling mixing and heat extraction in existing utility boiler furnaces, it is not considered realistic to expect the same low NO_x and soot emission levels by combustion

modifications. It is thought that the results of this study should be used as guidance in design strategy for low NO_x emission from the combustion of high nitrogen-bearing fuels rather than as an indication of the absolute levels of NO_x which can be achieved by staged combustion techniques in utility boilers.

Because of the significance of the flow and mixing pattern in the flame for both the formation of NO_x and carbonaceous particulates it is recommended that in the second phase of this study the effect of mixing and heat extraction along both single and multiple staged flames be studied in more detail with a view of application of these controls to the combustion in large utility boilers.

1. Introduction

It is recognized that one of the major problems associated with the clean combustion of certain liquid fuels, including shale oil and coal derived liquids, is due to their high nitrogen content. Fuel-bound nitrogen (FBN) is known to convert preferentially to NO_x under conventional turbulent diffusion flame conditions, and is often the major source of NO_x emission for these high nitrogen content fuels. There are two major sources of NO_x emissions from combustion processes: at high flame temperatures and oxidizing conditions atmospheric nitrogen reacts with the oxygen in the flame to form NO_x. The reaction mechanism—the Zeldovich "atom shuttle" reaction between N atoms and O_2 molecules, and O atoms and N_2 molecules respectively—is known and chemical kinetic rate parameters are available for its calculation in fuel lean flames.

The other source of NO_x in flames is the nitrogen organically bound mainly in heterocyclic compounds in the fuel. The mechanism of the conversion of fuel bound nitrogen (FBN) in flames is more complex as it involves a large number of gas phase and heterogeneous reactions but a general picture of the most significant steps in the reaction paths of FBN is evolving through a number of investigations carried out during the last decade. Research on the conversion of FBN in flames surveyed by Haynes [1] has been extended by Levy et al [2] in the course of a recent research study at MIT. Some details of the chemistry of FBN conversion relevant to the present study are discussed in Chapter 2 of this report. At this point in our introductory discussion it should be noted that the major difference from the point of view of NO_x control between "thermal NO" and "fuel NO" is that the former is produced predominantly at temperatures in excess of 1800 K and its rate of formation is strongly dependent upon the temperature, while the latter is little affected by the flame temperature, the rate of formation being primarily dependent upon local flame stoichiometry. It is important also to note that reactions of FBN in fuel rich, high temperature environments can lead to the formation of molecular nitrogen, N_2, which is the way of rendering the FBN innocuous for further oxidation to NO_x in the lean stage of staged combustion systems.

Because of the strong dependence of FBN conversion upon the local fuel/air mixing ratio in the flame NO_x control methods developed to reduce thermal NO_x formation by reducing peak flame temperatures, such as flue gas recirculation, will not be effective in suppressing "fuel NO"

formation; however, staged combustion techniques are found to be most effective. Staged combustion involves the delayed mixing of a proportion of the combustion air to permit the reactions which convert FBN to N_2 to proceed in the fuel rich part of the flame following which the combustion is completed in an oxidizing atmosphere. Staged combustion can be achieved by the appropriate management of the fuel/air mixing in a single combustor, or by the physical separation of the fuel-rich and lean combustion chambers. In the present first phase of our investigation the fuel rich-lean combustion system was chosen for study mainly because of the better control of mixing and heat extraction that this system permits. As will be seen from the discussion of the experimental program, however, one of the single stage flames chosen for establishing baseline data —a slowly mixing, long turbulent diffusion flame—is representative of the aerodynamical staging in a single combustion chamber.

Recent theoretical investigations at MIT have shed additional light on the FBN conversion processes involved in staged combustion [3].

These calculations indicate that some of the important fuel-nitrogen conversion reactions in the fuel-rich zone may well be kinetically limited at the low flame temperatures which exist in this zone, effectively preventing these reactions from reaching equilibrium within the available residence time. Consequently, it is very likely that increased temperatures in the fuel-rich zone will assist in maximizing fuel-nitrogen conversion to molecular nitrogen and thereby reducing overall NO_x emission. In practice increased temperatures can only be obtained by increasing air-preheat, and/or reducing heat loss from the fuel-rich zone.

A problem associated with maximizing the efficiency of fuel-nitrogen conversion to molecular nitrogen in a high temperature fuel-rich zone is that these conditions are conducive to the formation of large concentrations of soot or coke residues. Hence the research problem becomes one of optimizing the conditions within the fuel-rich zone to minimize both NO_x and soot formation.

The research approach which has been adopted in this program was aimed at demonstrating the practical feasibility of the staged combustion approach to NO_x control, using the MIT Combustion Research Facility (CRF). Thermodynamic and kinetic data on reactions known to play a significant role in fuel-nitrogen conversion were used to help formulate critical experiments and to identify parameters which are most likely to have a significant effect on the efficiency of conversion of fuel-nitrogen to molecular nitrogen.

The fuel equivalence ratio and the fuel rich stage temperature and residence time are parameters the significance of which to FBN conversion was clearly illustrated by results of the thermodynamic-chemical kinetic modeling studies. Correspondingly the experimental program was devised to determine the effects of these variables together with others which were expected to influence the emission of combustible gases and solids. The fuel rich stage temperature was varied by means of the variation of air preheat up to 500° C and the fuel rich stage residence time by varying the fuel input rate in the range of 1 to 2.0 MW (thermal).

In the following the details of the thermodynamic and chemical kinetic modeling studies are discussed followed by the presentation of the experimental program, and the results of the investigation.

Studies on a single fuel rich first stage, and on the second stage of a two-staged combustor have been completed. multiple staging has not been taken up to any extent yet. Studies have been carried out on a high nitrogen No. 6 fuel oil having an organic nitrogen content of about 0.7% by weight.

Descriptions of the experimental facility, the MIT Combustion Research Facility and the various measurement, sampling and analytical techniques can be found in Appendices A and B.

2. Theoretical Analysis: Chemical Equilibrium and Kinetic Studies on Nitrogen Species Formed in Staged Combustion of High Nitrogen No. 6 Fuel Oil

Thermodynamic and chemical kinetic computer studies on nitric oxides formed during staged combustion of high nitrogen-bearing fuels, were carried out to complement experimental work in the same area carried out at the MIT Combustion Research Facility (CRF). These studies are largely qualitative, and were intended to aid in the planning of the experimental program and in interpretation of data.

The theoretical studies examine a number of variables in the staged combustion process which are thought to have a strong effect on nitric oxides emissions. These are (1) combustion temperature in each stage (affected by air preheat and combustor heat losses), (2) fuel equivalence ratio (particularly in the fuel rich first stage(s)), (3) average residence time in each stage, (4) the number of stages, and (5) the organic nitrogen content of the fuel. Information on the effects of these variables on NO_x emissions should help in the formulation of an optimal staged combustion process strategy.

The theoretical studies make use of two computer programs, one which calculates equilibrium compositions of combustion mixtures, and the other which models the chemical kinetics of fuel nitrogen transformations. Both are used to calculate concentrations of nitrogen oxides (and other nitrogenous species) in combustion mixtures. A description of these programs is given in the following section. The results of the computer studies are presented next, and then finally some conclusions that may be drawn from them.

2.1 Descriptions of the Computer Programs Employed in the Theoretical Studies

The NASA Chemical Equilibrium Program

The computer program used to carry out chemical equilibrium calculations in this study is entitled COMPUTER PROGRAM FOR CALCULATION OF COMPLEX CHEMICAL EQUILIBRIUM COMPOSITIONS, ROCKET PERFORMANCE, INCIDENT AND REFLECTED SHOCKS, AND CHAPMAN-JOUGNET DETONATIONS, and was written at the NASA Lewis Research Center by S. Gordon and B. McBride in 1961-1962, and has since been updated and improved upon several times.

Program Basis

There are two approaches towards solving simultaneous chemical equilibria at a specified temperature and pressure, one involving equilibrium constants and the other minimization of Gibbs free energy. The NASA program is based upon the latter approach, which does not require an explicit formulation of an independent set of chemical reactions leading

to the formation of the chemical species being considered. (This information is implicit in the Gibbs energy formulation of a chemical equilibrium problem).

The Gibbs free energy of the combustion mixture may be written

$$\underline{G} = \sum_{i=1}^{n} u_i N_i$$

where

$\underline{G}$ is the total Gibbs free energy,

i refers to a chemical species,

N_i refers to the number of moles of species i present in the mixture,

u_i refers to the chemical potential of species i present in the mixture.

The criterion for equilibrium is that the Gibbs free energy of the combustion mixture is at a minimum (at a particular temperature and pressure):

$$\delta \underline{G} = \sum_{i=1}^{n} u_i \delta N_i = 0$$

The variations in N_i are not independent but are subject to a number of constraints consisting of elemental balances:

$$\sum_{i=1}^{n} N_i a_{ik} - A_k = 0$$

where

k refers to the k^{th} element in the mixture,

A_k refers to the total moles of the k^{th} element,

a_{ik} refers to the atoms of the k^{th} element present in species i.

The NASA program applies the Lagrangian multiplier approach towards simultaneously solving the equation defining chemical equilibrium and the accompanying constraints for the equilibrium composition of the mixture.

The program uses the ideal gas equation of state, even when small amounts of condensed species are present. The program is equipped with a thermodynamic data base that can handle over 60 reactants and 400 reactant species. Other state functions may be used to assign the thermodynamic state at which the equilibrium composition is to be determined, besides temperature and pressure (e.g., enthalpy and pressure).

The computer program is able to handle an adiabatic condition as well as isothermal. In the case of the adiabatic option, an energy balance is coupled with the equations for equilibrium, in the determination of the equilibrium composition and temperature.

The NASA program has been used in our study for the calculation of the sum of bound nitrogen concentrations including NO_x (i.e. all nitrogen compounds except N_2) in combustion mixtures at chemical equilibrium. Because of the departure from equilibrium conditions at shorter residence times in the fuel rich stage of the combustor the results of thermodynamic calculations were considered to give information on the trends in NO_x formation as combustor temperature and fuel equivalence ratio are varied. It was recognized that for more detailed information the chemical kinetics of fuel-nitrogen conversion reactions have to be taken into consideration.

2.2 Nitrogen Oxides Chemistry

A brief review of NO_x chemistry is given below to facilitate a better understanding of the second computer program used in the theoretical studies. A description of the program follows this review.

Nitrogen oxides are formed by direct oxidation of nitrogen (N_2) in the air (thermal NO_x), by fixation of nitrogen in the air by hydrocarbon fragments and their subsequent oxidation (prompt NO_x), and by direct oxidation of organic nitrogen (fuel NO_x).

2.2.1 Thermal NO_x

The formation of thermal NO_x is well understood, resulting from a small set of gaseous reactions referred to as the extended Zeldovich mechanism. These reactions are listed below.

$$N_2 + O = NO + N \quad (1)$$

$$N + O_2 = NO + O \quad (2)$$

$$N + OH = NO + H \quad (3)$$

These reactions are highly temperature sensitive; formation rates of nitric oxides via the Zeldovich mechanism begin to become noticeable at combustion temperatures above 1800 K. Thermal NO_x also increases with increasing oxygen concentration in the combustion mixture.

2.2.2. Prompt NO_x

In fuel rich hydrocarbon flames it is believed that molecular nitrogen can be fixed by unburnt hydrocarbon fragments in reactions

such as

$$CH + N_2 = HCN + N \qquad (4)$$

The bound nitrogen thus formed is believed to undergo oxidation to nitric oxides in reactions such as those described below.

2.2.3 Fuel NO_x

The process by which nitrogen oxides are formed from fuel nitrogen is complex and not fully understood. Figure 1 shows the paths that fuel nitrogen transformations are believed to take during the combustion process. The fuel nitrogen is first partially devolatilized to heterocyclic organic nitrogen compounds which then decompose mostly to HCN. The decomposition of the ring compounds is believed to proceed at a much greater rate than the initial pyrolysis step. The HCN proceeds through a set of homogeneous gas phase reactions to N_2 or NO_x. The condensed fuel nitrogen in the soot particles is believed to undergo a heterogeneous oxidation process to NO_x. There is also interaction between NO_x in the gas phase and the carbon in the soot particles, which is believed to catalyze a NO_x reduction reaction to N_2. Considerable progress has been made in understanding the homogeneous gas phase kinetics of fuel nitrogen reactions. Some of the reactions upon which the chemical kinetic program is based, are given below. The understanding of the kinetics of the heterogeneous reactions is not so well advanced, especially for liquid fuel combustion.

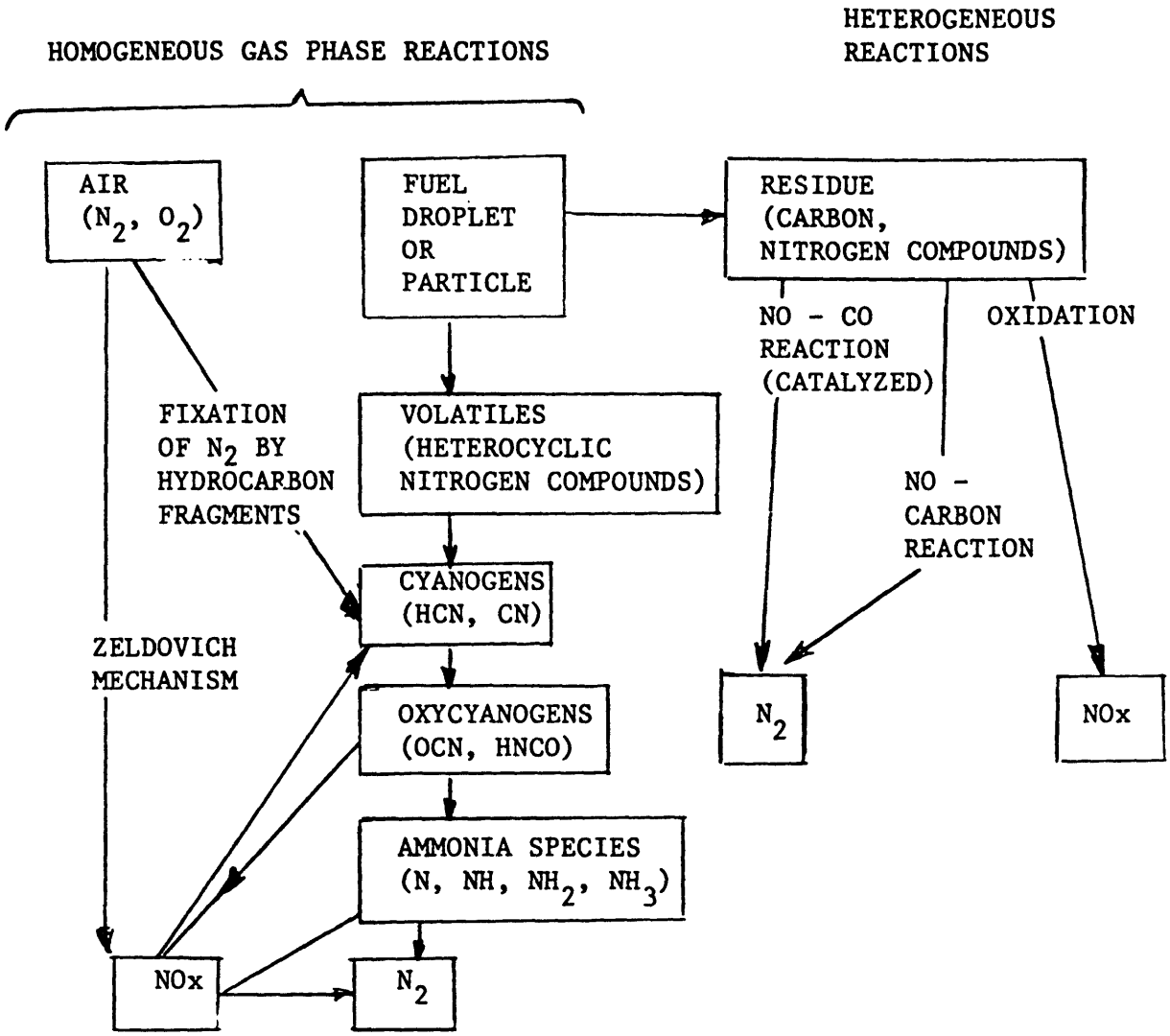

Figure 1. The formation of nitrogen oxides in fossil fuel combustion: mechanistic pathways.

2.3 Homogeneous Gas Phase Reactions of Fuel Nitrogen

The HCN formed from pyrolysis of the fuel nitrogen is believed to be initially oxidized to short-lived oxycyanogen intermediates in reactions such as the one presented below. (HCN is assumed to initially be partially equilibrated with CN.)

$$CN + OH = NCO + H \quad (5)$$
$$CN + O_2 = NCO + O \quad (6)$$
$$HCN + OH = HNCO + H \quad (7)$$
$$HCN + O = NCO + H \quad (8)$$

The oxycyanogens are in turn thought to be converted to ammonia species by H radicals.

$$NCO + H = NH + CO \quad (9)$$
$$HNCO + H = NH_2 + CO \quad (10)$$

The ammonia species and nitrogen atom, N, NH, NH_2, NH_3, undergo a number of hydrogen abstraction reactions which rapidly interconvert them to one another.

$$NH_3 + OH = NH + H_2O \quad (11)$$
$$NH_3 + O = NH_2 + OH \quad (12)$$
$$NH_2 + O = NH + OH \quad (13)$$
$$NH + OH = N + H_2O \quad (14)$$
$$NH + O = N + OH \quad (15)$$
$$NH + H = N + H_2 \quad (16)$$
$$NH_2 + OH = NH + H_2O \quad (17)$$
$$NH_2 + H = NH + H_2 \quad (18)$$
$$NH_3 + H = NH_2 + H_2 \quad (19)$$
$$NH + NH_2 = NH_3 + N \quad (20)$$

The fuel nitrogen is thought to form molecular nitrogen or nitric oxide by reactions through a common intermediate, probably being one or more of the N, NH, NH_2, and NH_3 species. The intermediate undergoes two parallel competing reactions:

1) with NO to produce N_2
2) with O or OH to produce NO.

The major rationale behind staged combustion is to create conditions which favor the first of the two reaction paths listed above.

Thus fuel nitrogen is converted to molecular nitrogen by the reaction

$$N + NO = N_2 + O \qquad (1)$$

Other reactions leading to N_2 include the reaction sequence shown below.

$$NH + NO = N\ O + H \qquad (21)$$
$$N_2O + H = N_2 + OH \qquad (22)$$

Interaction of ammonia species may also lead to N_2.

$$NH + N = N_2 + H \qquad (23)$$

The fuel nitrogen may be converted to nitric oxide by the reaction

$$N + OH = NO + H \qquad (3)$$

which competes with Reaction 1, or by

$$NH + O = NO + H \qquad (24)$$

which competes with the reaction sequence 21-22. Another source of NO from fuel nitrogen is believed to be the oxidation of NCO.

$$NCO + O = NO + CO \qquad (25)$$

In addition to reactions 25 and 26 a number of other elementary reactions have been postulated to lead to NO, such as reactions of HNO and N_2O with O, H, or OH radicals.

A number of other reactions are required to define concentrations of intermediate species. These include (1) hydrogen abstraction reactions between H_2, O_2, H, O, H_2O, and between CN and HCN, (2) 3-body recombination/ disassociation reactions, and (3) the CO to CO_2 oxidation reaction. Some of these are listed below.

$$H_2 + O = H + OH \qquad (26)$$
$$H_2O + O = OH + OH \qquad (27)$$
$$H_2 + OH = H_2O + H \qquad (28)$$
$$O_2 + H = O + OH \qquad (29)$$

$$H + OH + M1 = H_2O + M1 \qquad (30)$$
$$H + H + M1 = H_2 + M1 \qquad (31)$$
$$N\ O + M1 = N_2 + O + M1 \qquad (32)$$
$$H + O + M1 = OH + M1 \qquad (33)$$
$$O_2 + M1 = O + O + M1 \qquad (34)$$

$$CN + H_2 = HCN + H \qquad (35)$$
$$HCN + OH = CN + H_2O \qquad (36)$$
$$CO_2 + H = CO + OH \qquad (37)$$

All the reactions presented in this section are summarized in Table 1, and form the basis of the chemical kinetic program which is described shortly.

In general, fuel nitrogen reactions are sensitive to fuel-air stoichiometry, which plays an important role in determining whether the fuel nitrogen proceeds to N_2 or NO. Temperature has an important bearing on fuel nitrogen reactions

TABLE 1

CHEMICAL KINETICS STUDIES ON HIGH NITROGEN NO. 6 FUEL OIL.REACTIONS CONSIDERED TO INITIALLY BE PARTIALLY EQUILIBRATED

1. $H_2O + CO = CO_2 + H_2$
2. $O_2 + H_2 = OH + H$
3. $O + OH = O_2 + H$
4. $H_2 + OH = H + H_2O$
5. $HCN + H = CN + H_2$

REACTIONS CONSIDERED IN THE CHEMICAL KINETICS COMPUTER PROGRAM USED FOR PREDICTION OF BOUND NITROGEN SPECIES CONCENTRATIONS

Zeldovich Reactions

1. $N + NO = N_2 + O$
2. $NO + O = N + O_2$
3. $NO + H = N + OH$

Formation of oxycyanogens

4. $CN + OH = NCO + H$
5. $CN + O_2 = NCO + O$
6. $HCN + OH = HNCO + H$
7. $HCN + O = NCO + H$
8. $NCO + H_2 = HNCO + H$

Oxidation of CN to CO

9. $CN + O = CO + N$

Conversion of oxycyanogens to ammonia species

10. $NCO + H = NH + CO$
11. $HNCO + H = NH_2 + CO$

Ammonia species interconversions

12. $NH_3 + OH = NH + H_2O$
13. $NH_3 + O = NH_2 + OH$
14. $NH_2 + O = NH + OH$
15. $NH + OH = N + H_2O$
16. $NH + O = N + OH$
17. $NH + H = N + H_2$
18. $NH_2 + OH = NH + H_2O$
19. $NH_2 + H = NH + H_2$

20. $NH_3 + H = NH_2 + H_2$

21. $NH + NH_2 = NH_3 + N$

Formation of molecular nitrogen

1. $N + NO = N_2 + O$

22. $NH + NO = N_2O + H$

23. $N_2O + H = N_2 + OH$

24. $N_2O + M1 = N_2 + O + M1$

25. $NH + N = N_2 + H$

Formation of nitric oxide

26. $NCO + O = NO + CO$

3. $N + OH = NO + H$

27. $NH + O = NO + H$

Interconversions between O_2, O, H_2, H, and H_2O

28. $H_2 + O = H + OH$

29. $H_2O + O = OH + OH$

30. $H_2 + OH = H_2O + H$

31. $O_2 + H = O + OH$

Interconversions between HCN and CN

32. $CN + H_2 = HCN + H$

33. $HCN + OH = CN + H_2O$

CO - CO_2 reaction

34. $CO_2 + H = CO + OH$

3-body recombination/dissassociation

35. $H + OH + M1 = H_2O + M1$

36. $H + H + M1 = H_2 + M1$

37. $H + O + M1 = OH + M1$

38. $O_2 + M1 = O + O + M1$

under fuel rich conditions, because it greatly affects free radical concentrations, which in turn greatly affect the reaction rates.

2.4 The Chemical Kinetic Computer Program

The second computer program takes a large step forward as far as prediction of nitric oxide formation in fossil fuel combustion is concerned. Developed at MIT by Taylor,* Levy, and Sarofim, the program is an attempt at modeling fuel nitrogen transformations to nitric oxides by a comprehensive elementary reaction set. Included in the set are reactions from the well-established Zeldovich mechanism which accounts reasonably well for nitric oxides formed by direct oxidation of nitrogen (N_2) in the air at high combustion temperatures. The program does not account for interaction of nitrogenous species with hydrocarbon fragments or heterogeneous fuel nitrogen reactions.

The hydrocarbon fuel is assumed to initially combust to a partially equilibrated mixture of CO, CO_2, H_2, H_2O, O, and O_2. In addition the fuel nitrogen is assumed to have instantaneously been devolatilized and converted to HCN and CN, these species also being in partial equilibrium with those mentioned above. The elementary reaction set then models the kinetics of nitric oxide and other bound nitrogen species formation from this partially equilibrated mixture. The assumption of partial equilibrium is reasonable, since rates of formation of the CO, CO_2, H_2, H_2O, O, O_2, CH, and HCN are fast relative to the nitrogen species transformations that follow.

---

* The program version used in this study was developed by Barry Taylor (doctoral candidate in chemical engineering at MIT under Prof. Sarofim).

A list of the initially partially equilibrated reactions and the elementary kinetic reaction set is given in Table 1.

2.4.1 Limitations on the Applicability of the Chemical Kinetic Program Results to the CRF Combustor

The elementary reaction set is integrated into a simple plug-flow reactor model, which puts limitations on the quantitative accuracy of the computer calculated NO_x concentrations, when applied to the CRF combustor. The reactions in the program are assumed to take place in a homogeneous gas phase environment in which the oxidant and fuel have been introduced in a perfectly mixed state. In order to predict NO_x emissions quantitatively and accurately from a combustor such as is in use at the MIT CRF, the following processes would have to be taken into account in addition to the gas phase chemistry of NO_x formation from fuel nitrogen and N_2 in the air:

1) Atomization
   i) droplet sizes and size distribution
   ii) nature of the spray (e.g. dimensions and pattern).
2) Fuel droplet vaporization (both the hydrocarbons and the organic nitrogen compounds).
3) Decomposition of volatilized organic nitrogen compounds to HCN.
4) Mixing rates and patterns in the combustor, of air and fuel.

However, it is thought that the gas phase reactions of fuel bound nitrogen compounds in the fuel rich stage of a staged combustor are predominant and this prediction therefore gives good approximate quantitative information even when neglecting some of the above-mentioned physical and chemical processes.

2.4.2 Description of the Computer Runs and Results

All the computer studies carried out thus far have been on a high nitrogen No. 6 fuel oil having a composition similar to that studied at the CRF and reported in Chapter 3. The important characteristics of this fuel are listed in Table 2.

2.5 Thermodynamic Calculations

The thermodynamic equilibrium calculations were mainly aimed at the fuel rich first stage(s), in which combustor air inlet temperatures were selected at 298 K, 500 K, and 700 K, and fuel equivalence ratios at 0.8, 1.0, 1.2, 1.4, 1.6, 1.7, 1.8, 1.9, 2.0, 2.2, 2.4, 2.6, and 2.8. Other important parameters affecting the equilibrium combustion mixture compositions were left constant: pressure at 1 atmosphere, and inlet fuel temperature at 367 K. All calculations were carried out for adiabatic conditions.

Table 3 is a list of the most important combustion species considered by the program.

The results of these calculations are shown in:

1) Figure 2; equilibrium adiabatic flame temperatures as a function of fuel equivalence ratio at different combustor inlet air temperatures, and
2) Figure 3; the sum of the bound nitrogen species mole fractions at chemical equilibrium as a function of fuel equivalence ratio at different combustor inlet air temperatures.

TABLE 2

TRIAL NO. 6 FUEL OIL BLENDS

Description	Asphalt	Light Cycle Oil (cutter stk) X-4300	Trial No. 6 F.O. Blends A X-4321	Trial No. 6 F.O. Blends B X-4322
Blend Make-up: wt %				
Asphalt (X-4299)	100	-	50	75
Cutter Stock (X-4300)	-	100	50	25
Inspection				
Gravity: °API	8.0	25.9	16.5	11.8
Specific Gravity, 60°/60° F	1.0143	0.8990	0.9561	0.987
Viscosity, Kin. cSt				
100° F	-	22.74	726	19538
150°	-	11.72	120.3	1490
210°	2484	4.09	29.52	176.6
275°	257	-	-	-
Flash, P-M: °F	-	-	325	-
Sulfur, ASTM D1552: Wt %	1.91	-	-	-
Nitrogen, Gulf 811: Wt %	1.27	0.13	-	-
Carbon, Semi Micro: Wt %	85.48	87.17	-	-
Hydrogen, Semi Micro: Wt %	10.61	12.83	-	-
Spot Test, Gulf 856*				
Compatability with Phil. Dieselect	-	-	5	-
Compatability with PA No. 2 H.O.	-	-	5	-
Compatability with FCC No. 2 F.O.	-	-	5	-
Spot Test, Homogeneity Rating Gulf 986†				
Spotted at 140° F	-	-	5	-
Spotted and Dried at 140° F	-	-	1	-

* No. 5 spots were obtained using procedure A (HOT) and procedure B (COLD).

† This test is for intermediate fuels. Sample tested (X-4321) is outside the suggested viscosity range of the test.

TABLE 3

LIST OF HYDROCARBON, HYDROGEN, AND OXYGEN SPECIES CONSIDERED IN THE NASA CHEMICAL EQUILIBRIUM COMPUTER PROGRAM FOR A FUEL CONTAINING HYDROGEN, CARBON, AND NITROGEN (Nitrogenous species are listed separately)

CO	OH	C_3H_8	C_8H_{18}
CO_2	O_2	CH_2	CH_4
H	C (s)	C_2H	C_2H_6
HCO	C_3	C_4	CH_3OH
HO_2	H_2O (l)	CH_2O	O_3
H_2	C	C_2H_2	C_2O
H_2O	C_3O_2	C_5	H_2O (s)
H_2O_2	CH	CH_3	
O	C_2	C_2H_4	

LIST OF NITROGENOUS SPECIES CONSIDERED IN THE NASA CHEMICAL EQUILIBRIUM COMPUTER PROGRAM FOR A FUEL CONTAINING HYDROGEN, CARBON, AND NITROGEN

HCN	HNO	NH_3
CN	HNO_2	NO
HNCO	HNO_3	NO_2
NCO	N	NO_3
CNN	N_2	N_2O
C_2N_2	N_3	N_2O_4
CN_2	NH	N_2O_5
C_2N	NH_2	N_2H_4

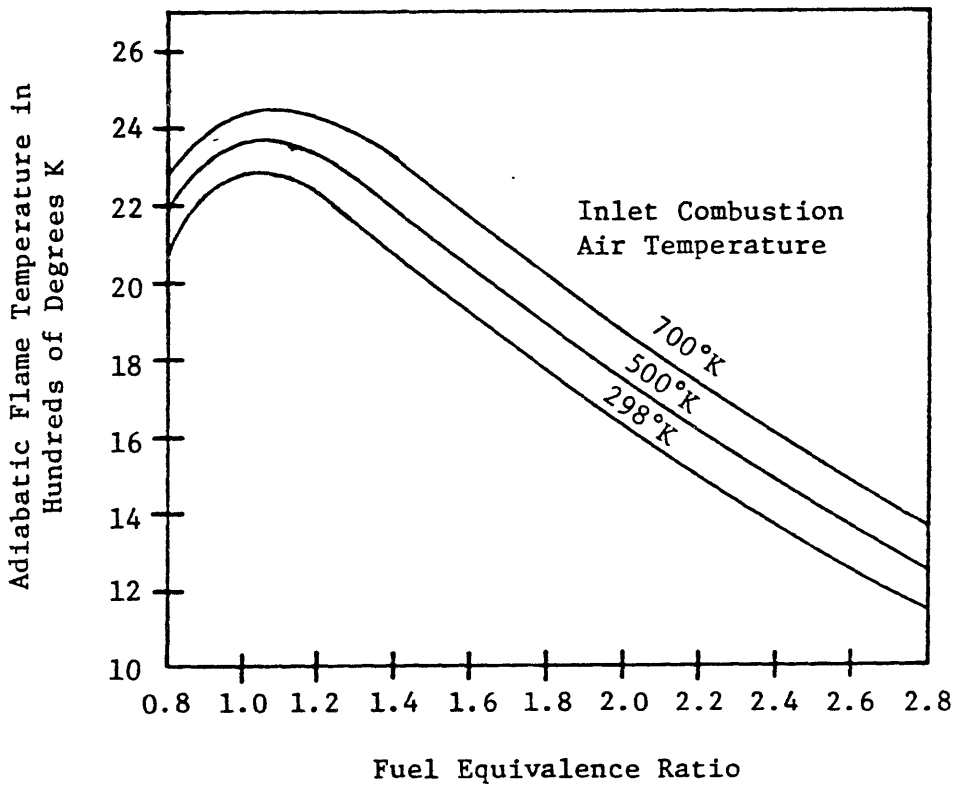

Figure 2. --Equilibrium adiabatic flame temperature as a function of fuel equivalence ratio at different combustor inlet air temperatures.

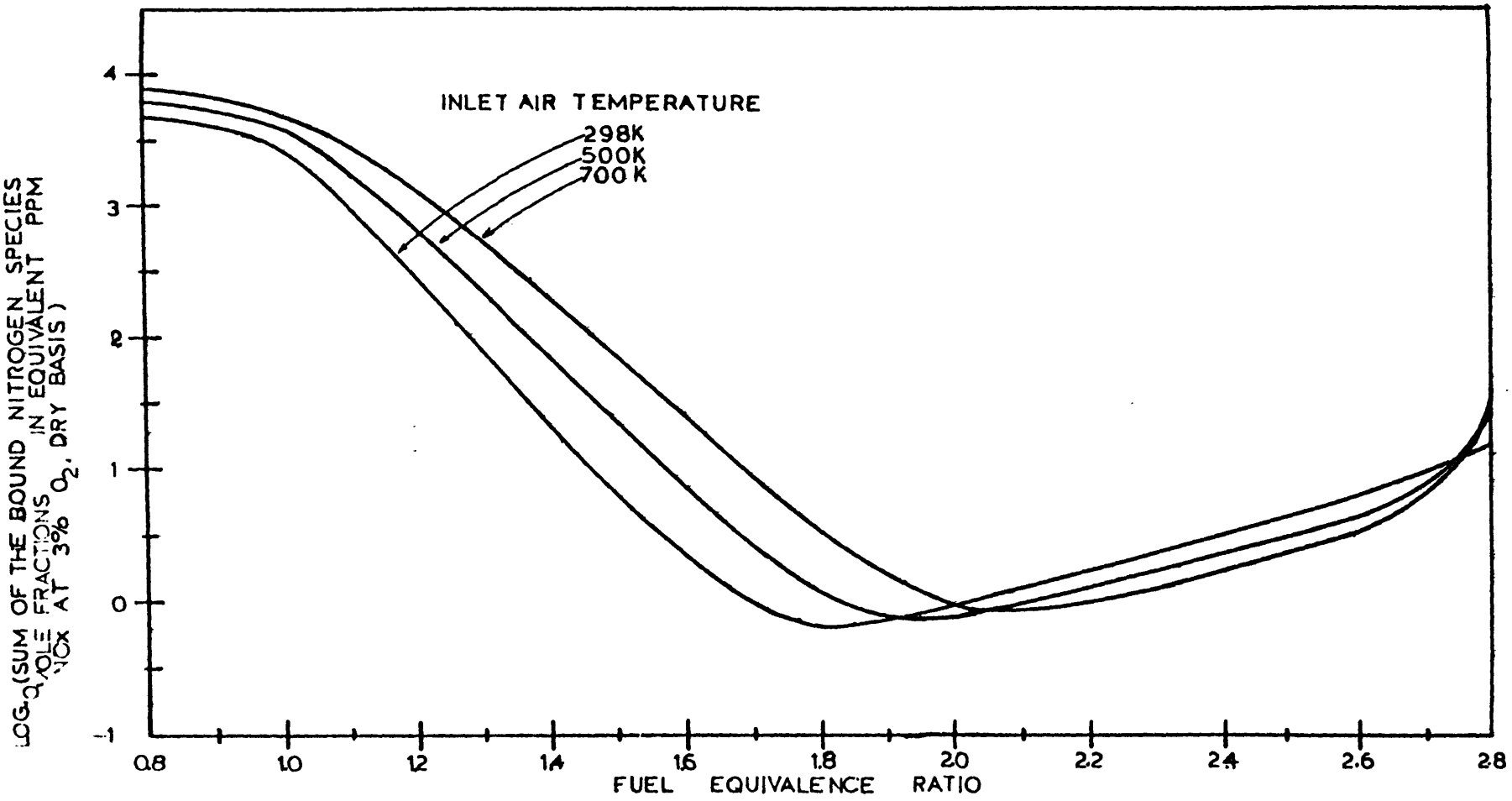

Figure 3. --The sum of the bound nitrogen species mole fractions (in equivalent ppm NOx at 3% O_2) at chemical equilibrium as a function of fuel equivalence ratio at different combustor inlet air temperatures.

2.6 Chemical Kinetic Calculations

Single Stage Study

The first set of computer runs, performed with the chemical kinetic computer program, were devoted to a single fuel rich first stage. The effects of air preheat and fuel equivalence ratio were investigated: the air temperatures were again selected at 298 K, 500 K, and 700 K, and the fuel equivalence ratios, at 1.4, 1.6, 1.8, and 2.0. The pressure was left constant at 1 atmosphere, inlet temperature at 367 K, conditions were adiabatic, and the reactor model was plug flow. Calculations were carried out to residence times of 4 seconds.

Table 4 lists the major combustion species considered by the kinetic program.

Results from the chemical kinetic computer runs in the first stage study are as follows:

1) Figures 4-7; the sum of the bound nitrogen species mole fractions as a function of residence time at different combustor inlet air temperatures for fuel equivalence ratios of 1.4, 1.6, 1.8, and 2.0.

2) Figures 8-12; the sum of the bound nitrogen species mole fractions as a function of fuel equivalence ratio at different inlet air temperatures for residence times of 0.5, 1.0, 2.0, 3.0, and 4.0 seconds.

3) Figures 13-17; the sum of the bound nitrogen species mole fractions as a function of adiabatic flame temperature at different fuel equivalence ratios for residence times of 0.5, 1.0, 2.0, 3.0, and 4.0 seconds.

TABLE 4

A LIST OF THE COMBUSTION SPECIES CONSIDERED
BY THE CHEMICAL KINETIC COMPUTER PROGRAM

Nitrogenous Species

N	NH	HCN	HNCO
NH	NO	CN	N
NH	N O	NCO	

Others

H	H_2	CO
O	O_2	CO_2
OH	H_2O	Ar

4) Figure 18; the effect of combustor inlet air temperature on the position of the minimum of the sum of the bound nitrogen species mole fractions: a comparison between chemical equilibrium and kinetic calculations.

5) Figure 19; the effect of combustor inlet air temperature on the value of the sum of the bound nitrogen species mole fractions: a comparison between chemical equilibrium and kinetic calculations.

Two-Staged Study

The chemical kinetic study was extended here to two stages where fuel burnout was completed in the second stage with an overall excess of air. Nitric oxide concentrations leaving the second stage were calculated by means of the chemical kinetic program.

The results of the two-staged study are shown in Figures 20-24 where the sum of bound nitrogen species in equivalent ppm NO_x at 3% O_2, is given as a function of residence time in a two-staged combustor for various combinations of conditions in the first and second stage. These conditions are described in Table 5. (The factor for converting from lbs. $NO_2/10^6$ Btu to ppm NO_x at 3% O_2 for this particular high nitrogen No. 6 fuel oil is 781.38 [multiply by this factor to arrive at ppm at 3% O_2].)

2.7 Discussion of Thermodynamic and Chemical Kinetic Modeling Results

2.7.1 Chemical Equilibrium Studies

1) The sum of the bound nitrogen species mole fractions passes through a minimum as fuel equivalence ratio is varied (see Fig. 3).

TABLE 5

TWO-STAGE COMBUSTION STUDY: VALUES FOR OPERATING VARIABLES FOR EACH COMPUTER RUN

	1st Stage	2nd Stage
1) Figure 3.22:	ϕ = 1.6 T_{air} = 298°K T_f = 1915°K	Case A, T_f = 2193°K T_{air} = 298°K Case B, T_f = 1600°K Case C, T_f = 1800°K
2) Figure 3.23:	1st Stage ϕ = 1.6 T_{air} = 500°K T_f = 2036°K	2nd Stage Case A, T_f = 2288°K T_{air} = 500°K Case B, T_f = 1600°K Case C, T_f = 1800°K
3) Figure 3.24:	1st Stage ϕ = 1.6 T_{air} = 700°K T_f = 2159°K	2nd Stage Case A, T_f = 2377°K T_{air} = 700°K Case B, T_f = 1600°K Case C, T_f = 1900°K
4) Figure 3.25:	1st Stage ϕ = 1.8 T_{air} = 500°K T_f = 1892°K	2nd Stage Case A, T_f = 2287°K T_{air} = 500°K Case B, T_f = 1600°K Case C, T_f = 1900°K
5) Figure 3.26:	1st Stage ϕ = 1.8 T_{air} = 700°K T_f = 2015°K	2nd Stage Case A, T_f = 2377°K T_{air} = 700°K Case B, T_f = 1600°K Case C, T_f = 1800°K

ϕ = fuel equivalence ratio, T_{air} = inlet combustion air temperature, and T_f = combustion temperature.

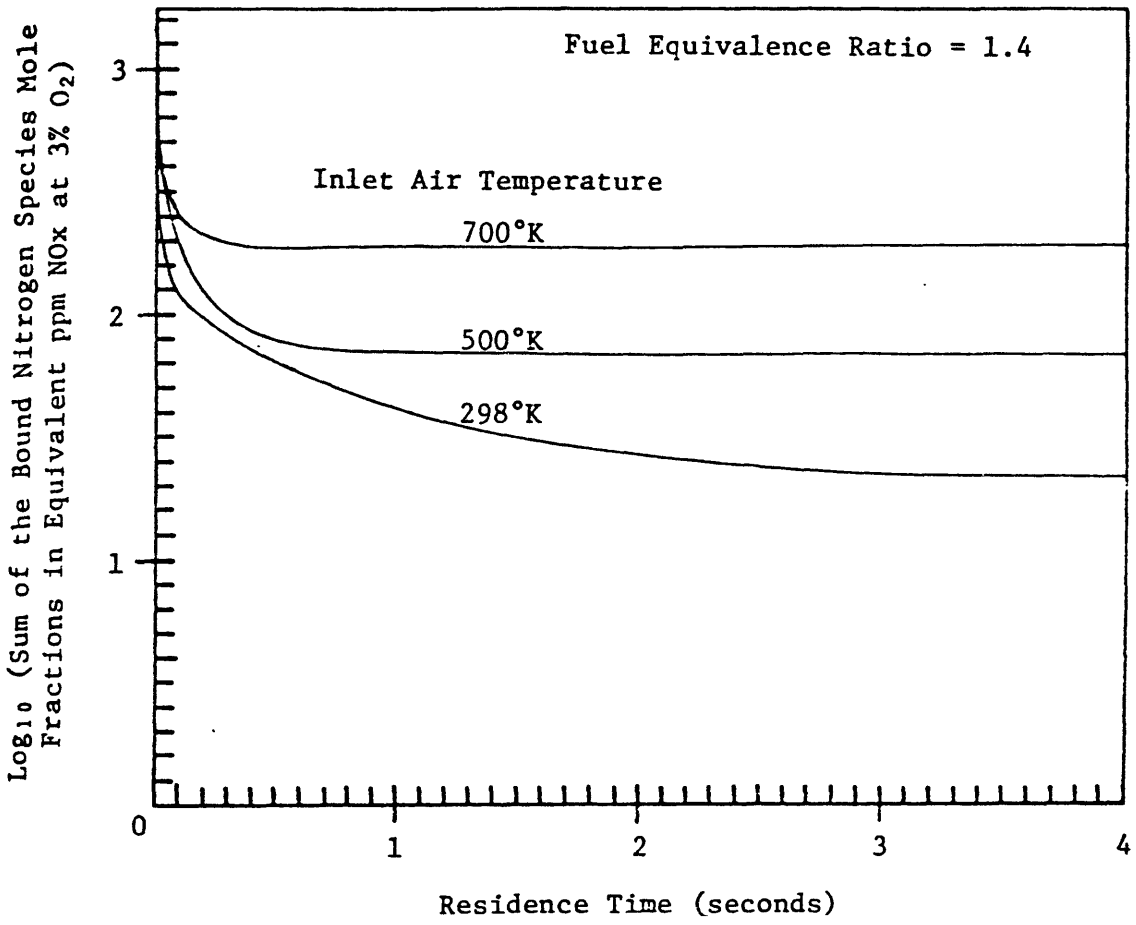

Figure 4. --The sum of the bound nitrogen species mole fractions (in equivalent ppm NOx at 3% O_2), as a function of residence time at different combustor inlet air temperatures.

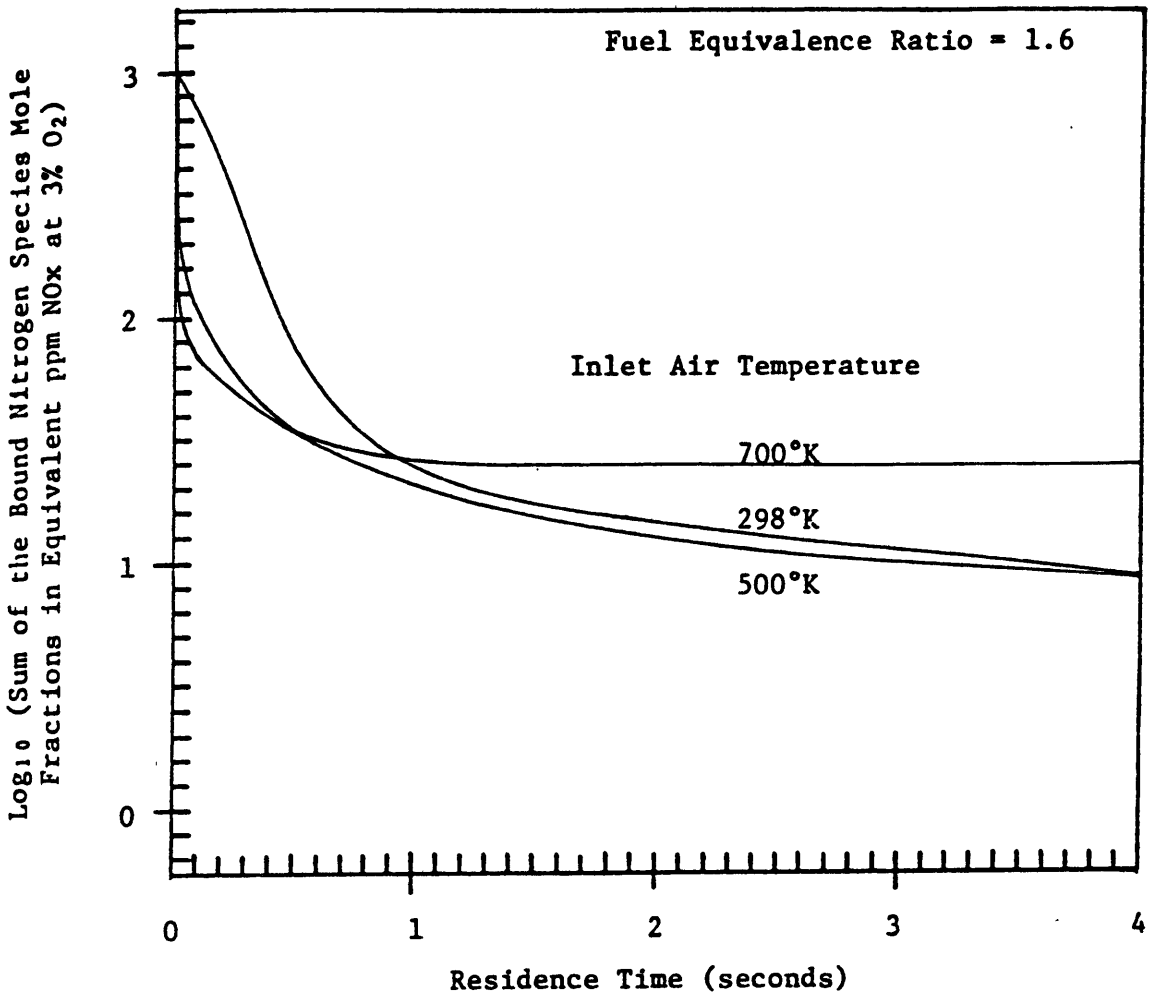

Figure 5. --The sum of the bound nitrogen species mole fractions (in equivalent ppm NOx at 3% O_2), as a function of residence time at different combustor inlet air temperature.

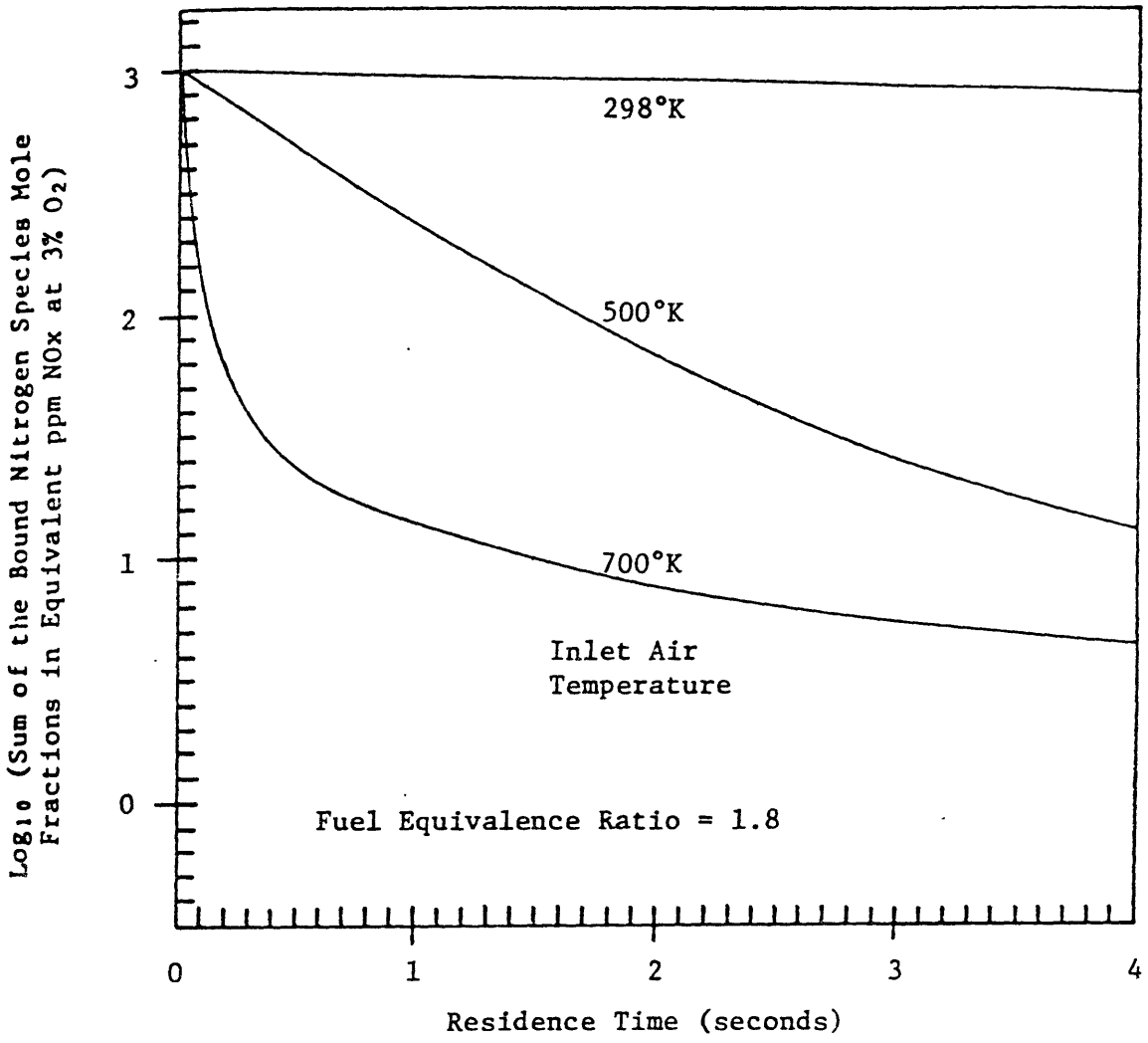

Figure 6. --The sum of the bound nitrogen species mole fractions (in equivalent ppm NOx at 3% O_2), as a function of residence time at different combustor inlet air temperatures.

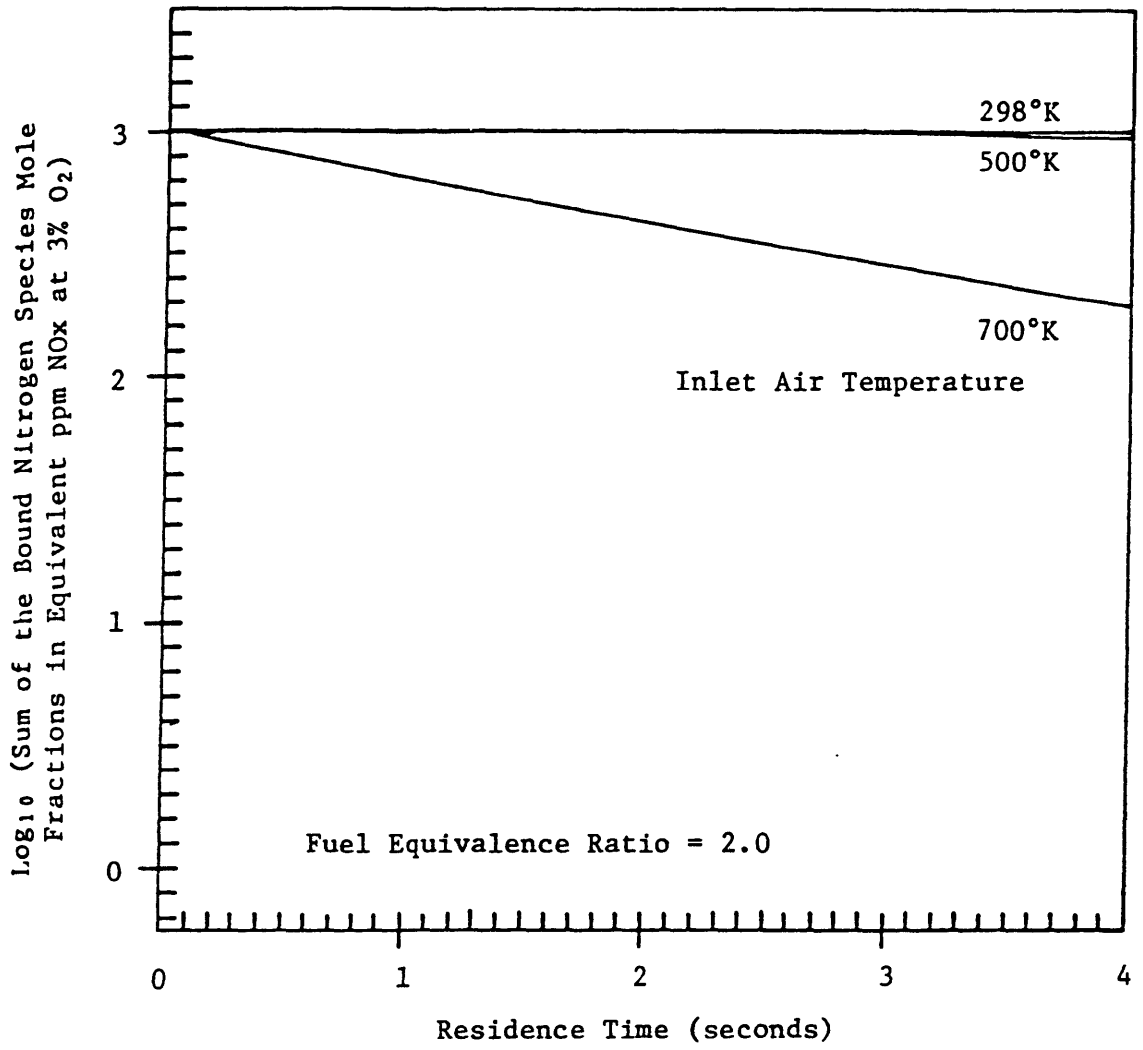

Figure 7. --The sum of the bound nitrogen species mole fractions (in equivalent ppm NOx at 3% O_2), as a function of residence time at different combustor inlet air temperatures.

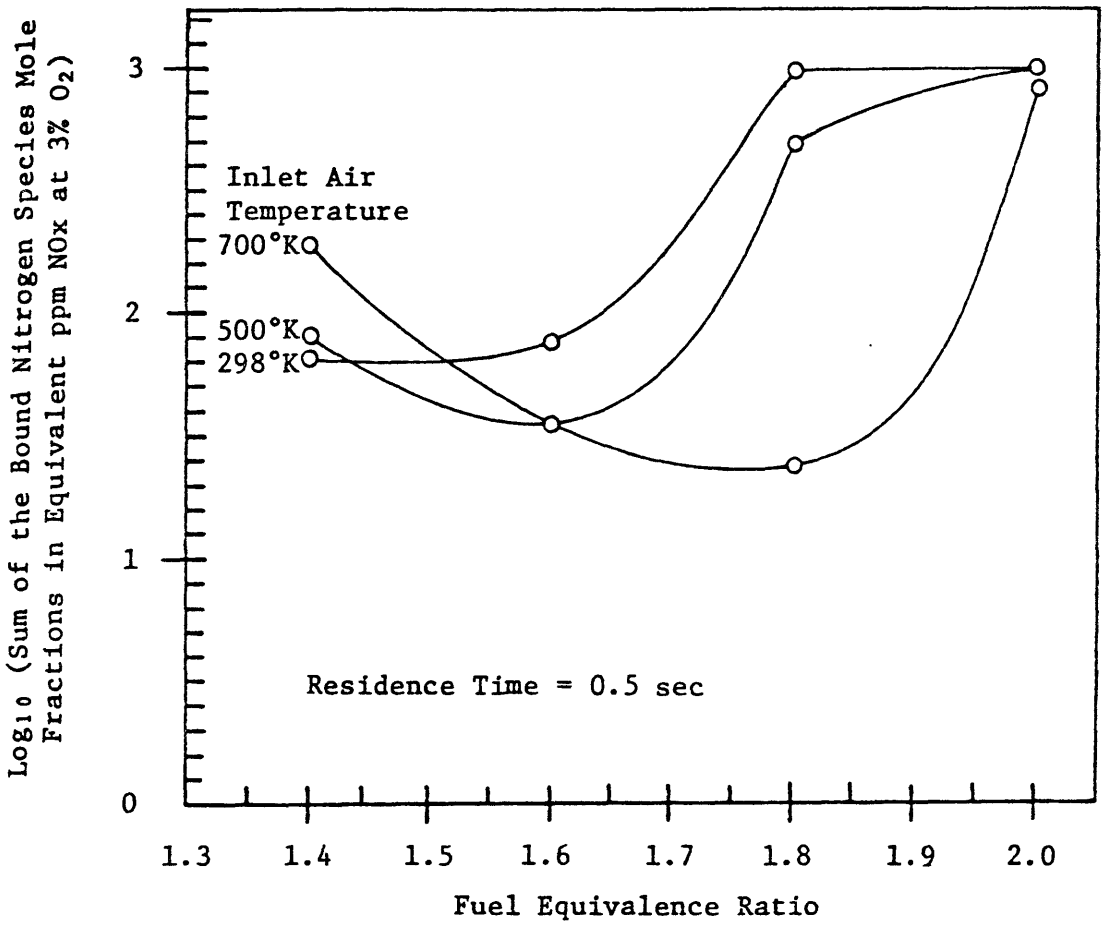

Figure 8. --The sum of the bound nitrogen species mole fractions (in equivalent ppm NOx at 3% O_2), as a function of fuel equivalence ratio at different combustor inlet air temperatures.

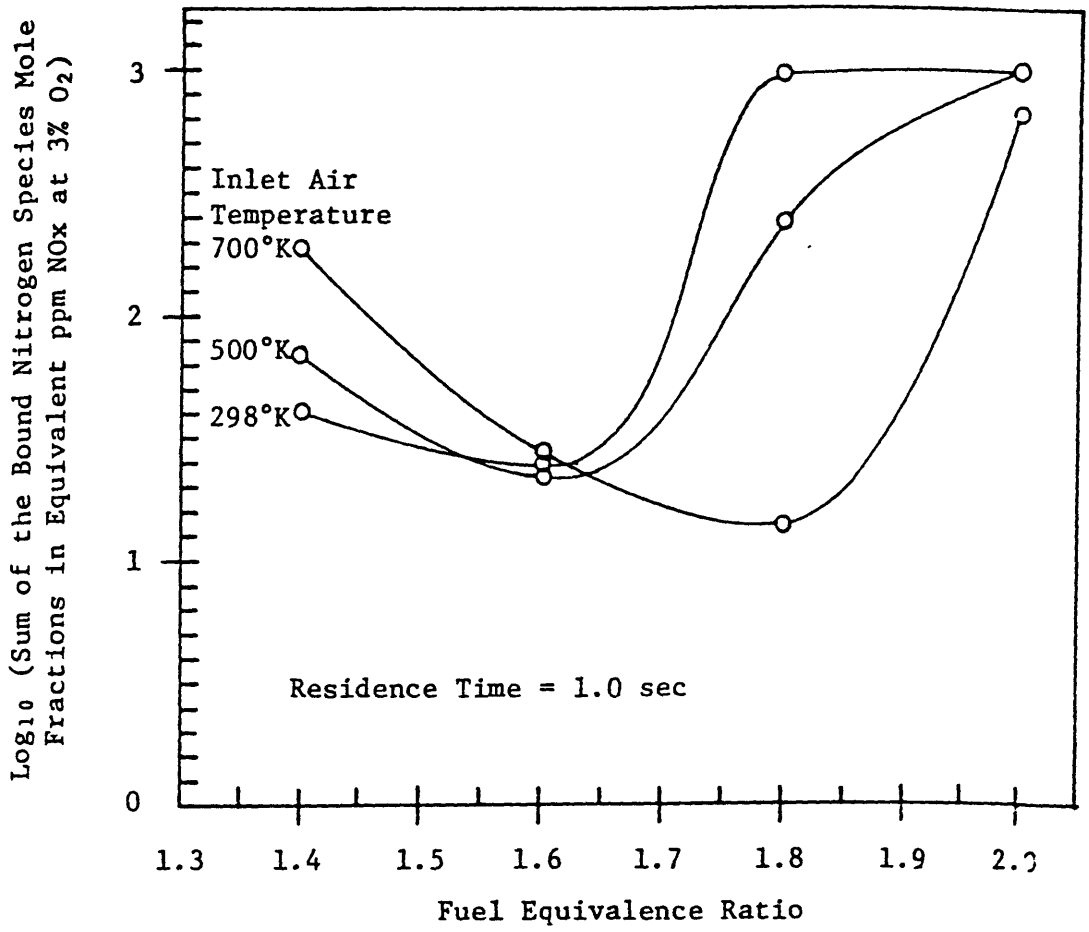

Figure 9. --The sum of the bound nitrogen species mole fractions (in equivalent ppm NOx at 3% O_2), as a function of fuel equivalence ratio at different combustor inlet air temperatures.

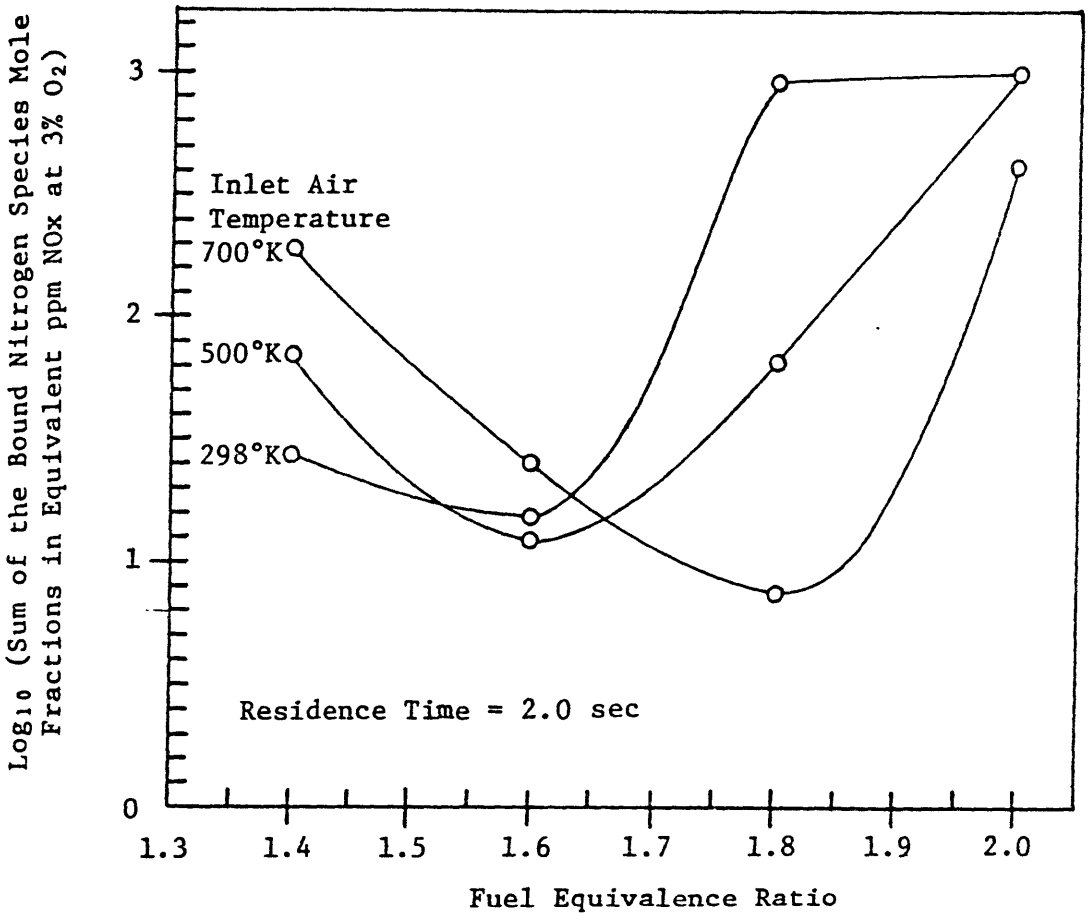

Figure 10. --The sum of the bound nitrogen species mole fractions (in equivalent ppm NOx at 3% O_2), as a function of fuel equivalence ratio at different combustor inlet air temperatures.

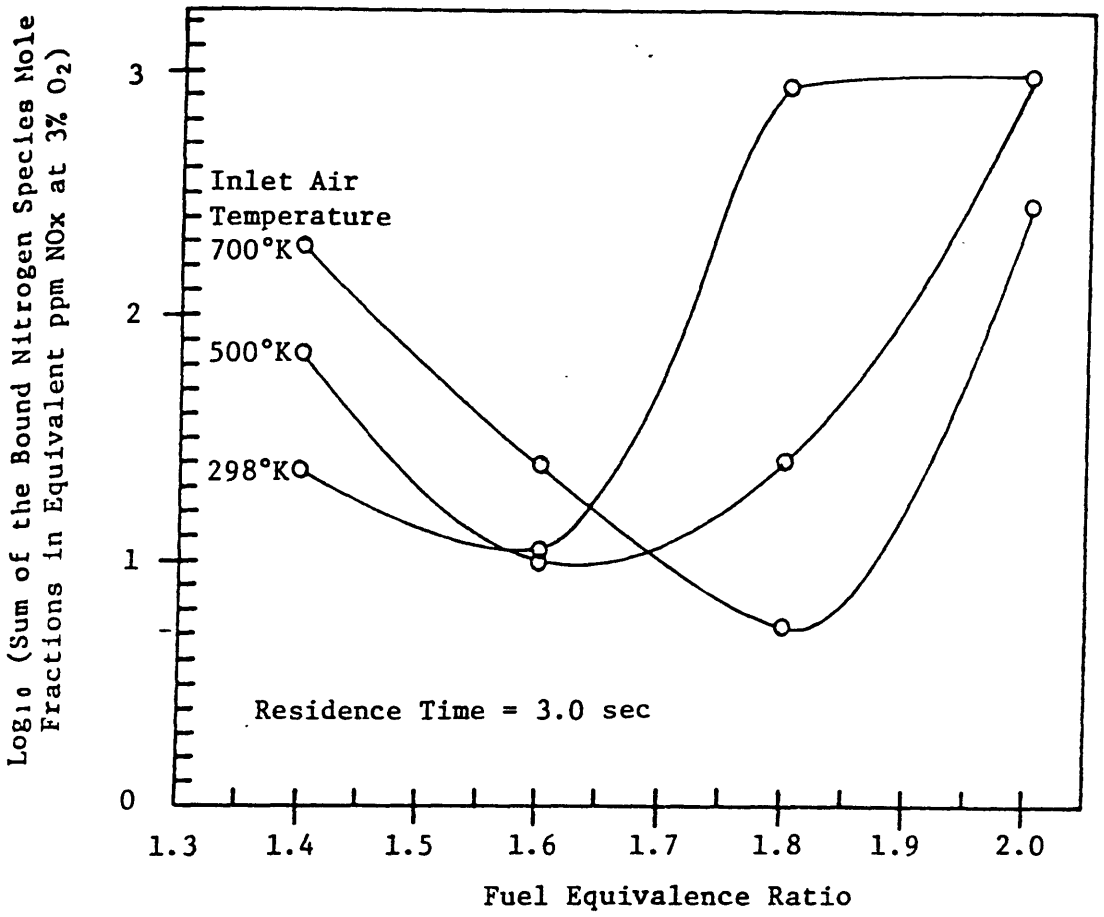

Figure 11. --The sum of the bound nitrogen series mole fractions (in equivalent ppm NOx at 3% O_2), as a function of fuel equivalence ratio at different combustor inlet air temperatures.

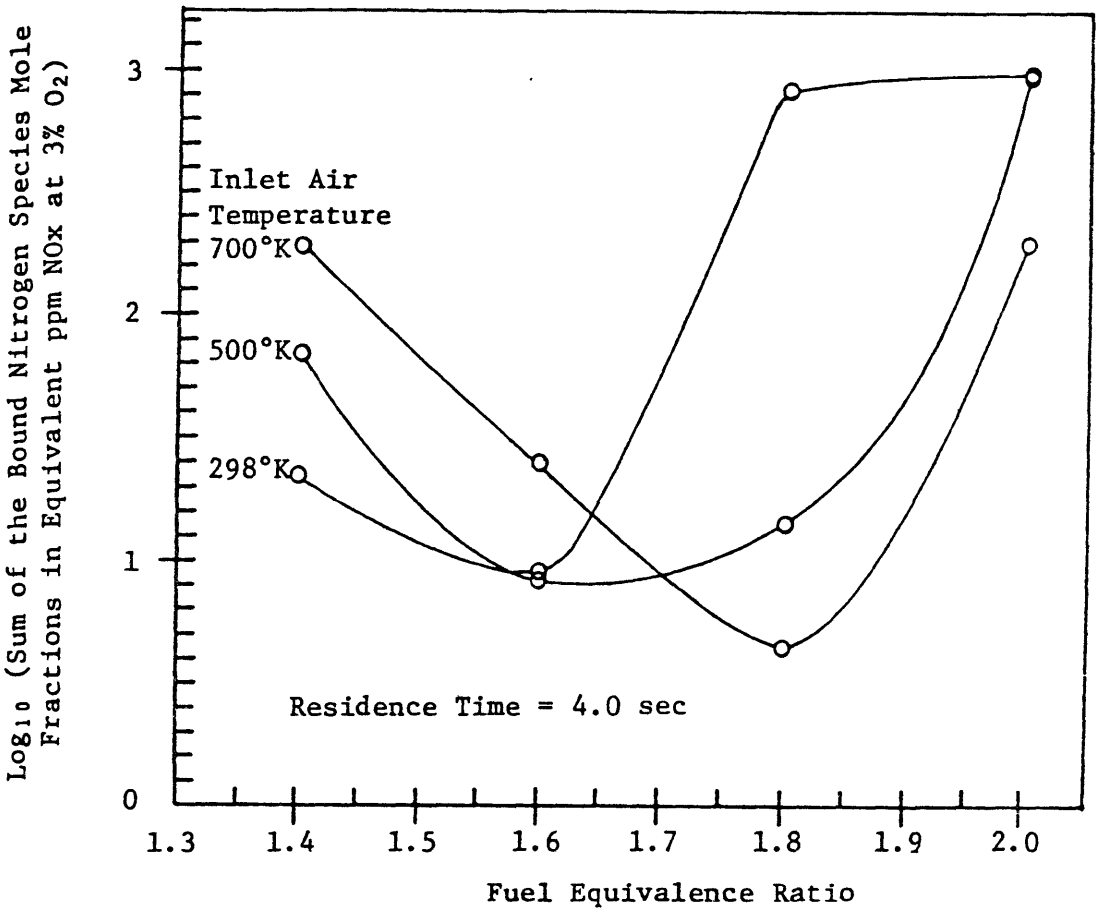

Figure 12 --The sum of the bound nitrogen species mole fractions (in equivalent ppm NOx at 3% O_2), as a function of fuel equivalence ratio at different combustor inlet air temperatures.

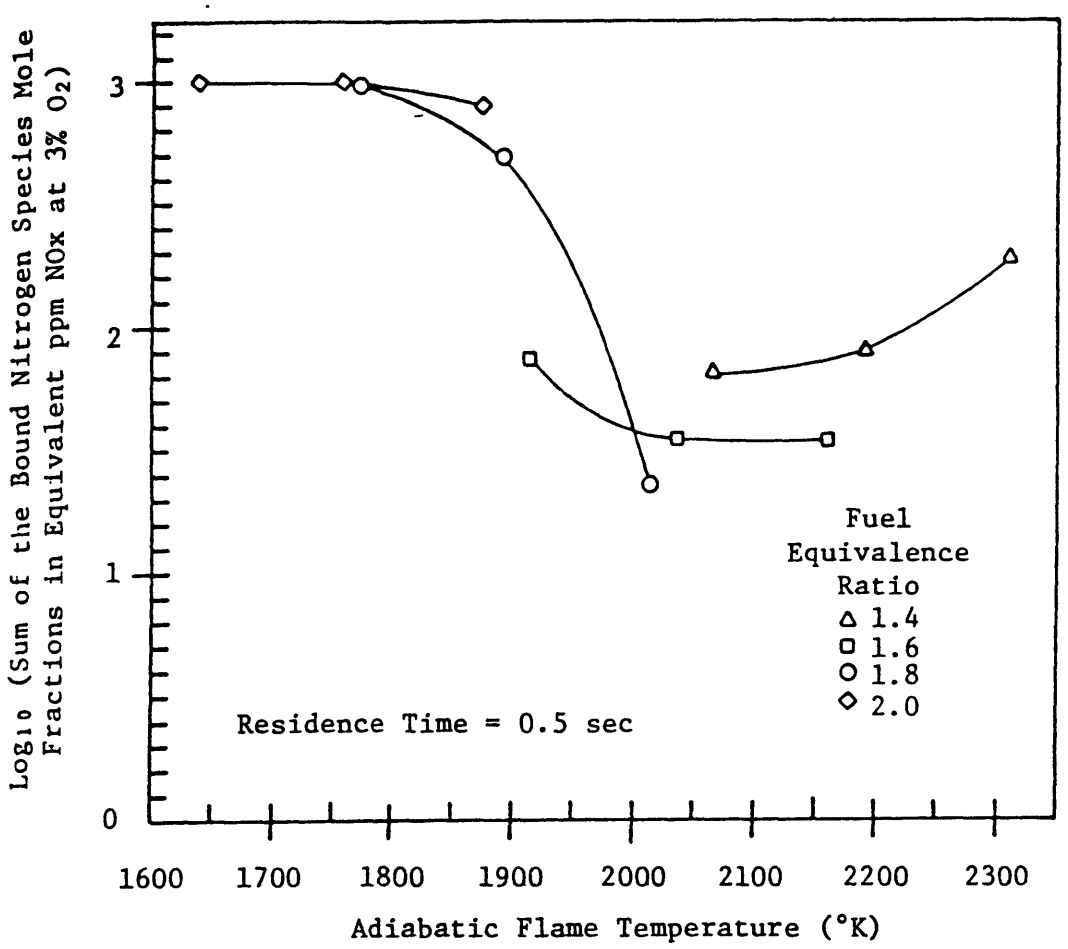

Figure 13 --The sum of the bound nitrogen species mole fractions (in equivalent ppm NOx at 3% O_2), as a function of adiabatic flame temperature at different fuel equivalence ratios.

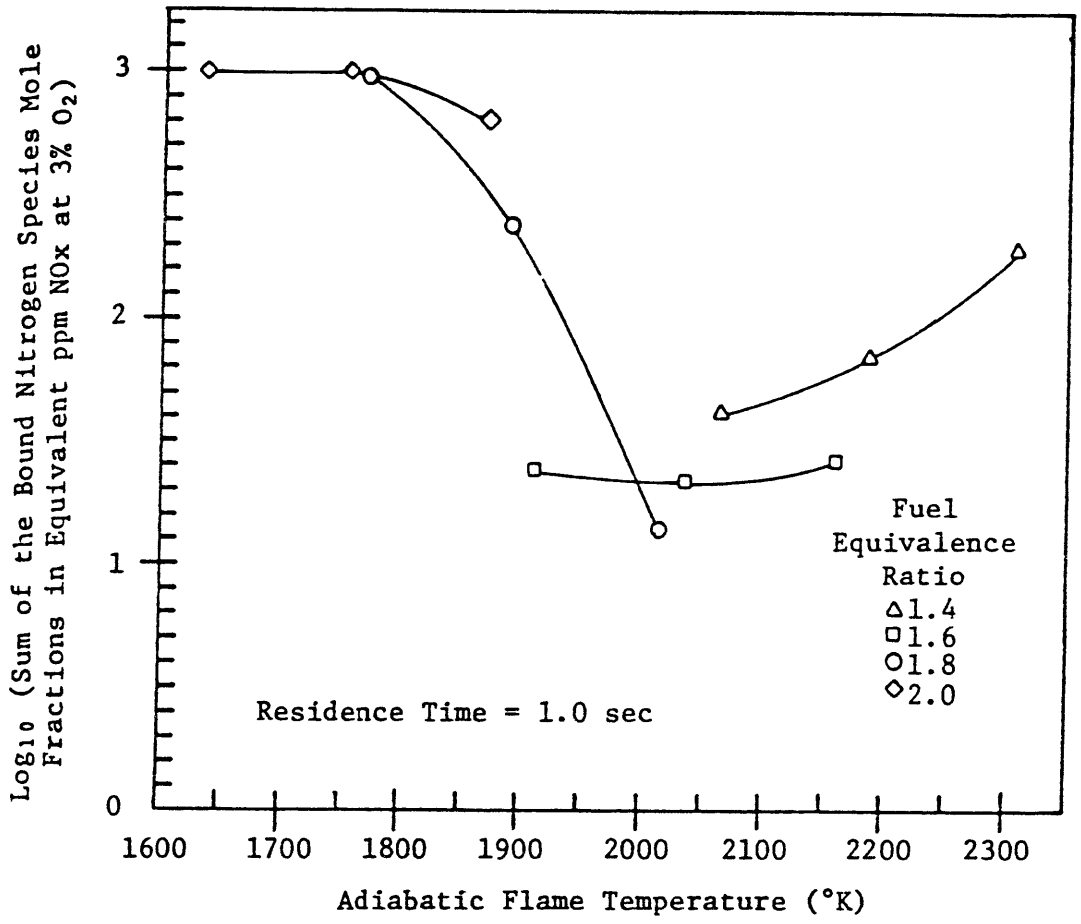

Figure 14. --The sum of the bound nitrogen species mole fractions (in equivalent ppm NOx at 3% O_2), as a function of adiabatic flame temperature at different fuel equivalence ratios.

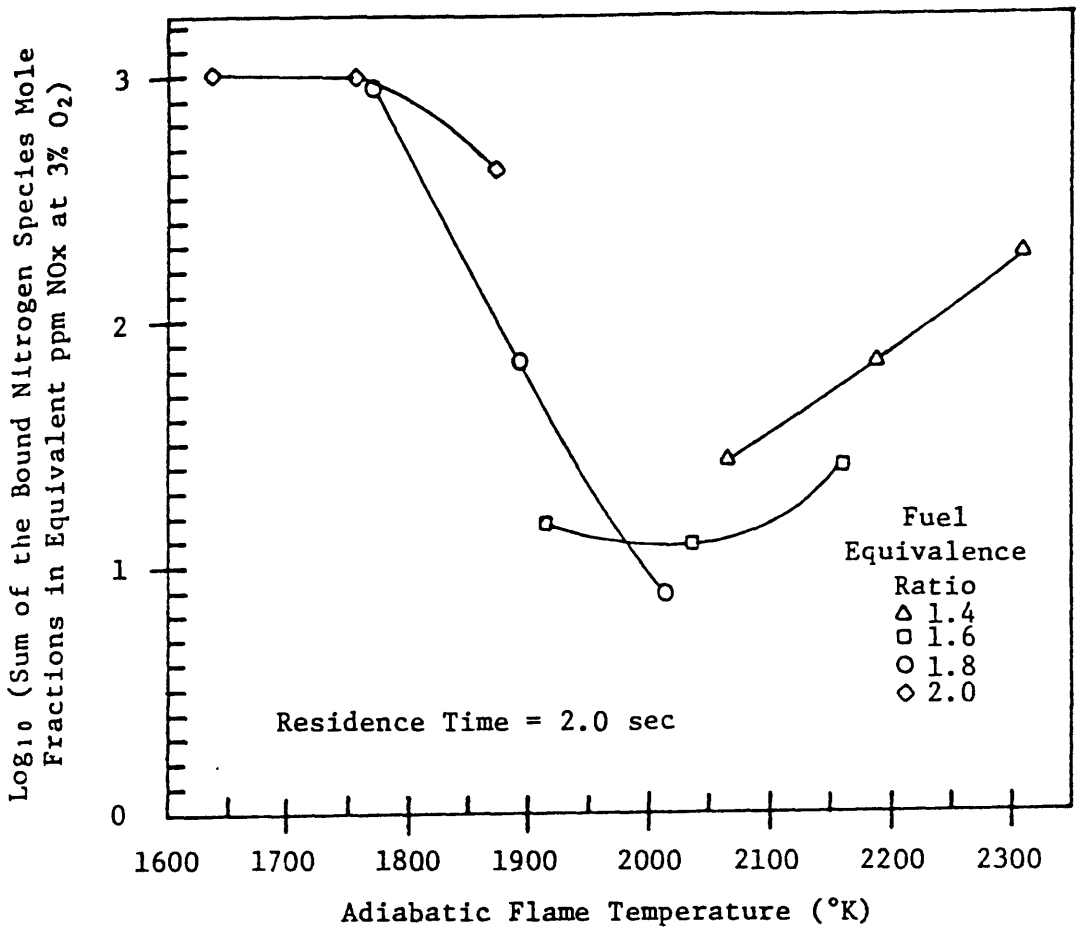

Figure 15 --The sum of the bound nitrogen species mole fractions (in equivalent ppm NOx at 3% O_2), as a function of adiabatic flame temperature at different fuel equivalence ratios.

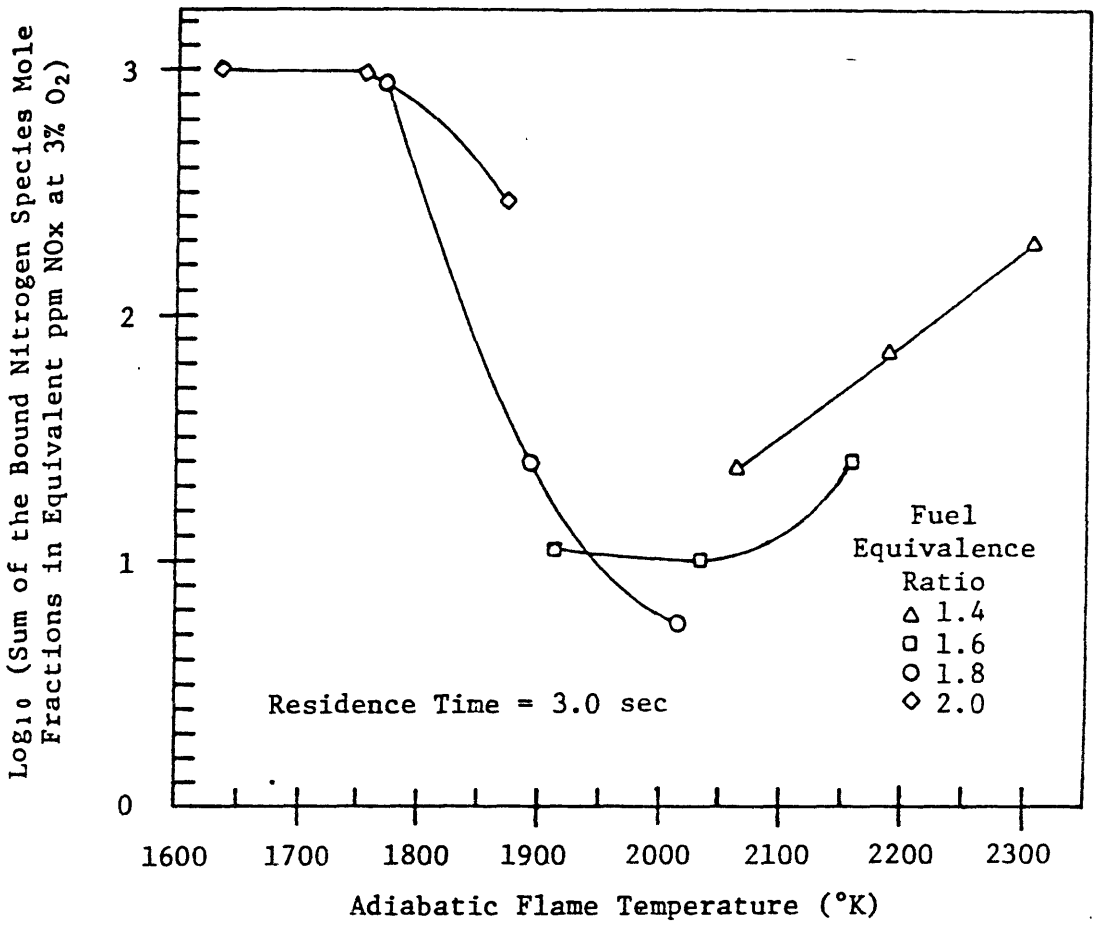

Figure 16 --The sum of the bound nitrogen species mole fractions (in equivalent ppm NOx at 3% O_2), as a function of adiabatic flame temperature at different fuel equivalence ratios.

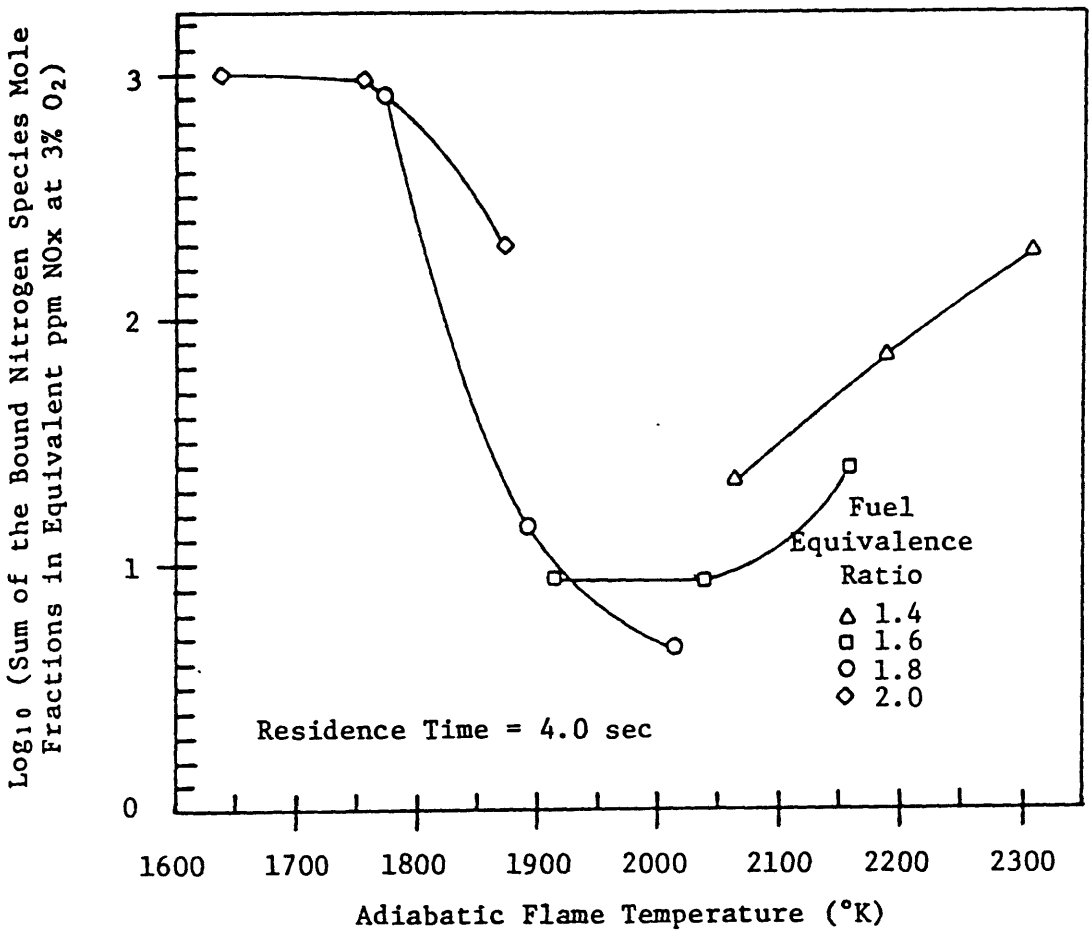

Figure 17 --The sum of the bound nitrogen species mole fractions (in equivalent ppm NOx at 3% O_2), as a function of adiabatic flame temperature at different fuel equivalence ratios.

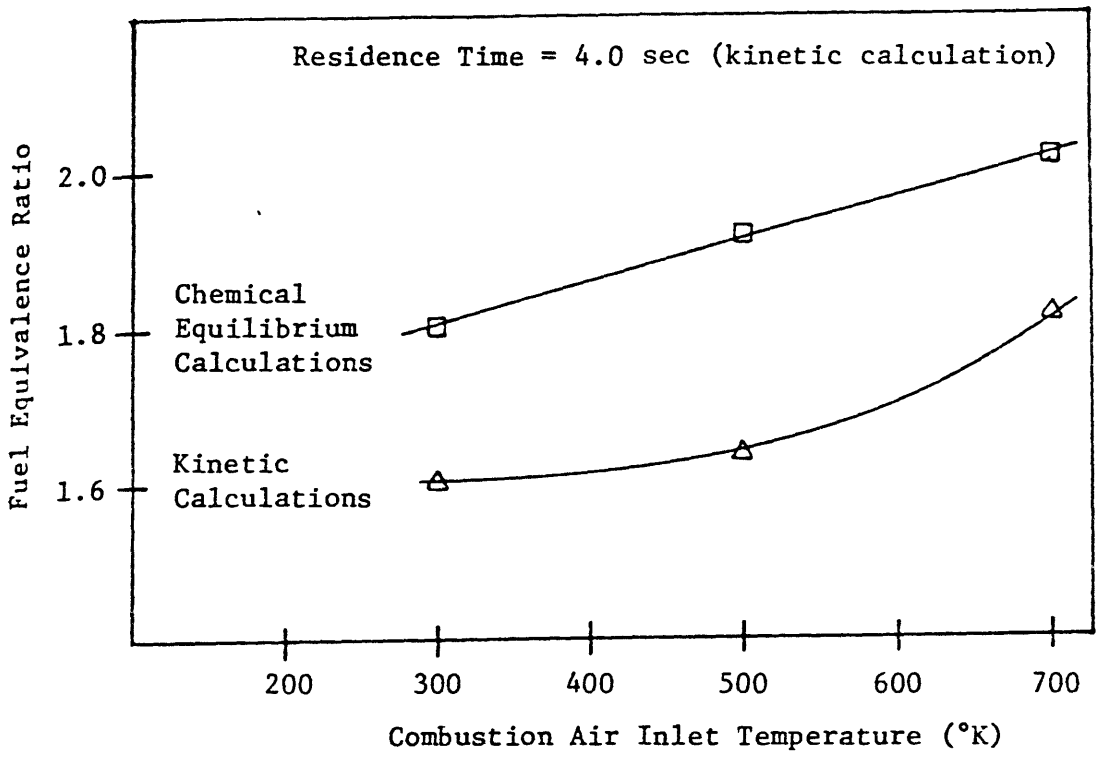

Figure 18 --The effect of combustor inlet air temperature upon the position (with respect to fuel equivalence ratio) of the minimum of the sum of the bound nitrogen species mole fractions: a comparison between chemical equilibrium and kinetic calculations.

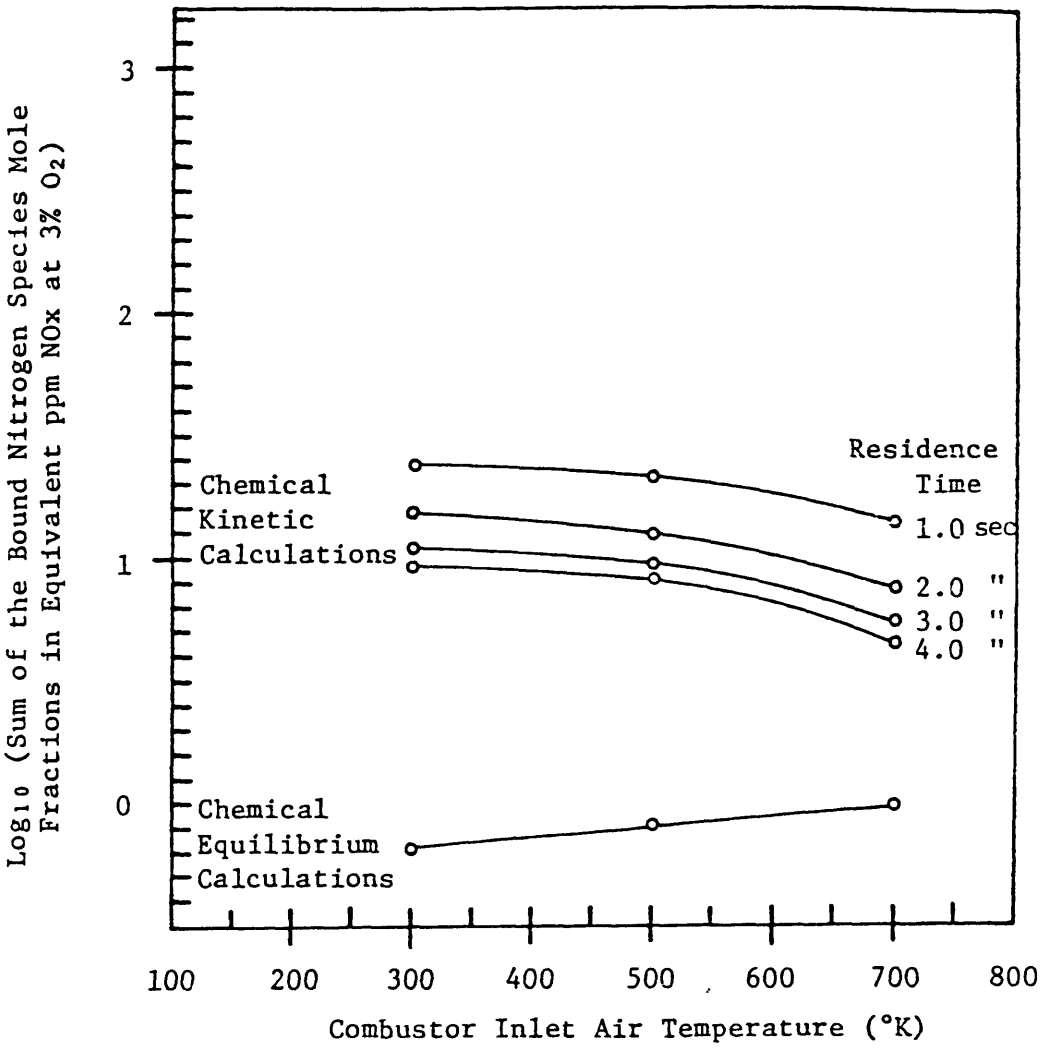

Figure 19 --The effect of combustor inlet air temperature on the value of the minimum of the sum of the bound nitrogen species mole fractions: a comparison between chemical equilibrium and kinetic calculations.

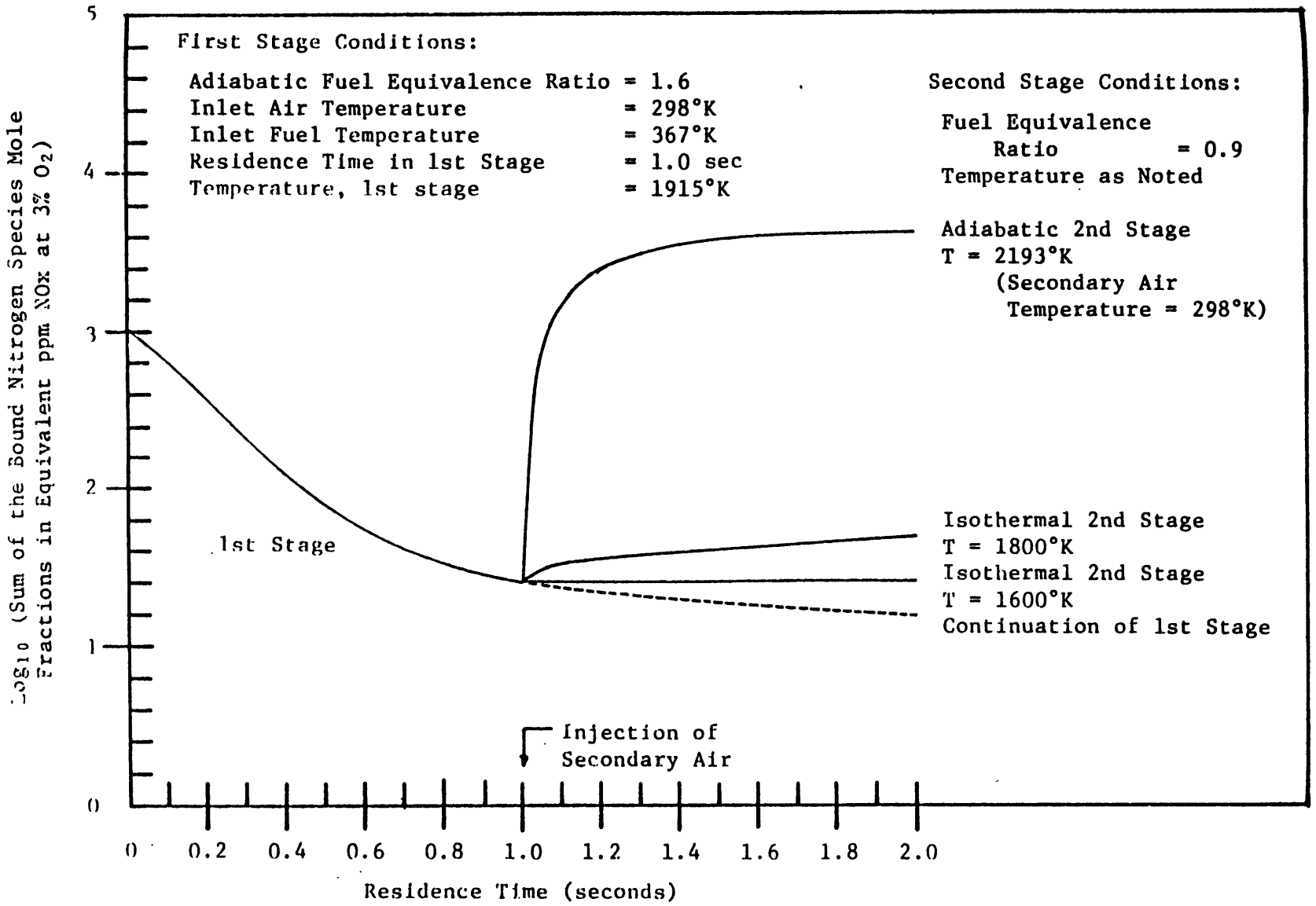

Figure 20 .--Two-stage combustion study: equivalent ppm NOx at 3% O_2, as a function of residence time in the combustor.

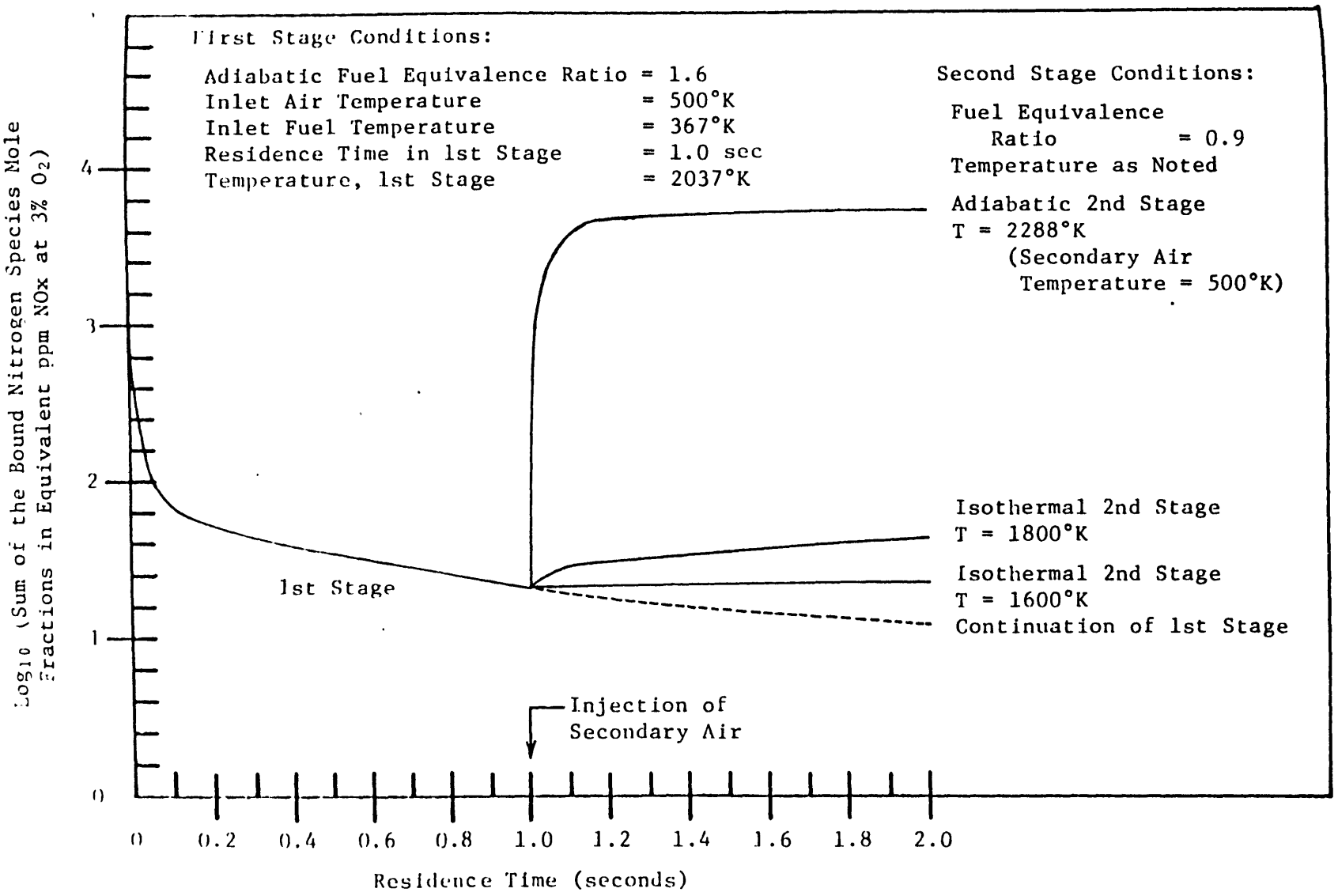

Figure 21 --Two-stage combustion study: equivalent ppm NOx at 3% O_2, as a function of residence time in the combustor.

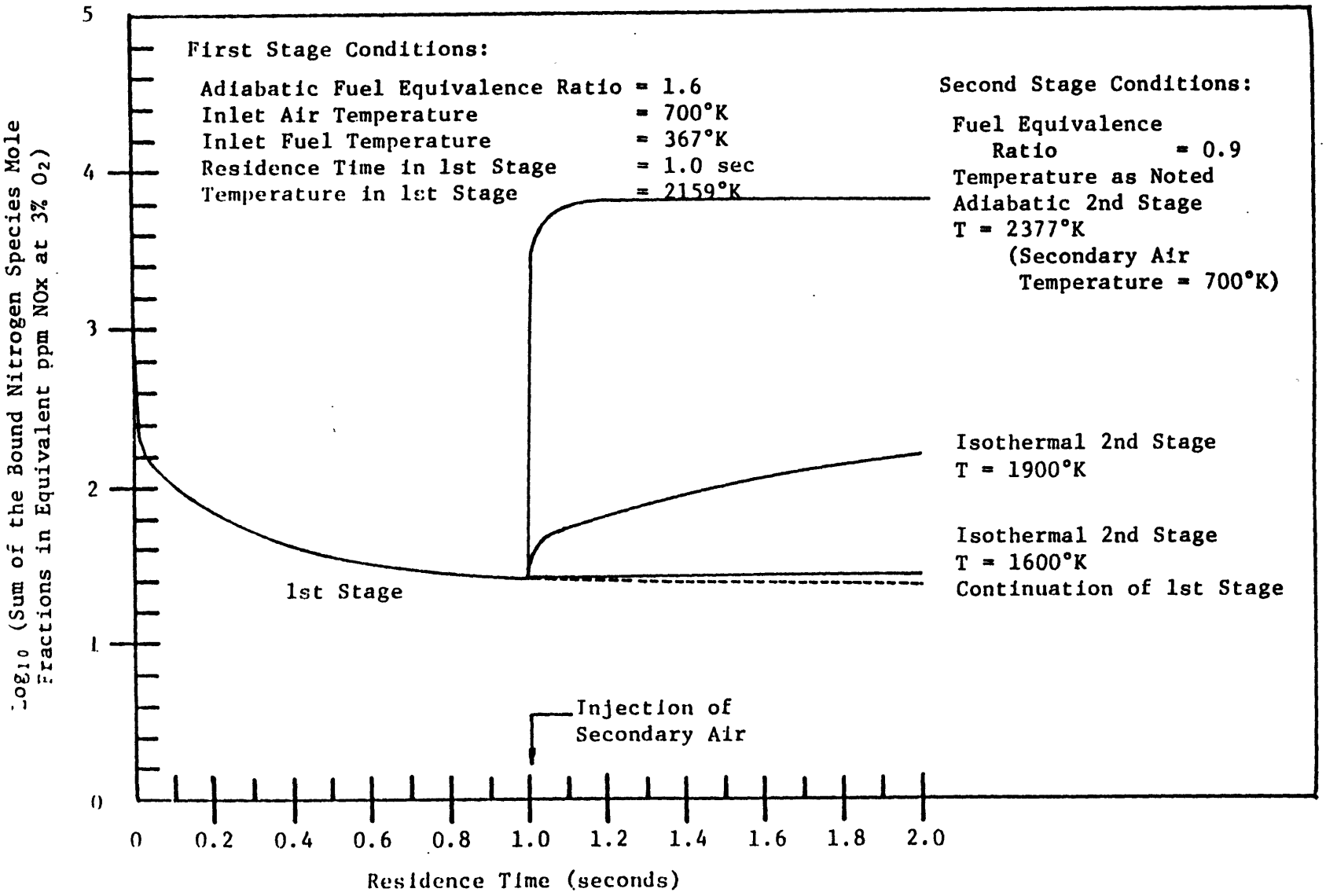

Figure 22 .--Two-stage combustion study: equivalent ppm NOx at 3% O_2, as a function of residence time in the combustor.

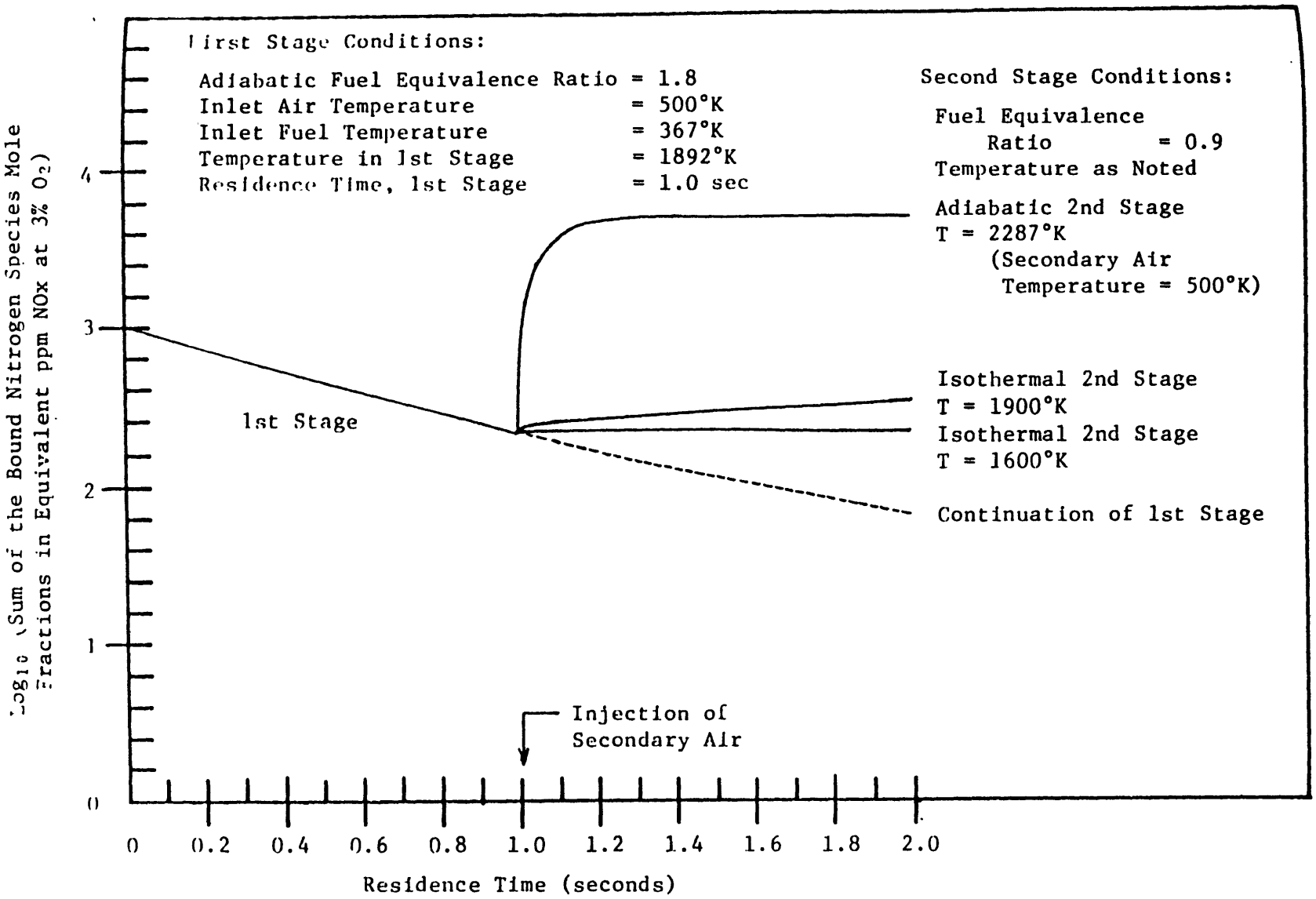

Figure 23 --Two-stage combustion study: equivalent ppm NOx at 3% O_2, as a function of residence time in the combustor.

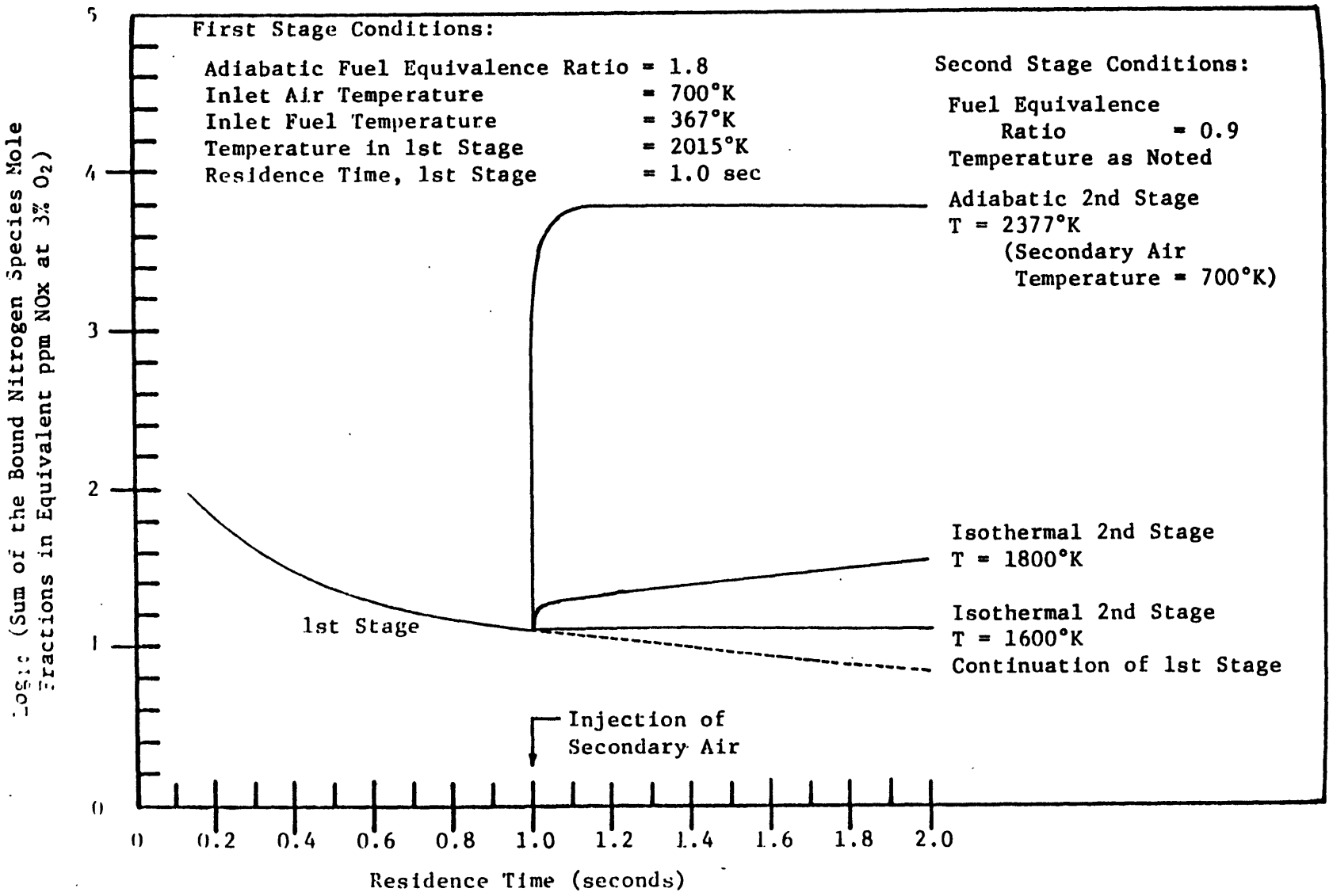

Figure 24 --Two-stage combustion study: equivalent ppm NOx at 3% O_2, as a function of residence time in the combustor.

This information suggests that fuel equivalence ratio is a very important parameter in the staged combustion process, and that it may be optimized. From the standpoint of chemical equilibrium the optimal fuel equivalence ratio that should be applied to the first stage lies between 1.75 and 2.0 depending on air preheat.

2) It is important to look at the sum of the bound nitrogen species mole fractions, since they all have the potential of being oxidized to pollutant NO_x, especially if combustion is completed with an overall excess of air after the fuel rich first stage(s).

3) The combustion temperature (which may be controlled to some degree by air preheat) affects the position of the minimum of the sum of the bound nitrogen species mole fractions with respect to fuel equivalence ratio. Equilibrium calculations indicate that the minimum shifts toward higher fuel equivalence ratios with increasing inlet air temperatures. (In observing this trend, particular notice should be made that rates of fuel nitrogen reactions are not taken into account.)

4) The equilibrium adiabatic flame temperature drops as fuel equivalence ratio is increased beyond 1 (see Fig. 2). This trend is important to bear in mind since 1) temperatures in the fuel rich first stage may drop to unacceptably low levels (e.g. poor carbon burnout) and 2) the introduction of secondary air to later stages may result

in sudden temperature rises or hot spots. Figure 2 indicates that combustion temperature may be raised by air preheat thus suggesting a means of solution to the possible occurrence of unacceptably low temperature in the first stage.

5) The chemical equilibrium calculations do not provide information on rates of fuel nitrogen reactions, on effects of residence times on NO_x concentrations, on effects of increased organic nitrogen content in the fuel, or on the actual quantitative values of nitric oxides concentrations in the flue gases of the CRF combustor.

2.7.2 Chemical Kinetic Calculations

Single Stage Study — Examination of the Fuel Rich Stage

6) The kinetic computer calculations demonstrate the importance of rates of fuel nitrogen reactions in the optimization of conditions for the fuel rich stage. At high fuel equivalence ratios (see Fig. 7) the rates of fuel nitrogen reactions are so low that the sum of the bound nitrogen species mole fractions does not come close to the equilibrium value even within 4 seconds of residence time, a period of time much longer than encountered in most utility boilers. At the other extreme (see Fig. 4), at low fuel equivalence ratios, rates are so fast that near-equilibrium values are achieved within half-a-second. Hence, though thermodynamic equilibrium calculations might indicate an optimal fuel equivalence

ratio of 2.0 at high air preheat (see Fig. 3) the kinetic calculations indicate that from a rate standpoint, within' the constraints imposed by typical utility boilers this value is unacceptable.

7) Examination of the computer results indicate that temperature is a key variable in affecting the rates of fuel nitrogen transformations, and may possibly be as important a variable in optimizing the fuel rich stage as fuel equivalence ratio. The combustion temperature is affected by 1) fuel equivalence ratio and 2) air preheat. Observation of Figures 13-17 will illustrate that from the point of view of fuel nitrogen chemistry, the optimal temperature in the first stage lies between 1900 K and 2100 K at any residence time.*

It might be added that these high temperatures are required to produce high radical concentrations (particularly the OH radical), which are necessary for the fuel nitrogen reactions to proceed rapidly.

In looking at Figures 13-17 the sum of the bound nitrogen species concentrations is observed to pass through a minimum with respect to temperature. The rise in the sum to the left of the minimum is indicative of kinetic constraints, and the rise to the

---

* Results from the MIT CRF indicate a weak dependence on temperature of fuel nitrogen reactions. Special note should be made though, that the combustion temperatures in the CRF are considerably below the optimal temperatures indicated by the computer calculations, i.e., 1600 to 1800 K as opposed to 1900 to 2100 K.

right, of thermodynamic constraints, in the NO_x minimization problem.

8) The minimum of the sum of the bound nitrogen species concentrations occurs at somewhat lower fuel equivalence ratios than those indicated by the equilibrium calculations (see Fig. 18). The kinetic calculations indicate that the position of the minimum with respect to fuel equivalence ratio lies between 1.6 and 1.8.

9) The chemical kinetic calculations indicate that the value of the minimum decreases with increasing temperature, a trend opposite to that indicated by the thermodynamic calculations (see Fig. 19). This discrepancy is due of course to the rates of the fuel nitrogen reactions being accounted for in the kinetic calculations.

10) The calculated nitrogenous species concentrations, made by the chemical kinetic computer program, are not acceptable from a quantitative viewpoint because of lack of a realistic reactor model accounting for effects on nitrogenous species formation, of quality of atomization, volatilization rates, and fuel-air mixing patterns and rates. However the modeling of the fuel nitrogen chemistry is good and provides reliable qualitative information.

Two-Stage Study — Examination of the Second Stage

11) The chemical kinetic study of the second stage of a two-staged combustor demonstrates above all the importance of temperature regulation in the second stage (see Figures 20-24). If

temperatures are allowed to increase above approximately 1800 K, thermal NO_x production via the Zeldovich mechanism becomes so great that it nullifies efforts to minimize concentrations of bound nitrogen species in the first stage. (Observe the adiabatic case in the second stage runs in Figures 20-24).

The introduction of secondary air in the second stage results in sudden temperature rises which exacerbate the thermal NO_x problem. In a real combustor, the rise in temperature is fortunately not so sharp due to finite mixing rates of air and fuel. However, some form of temperature control by means of heat removal may be necessary to keep thermal NO_x to a minimum. Temperature control may be rendered easier by multiple staging, where the combustion air is introduced a small amount at a time, rather than all at once.

12) The results of the single and two-stage studies indicate that optimally for the case of a two-staged combustor, the first stage should be run at a temperature between 1900 K and 2100 K, and a fuel equivalence ratio between 1.6 and 1.8, and the second stage at a temperature at least below 1800 K. The overall equivalence ratio of the staged combustor should be about .9 to .95, slightly air-rich so as to achieve complete fuel burnout.

3. Experimental Investigation of Staged and Unstaged High-N #6 Fuel Oil in the MIT CRF

High-N Content #6 Fuel Oil

A high nitrogen content #6 fuel oil was obtained from the Santa Fe Springs Refinery of the Gulf Oil Company in California.

The fuel oil consists of a blend of a cutter-stock and a high nitrogen content asphalt. The compatability and homogenity of blends of these oils were determined by Gulf Research and Development Company. The results of their analyses are presented in Table 2.

A 50:50 wt % blend was chosen because of its lower viscosity, permitting easier fuel handling. The fuel was blended by simply loading the cutter-stock and asphalt separately into a road tanker and relying on natural mixing during transportation from Los Angeles to Boston.

It is not possible to classify the resultant high nitrogen content #6 fuel oil as coming from any particular oil field since the asphalt itself consisted of a blend of the residues and vacuum tower bottoms of a range of crude oils.

3.1 Single Stage Combustion Studies

The objective of the unstaged or single-stage combustion studies was to establish baseline data on NO_x emissions. The influence of air preheat, atomizer type and degree of swirl (flame aerodynamics) was established.

The operating conditions of the CRF which were maintained constant throughout each test were:

Thermal Input	1 MW (3.4×10^6 Btu/hr ∿25 gph)
Fuel Temperature	200° F
Excess Air	5% (∿1% O_2 in flue gas)
Wall Temperature (average)	∿1200° C
Flue Gas Exit Temperature	∿1000° C

A total of eight flames were investigated; the input conditions for each flame are given in Table 6.

Air preheat levels of 500° F and 850° F were obtained using the independently fired air preheater. The atomizer types consisted of a pressure jet nozzle (Lucas 14 M80B) shown schematically in Figure 25(a), and a twin-fluid steam atomizing nozzle shown schematically in Figure 25(b). Fuel temperature was maintained at ∿200° F at which temperature the oil viscosity was ∿30 Cp.

The measurements taken for each of the eight unstaged flames were:

- Axial temperature profiles — using suction pyrometer
- Axial NO_x, CO, CO_2 and O_2 profiles — using gas sampling probe
- Flue gas NO_x, CO, CO_2, O_2 and particulate concentrations

3.1.1 The Axial Gas Composition and Temperature Profiles

The NO_x concentration profiles for the unstaged flames are presented in Figures 26 to 29. The results clearly show the effect of burner swirl number on NO_x formation and emission. The high swirl flames exhibit NO_x concentrations ∿120 ppm higher throughout than the low swirl flames. The higher NO_x values are attributed to higher peak flame temperatures in the high swirl flame which result in an increased proportion of thermal NO_x.

TABLE 6

INPUT CONDITIONS FOR UNSTAGED FLAMES
[See also Tables B1(a) and (b)]

Flame	Nozzle Type*	Air Preheat	Swirl #†	Run #
1	Pressure Jet	500° F	2.7	21(a)
2	Pressure Jet	500° F	0.42	21(b)
3	Pressure Jet	850° F	2.7	24(a)
4	Pressure Jet	850° F	0.42	24(b)
5	Twin Fluid	500° F	2.7	29(a)
6	Twin Fluid	500° F	0.53	29(b)
7	Twin Fluid	850° F	2.7	30(a)
8	Twin Fluid	850° F	0.53	30(b)

* The pressure jet nozzle shown in Figure 25(a) was operated at a pressure of $\sim$180 psi; the twin fluid steam atomizer shown in Figure 25(b) was operated with a steam pressure of 95 psia and an oil pressure of $\sim$60 psia.

† The swirl number S of a free air jet is defined as the ratio of the angular momentum (G_ϕ) to the product of axial thrust (G_x) and the nozzle radius (R).

$$\text{i.e.,} \qquad S = \frac{G_\phi}{G_x} R$$

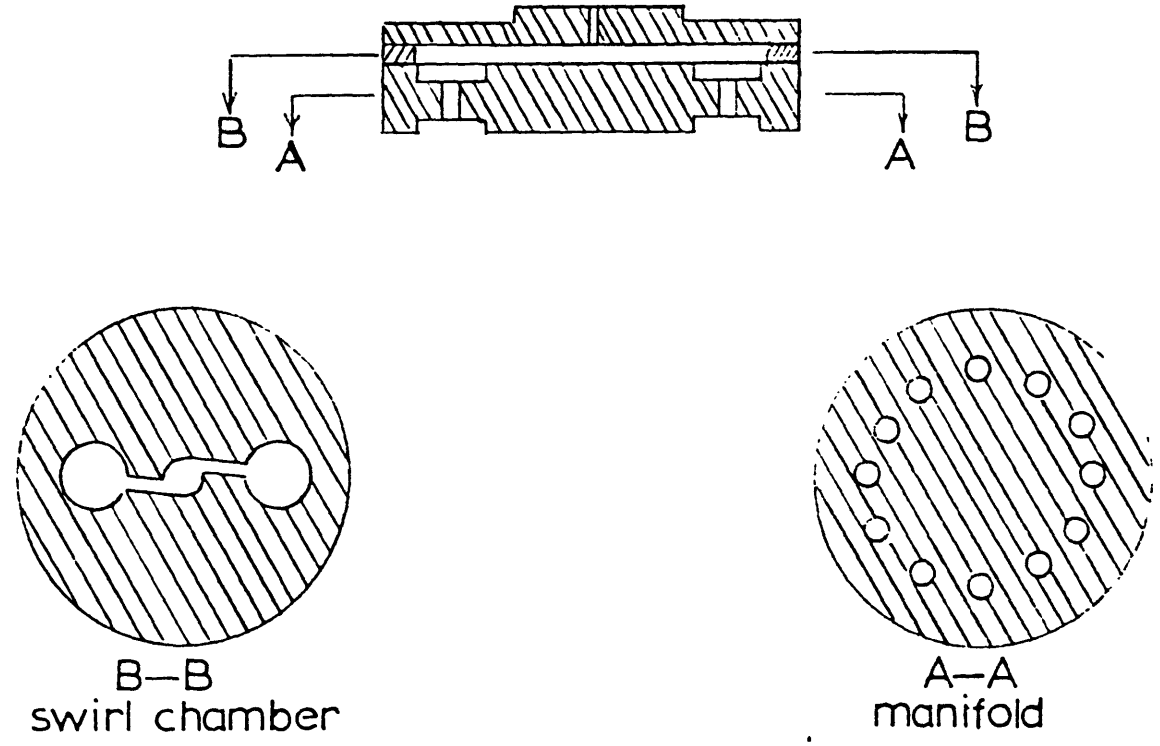

FIGURE 25(a)
LUCAS PRESSURE JET NOZZLE

FIGURE 25(b)
TWIN-FLUID STEAM-ASSISTED
ATOMIZING NOZZLE

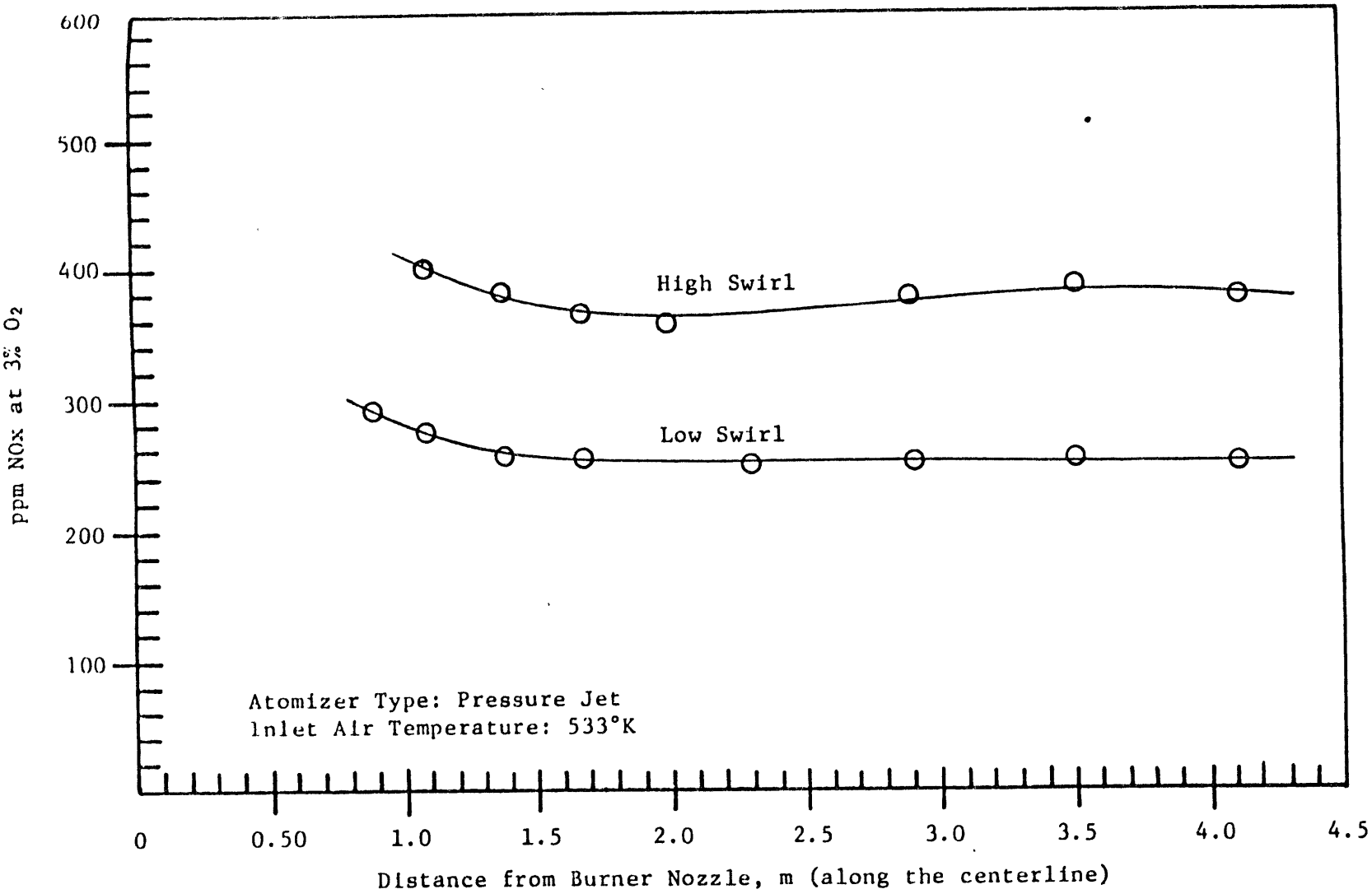

Figure 26 --Axial NOx (ppm at 3% O_2) concentration profiles, single stage baseline study.

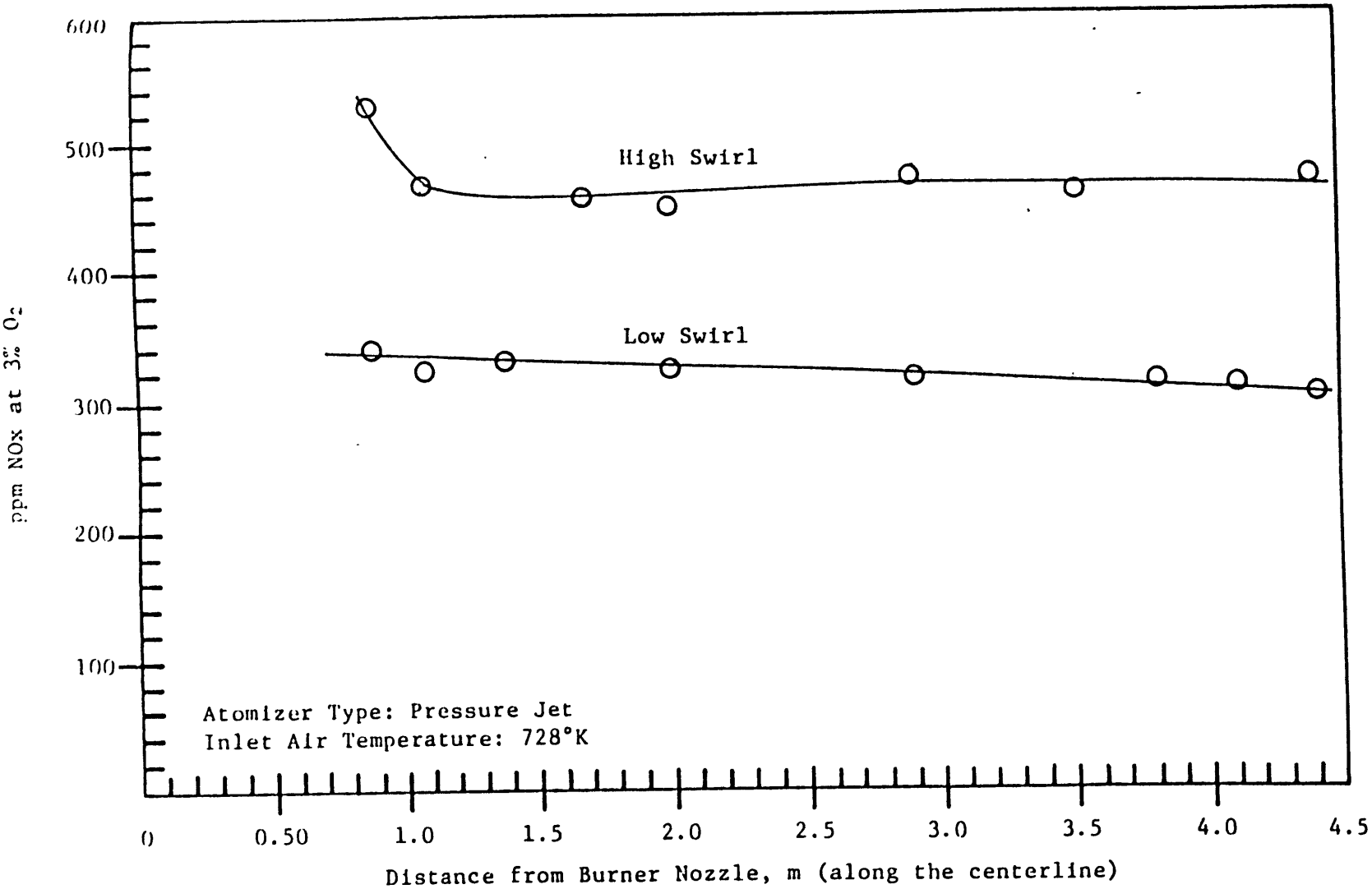

Figure 27 --Axial NOx concentration (ppm at 3% O_2) profiles, single stage baseline study.

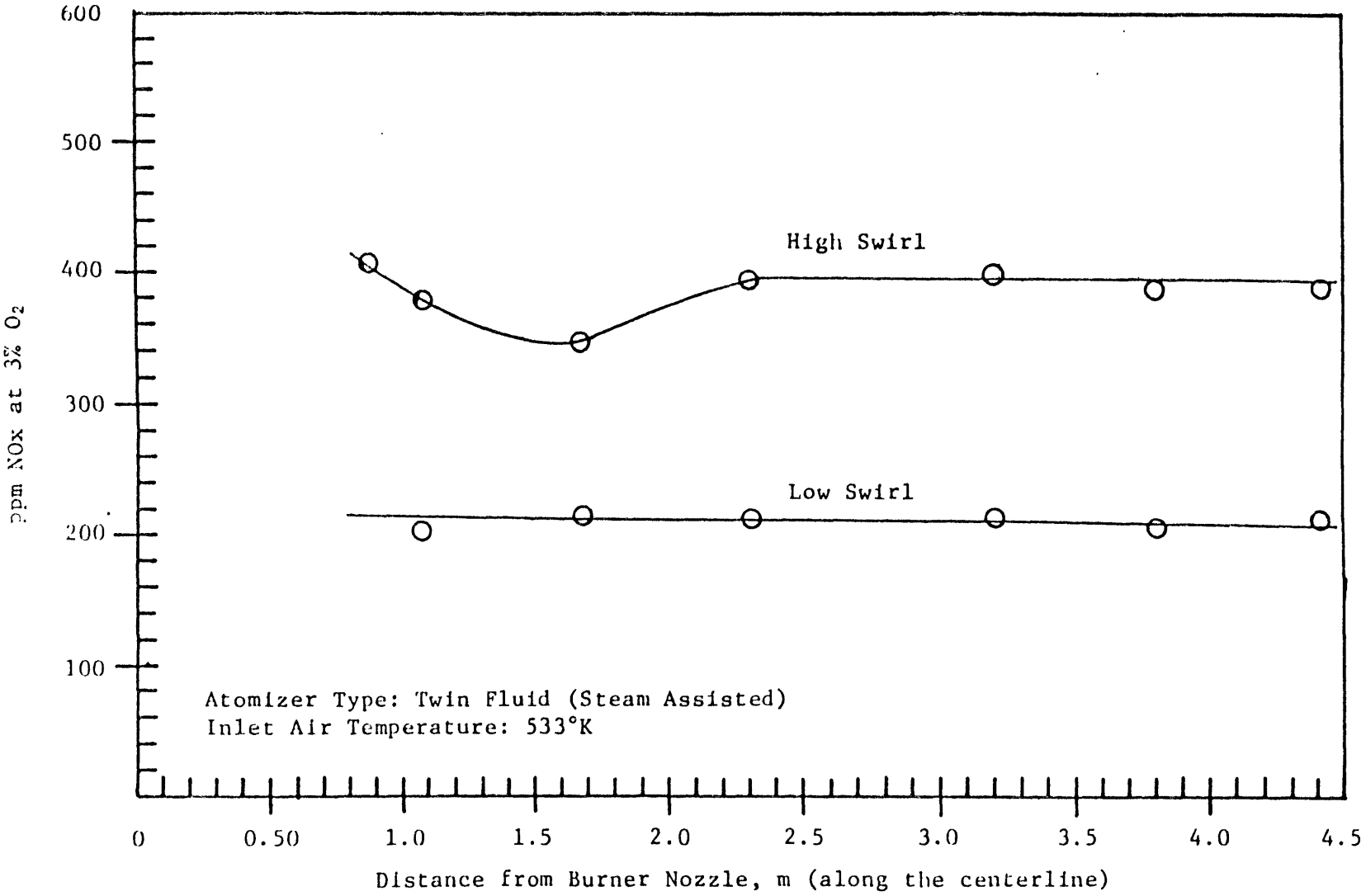

Figure 28 --Axial NOx concentration (ppm at 3% O_2) profiles, single stage baseline study.

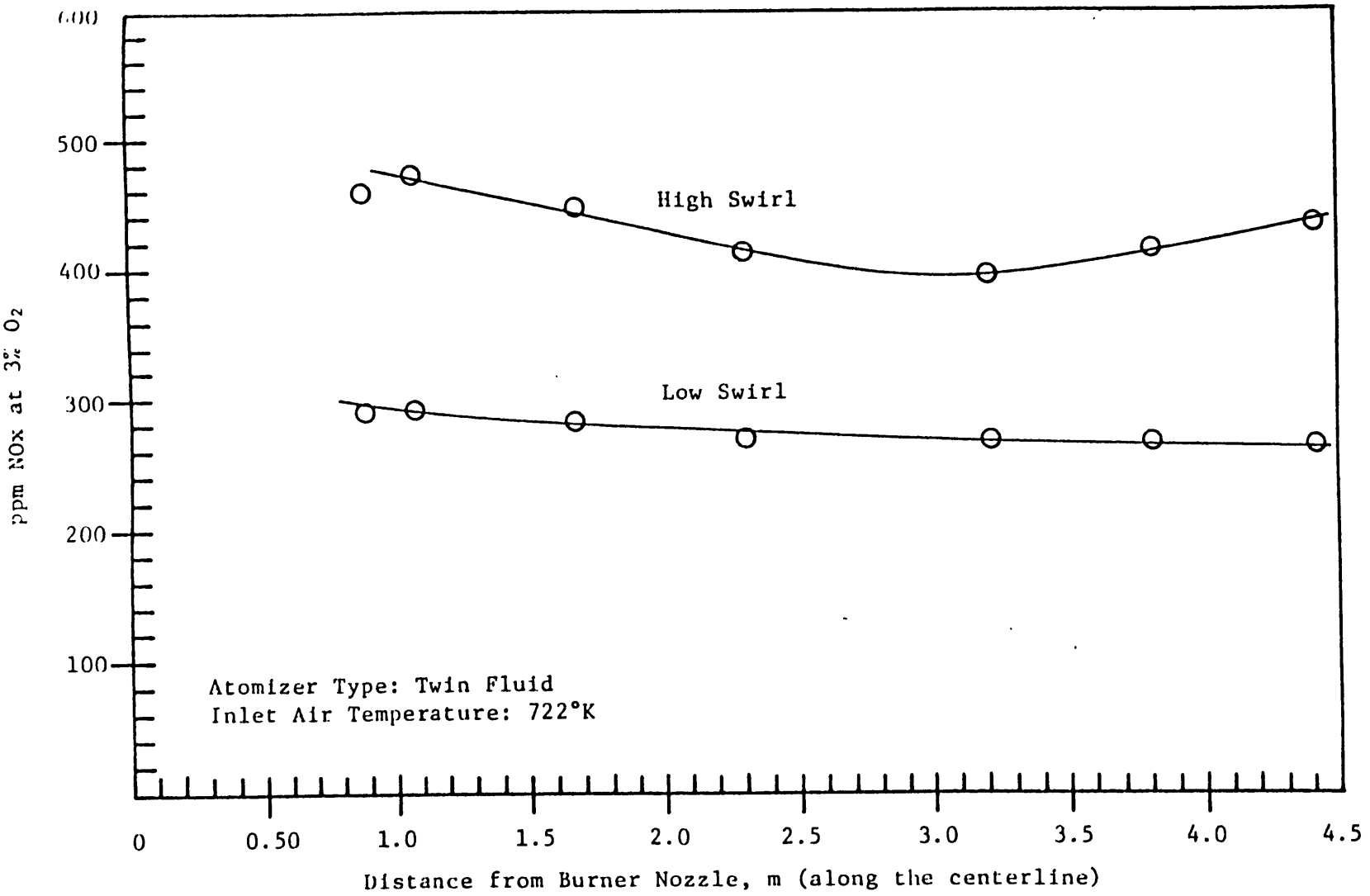

Figure 29 --Axial NOx concentration (ppm at 3% O_2) profiles, single stage baseline study.

A common feature of most of the profiles is that they remain essentially flat after 3-4 ft. from the burner. Visible flame lengths were typically 6-9 ft. These results indicate that NO_x formation is completed early in the flame. The slight upwards turn in some of the NO_x profiles near the burner nozzle, particularly at high swirl numbers, is probably due to increased formation of both thermal and fuel NO_x in this region. The increased formation of thermal and fuel NO_x near the burner nozzle in turn may be attributed to higher flame temperatures which occur in this region, and to the effects of swirl.

A close look at some of the NO_x profiles shown in Figures 26-29, especially at high swirl numbers, will show that in several instances there is a slight dip in the ppm NO_x at intermediate distances from the burner nozzle. This trend occurs too frequently to be dismissed as a random phenomenon due to experimental errors (see Figures 26, 28, and 29, high swirl), and most likely is attributable to the internal recirculation of gases within the flame. The recirculation of combustion gases, caused by an adverse pressure gradient produced in the flame at high swirl numbers, probably creates a reduction in oxygen concentration and temperature at intermediate distances from the burner nozzle. The reduction in oxygen concentration and temperature would result in a lowering of both thermal and fuel NO_x formation rates.

The dip in the axial NO_x profiles observed in the recirculation zone may reflect not simply a lowering of NO_x formation rates, but actually the destruction of NO_x in this region, perhaps due to nitrogenous species—hydrocarbon fragment interactions. Further experimentation is required in

the form of more detailed temperature and gas composition* mapping throughout the unstaged flames to provide a thorough and conclusive explanation for the dip in the NO_x profiles shown in Figures 26, 28 and 29.

Figure 30 illustrates the effect of burner nozzle type on the NO_x profiles from low swirl flames #2 and #6, using 500° F air preheat. The NO_x emission from the steam atomized jet flame is lower, 200 ppm compared to 250 ppm for the pressure jet case. Visual observation of these two flames indicated that the pressure jet flame was much shorter than the steam atomized flame.

The effect of air preheat on the NO_x profiles of a low swirl, pressure jet flame is shown in Figure 31. The overall effect of increased air preheat is to increase NO_x emission from 250 ppm at 500° F air preheat to 300 ppm at 850° F air preheat. The axial NO_x profiles are also somewhat different, the high air preheat flame exhibiting a flatter profile. This is attributed to a combination of the increased rates of the NO_x forming reactions due to increased flame temperature, and also the better mixing early in the flame due to the increased axial velocity of the combustion air at the high preheat temperature. Burner throat velocities increased from 23 m/sec at 500° F air preheat to 35 m/sec at 850°F.

Figure 32 is an example of O_2 and CO_2 concentration profiles obtained from the unstaged experiments. The sharp dip downwards in the CO_2 concentration profile near the burner nozzle is typical of all the data,

---

* It would be desirable to measure concentrations of cyanogens, ammonia species, and hydrocarbon fragments, in addition to nitrogen oxides, since these other species are involved in reactions which might destroy NO_x (see Chapter 2).

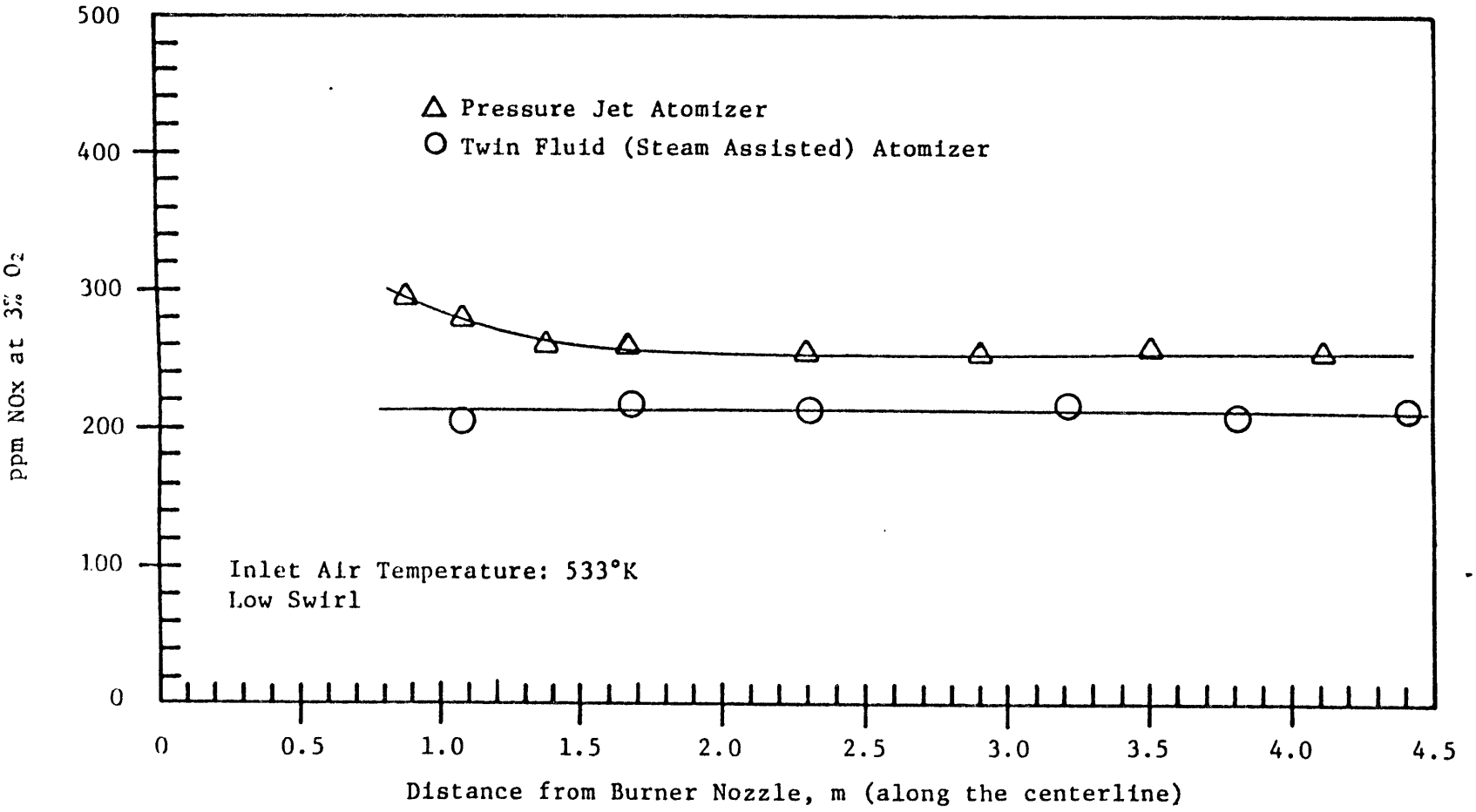

Figure 30 --An example of the effect of atomizer type on the NOx concentration (ppm at 3% O_2) profile in conventional unstaged combustion.

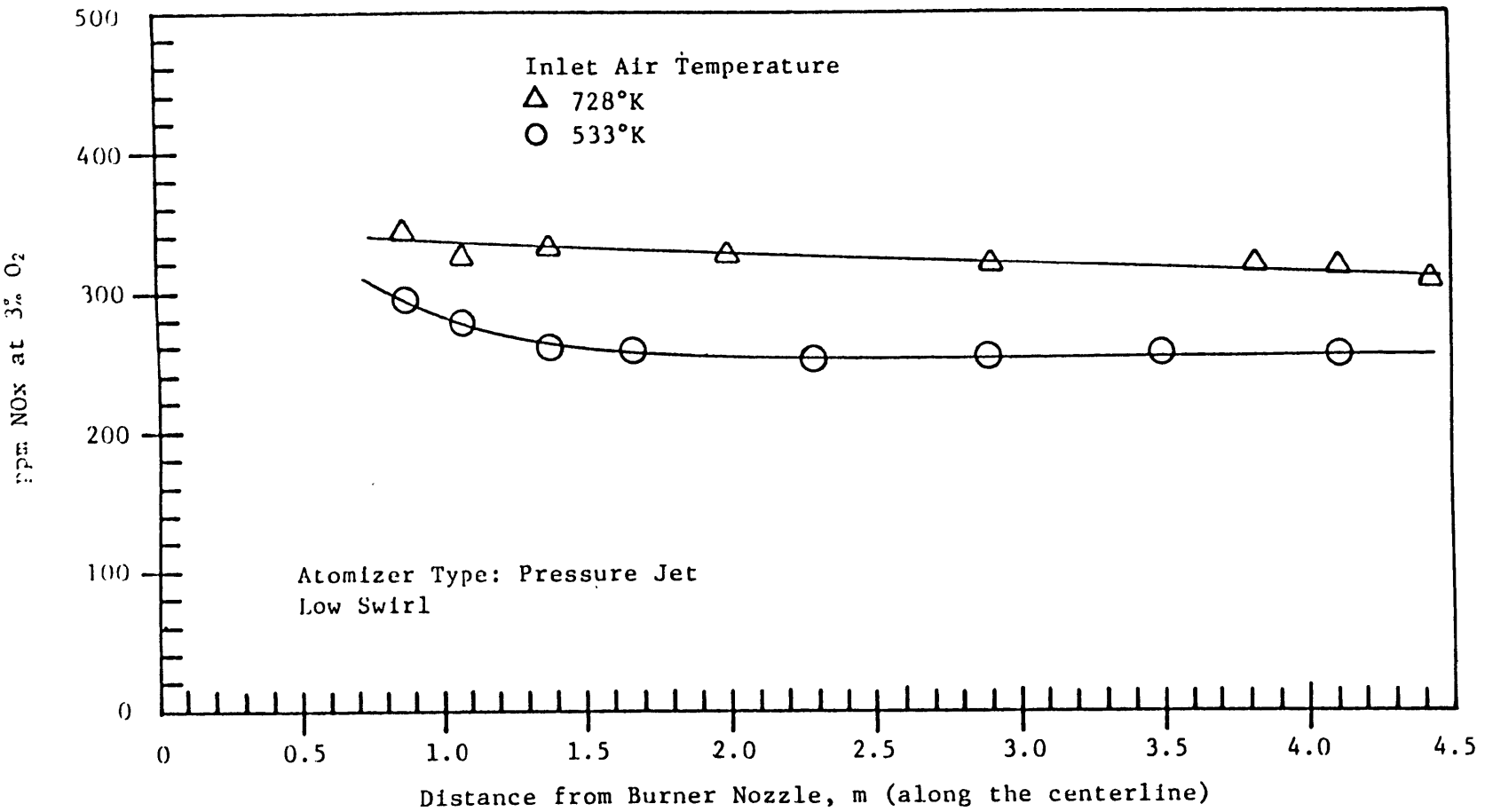

Figure 31 --An example of the effect of inlet combustion air temperature on the NOx concentration (ppm at 3% O_2) profile in conventional unstaged combustion.

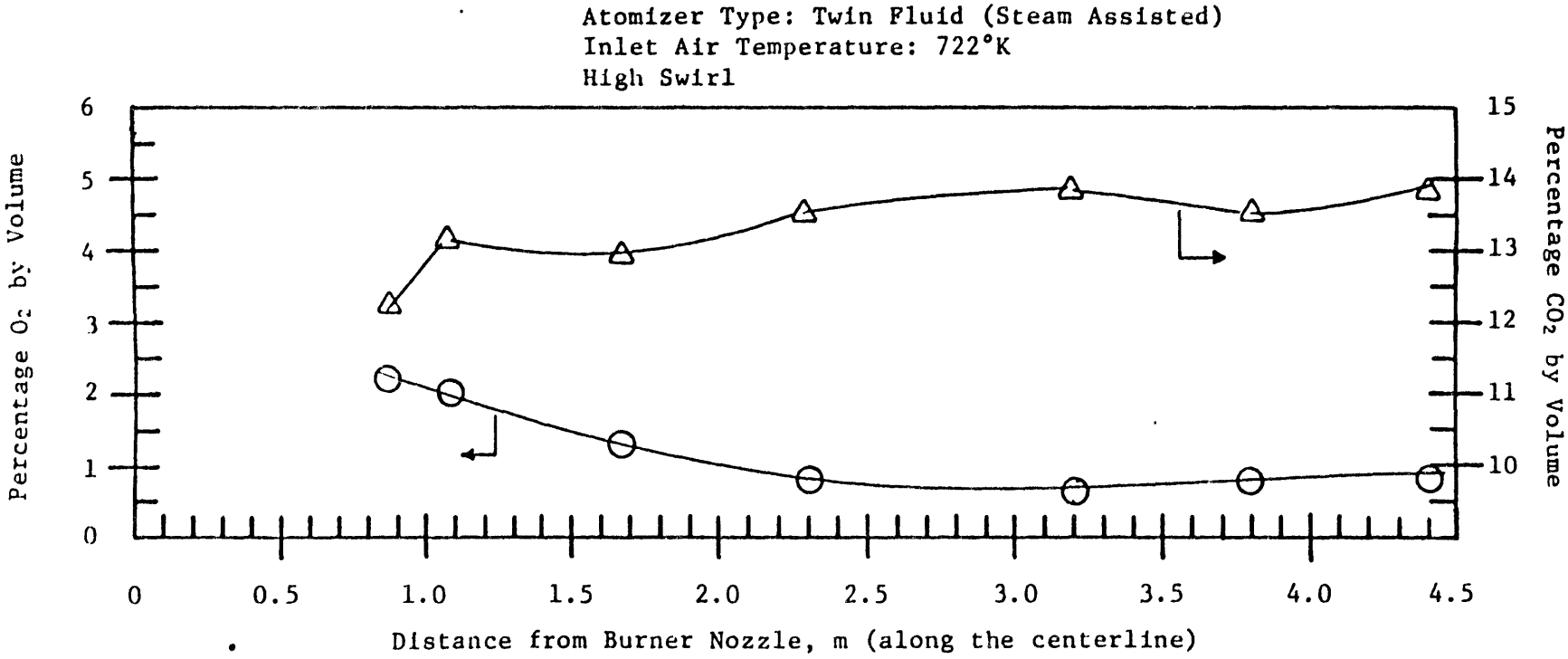

Figure 32 --Axial CO_2 and O_2 concentration profiles, single stage baseline study.

and is an indication of incomplete combustion of the fuel at this position in the combustion chamber. The slight increase in oxygen concentration in the direction towards the burner nozzle is believed to be due to imperfect mixing of air and fuel, and also to leakage of air into the furnace chamber through the viewing ports when the gas probe was inserted into the furnace. This problem, discovered at the beginning of the experimental studies, was remedied by closely monitoring the furnace chamber pressure and making sure it was maintained at a value slightly above that of atmospheric.

Axial temperature profiles are shown in Figures 33-36, again for the low and high swirl flames. Two general points concerning the temperature profiles might be made. First, it should be noted that the axial temperature profiles, especially at high swirl, do not display the absolute maximum temperatures of the flame. Temperatures along the centerline, near the burner nozzle, of flames at high swirl, are somewhat cooler than temperatures at a small distance to the side of the centerline, because of internal recirculation which tends to cool the central core. For this reason, direct comparison of the low swirl and high swirl temperature profiles may be somewhat misleading since it would appear that temperatures in the low swirl flames are higher. In actual fact peak temperatures in the high swirl flames are higher, but occur off the centerline and hence are not indicated by the axial profiles in Figures 33-36.

Secondly, observation of the unstaged flame temperature profiles at high swirl show that the profiles tend to flatten out at intermediate

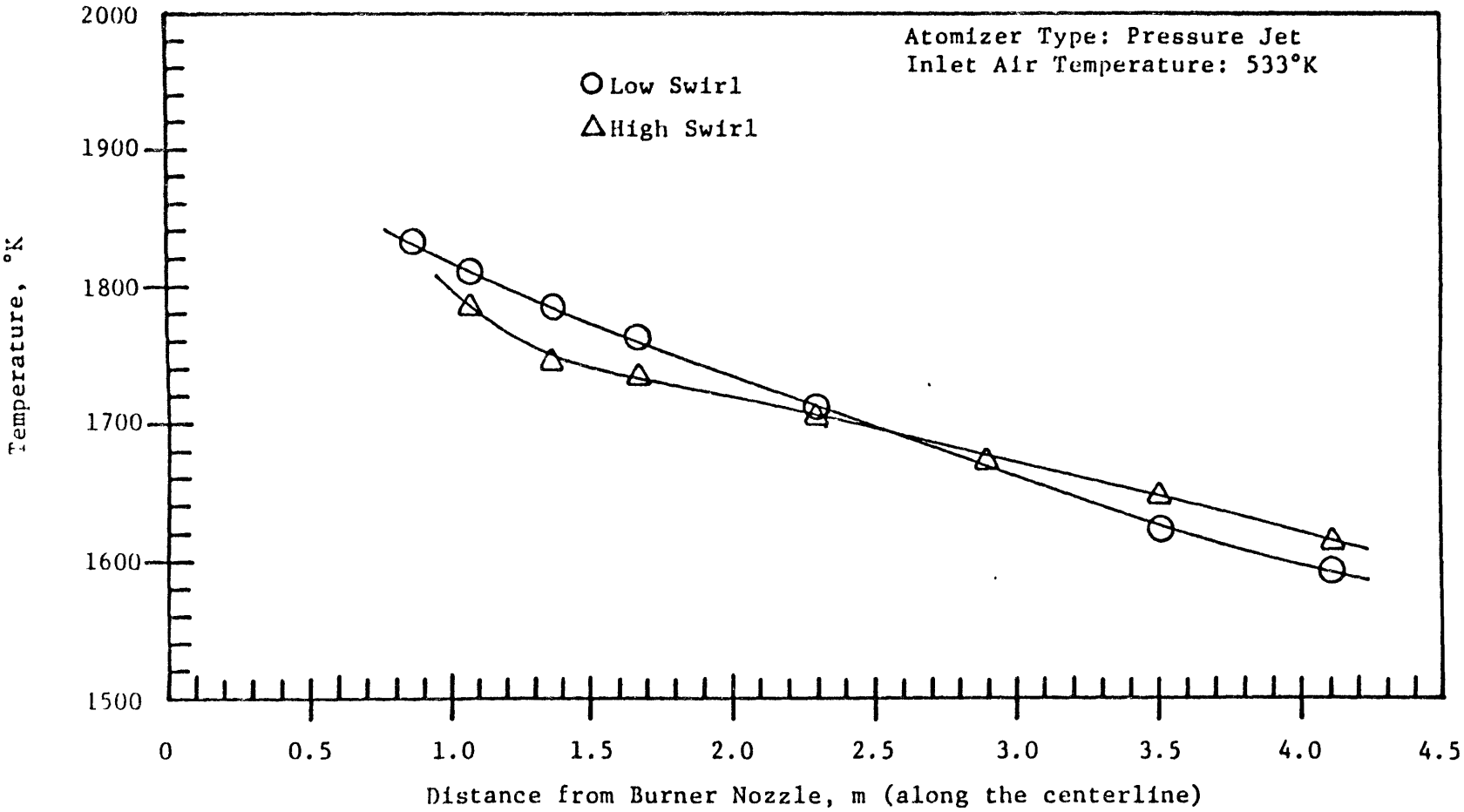

Figure 33 --Axial temperature profiles, single stage baseline study.

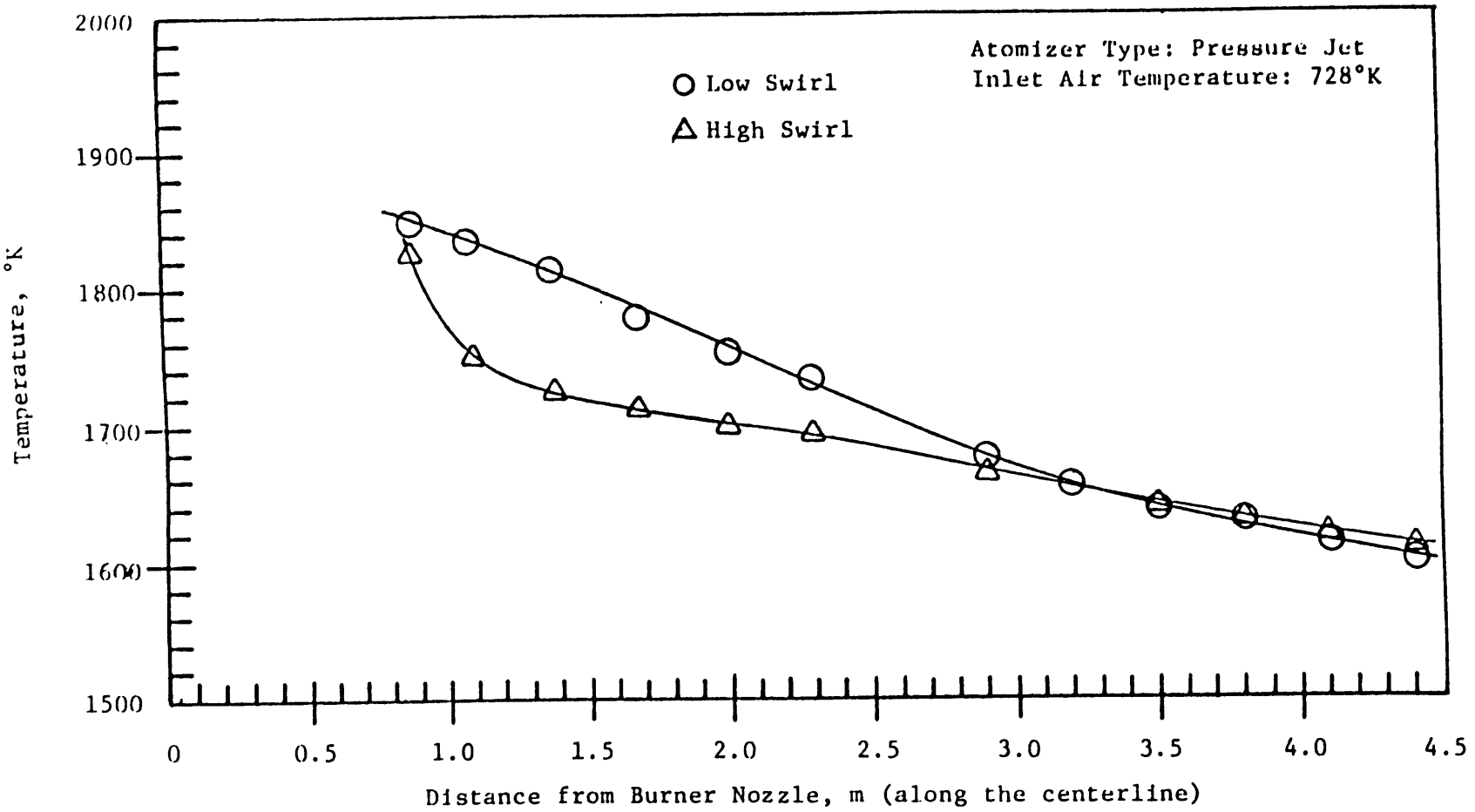

Figure 34 --Axial temperature profiles, single stage baseline study.

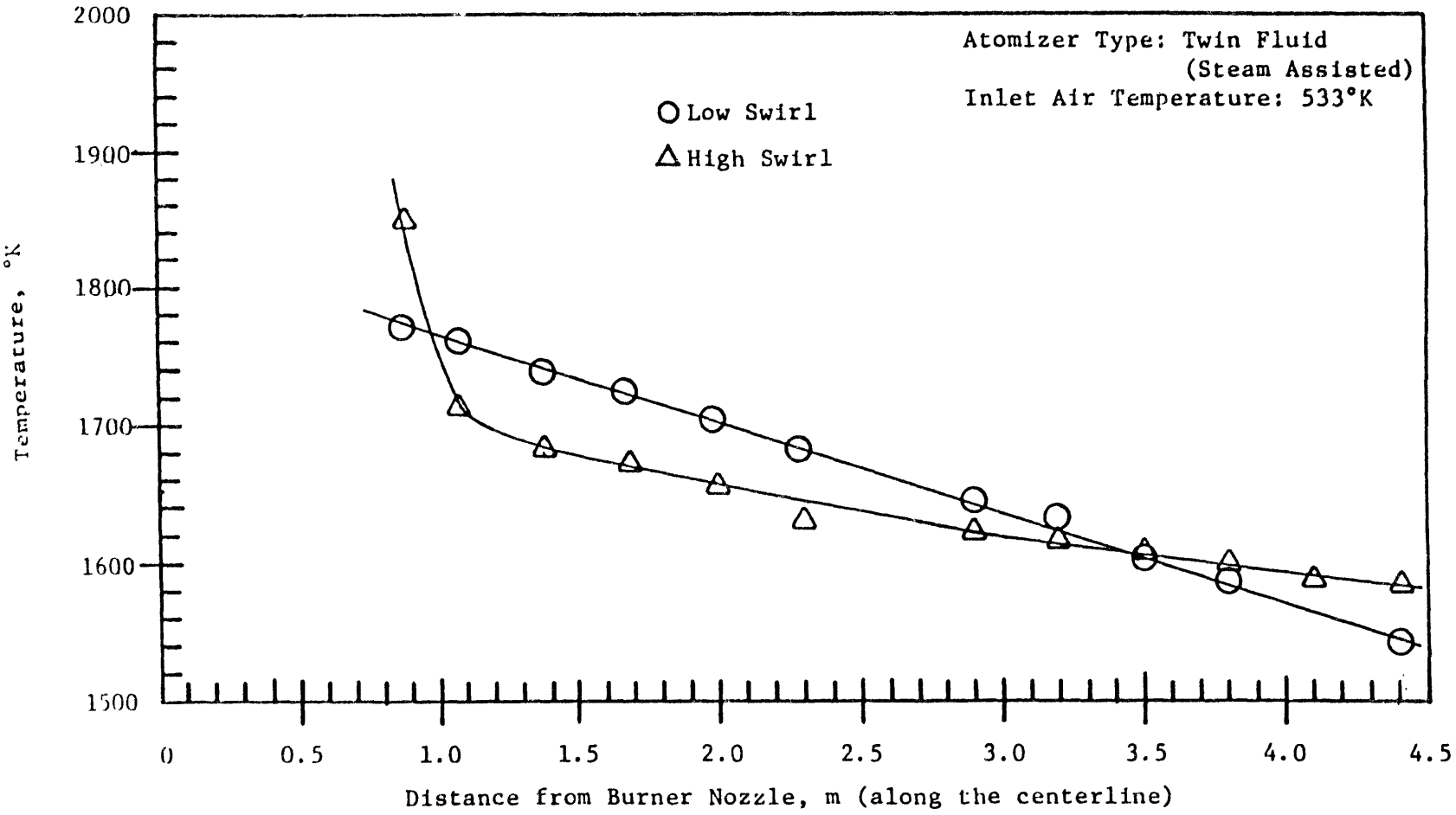

Figure 35 --Axial temperature profiles, single stage baseline study.

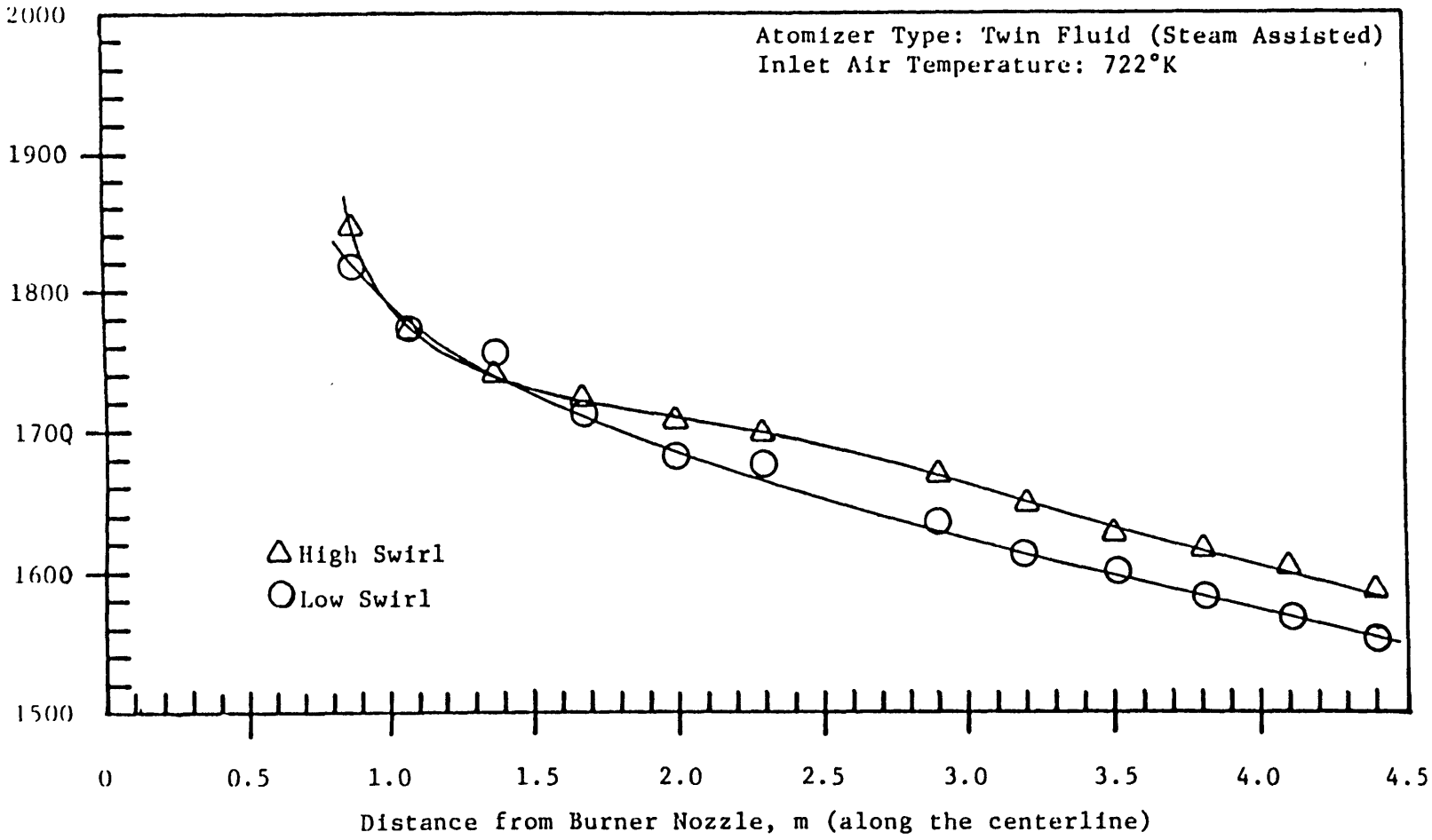

Figure 36 --Axial temperature profiles, single stage baseline study.

distances from the burner. This behavior, again, may probably be attributed to recirculation of gases at the high swirl condition.

3.1.2 Discussion

The general conclusion which was drawn from the study of these eight unstaged flames was that each of the variables chosen for investigation i.e., nozzle type, swirl number and air preheat level, did have an influence on the NO_x emission. However, when the average level of emission was evaluated separately for each of these three variables it was found that swirl number had the largest effect, followed by air preheat, with nozzle type having the least effect. Table 7 summarizes these general observations based on the averages of the measured NO_x emission. These data were obtained by separating the three parameters, swirl, air preheat and nozzle type, from the $2 \times 2 \times 2 = 8$ matrix of unstaged flame conditions. Hence, the average NO_x emission from, say, the low swirl flames, is obtained by averaging the measured emissions from flames #2, #4, #6, #8, which include changes in air preheat and nozzle type. Similarly, the average values of the measured NO_x emissions with nozzle type as the parameter include changes in swirl number and air preheat, etc.

This method of averaging identifies which of the parameters have the most significant influence on the NO_x emission for the range of variables investigated.

TABLE 7

SUMMARY OF INFLUENCE OF SWIRL NUMBER, AIR PREHEAT, AND BURNER NOZZLE TYPE ON NO_x EMISSIONS FROM UNSTAGED FLAMES

Parameter	Averaged NO_x emission, ppm @ 3% O_2 (Averaged from 4 flame conditions)		Difference in Average NO_x Emission
Swirl	Low Swirl (S = 0.4) 266 ppm	High Swirl (S = 2.7) 436 ppm	170 ppm
Air Preheat	Low Preheat (500° F) 308 ppm	High Preheat (850° F) 394 ppm	88 ppm
Burner Nozzle	Pressure Jet 365 ppm	Steam Atomized 337 ppm	28 ppm

3.2 Staged Combustion Studies

A schematic arrangement of the MIT Combustion Research Faciltiy set up for staged combustion experiments is shown in Figure 37. The second stage air was admitted perpendicular to the furnace axis through two sets of simple 1-inch nozzles arranged directly opposite each other through the furnace sidewalls, as shown in Figures 38 and 39. Operating conditions were maintained similar to those employed in the unstaged flame tests listed earlier, with the exception of two flames run at increased throughput to study the effect of residence time on NO_x emissions.

The injection air velocity is dependent upon both the primary stage fuel equivalence ratio ϕ_b and the value of the air preheat temperature for a fixed firing rate and overall equivalence ratio ϕ_o. However, the range

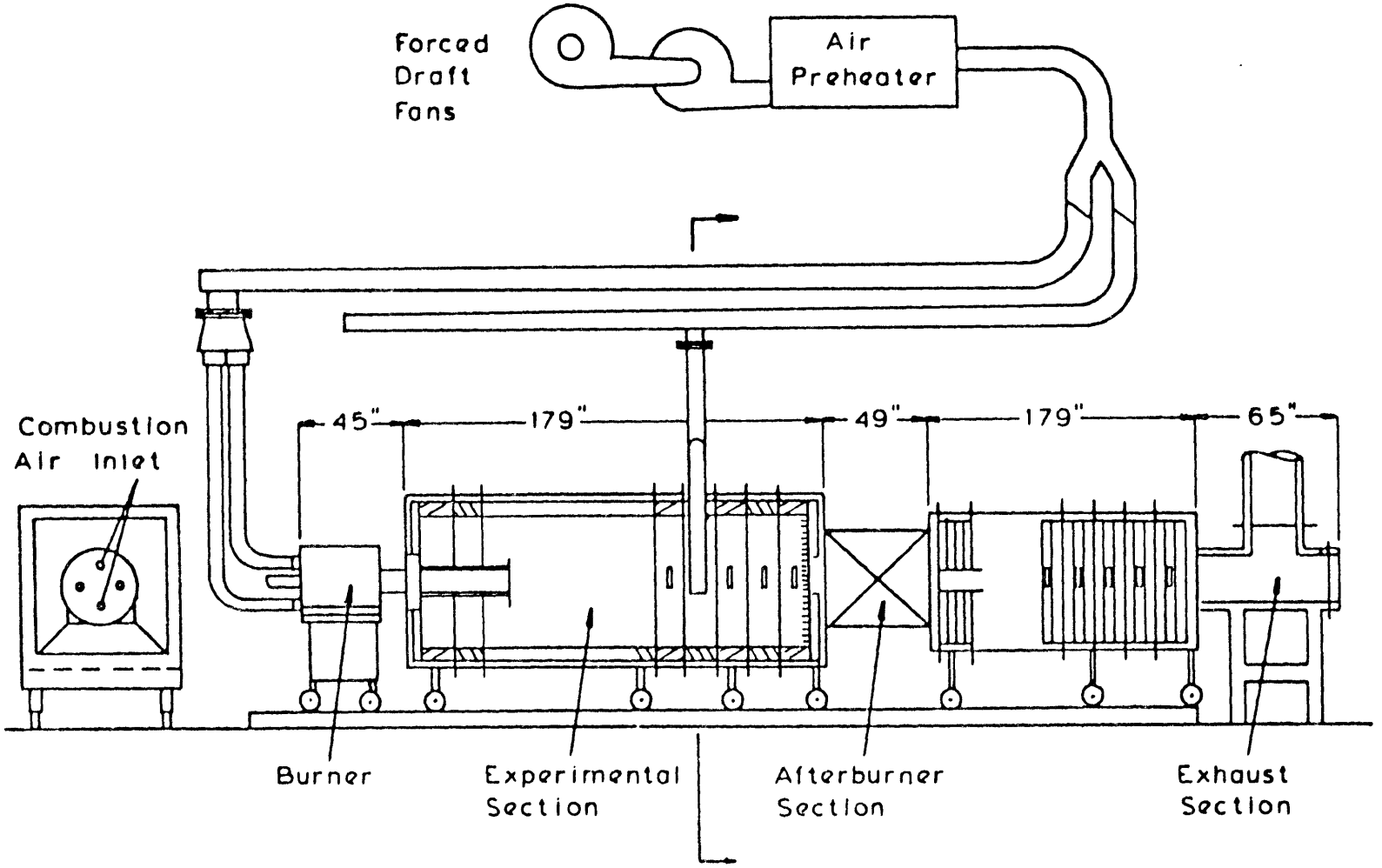

Figure 37 --Furnace assembly and air staging system.

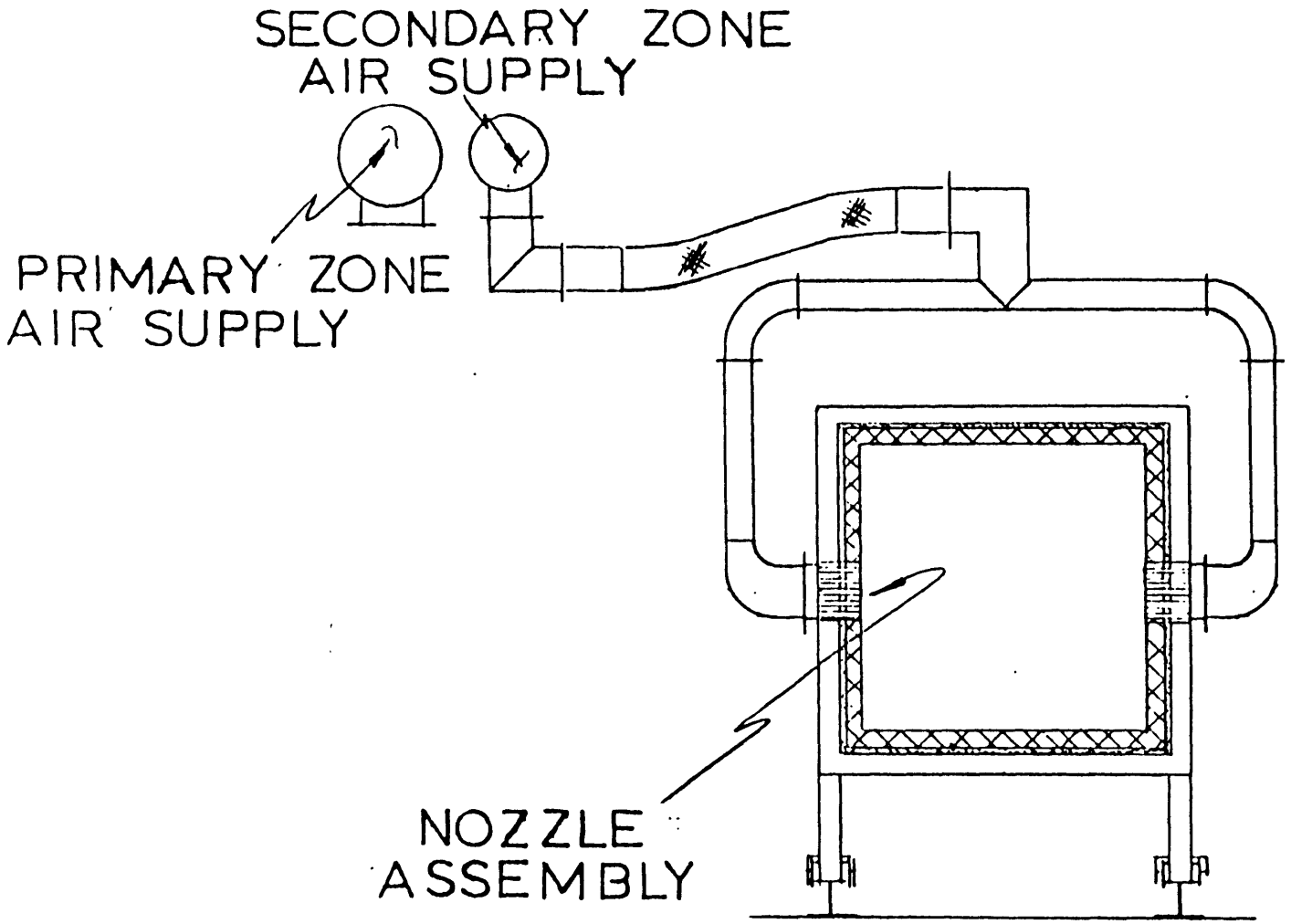

Figure 38 --Cross-section of the secondary air injection system.

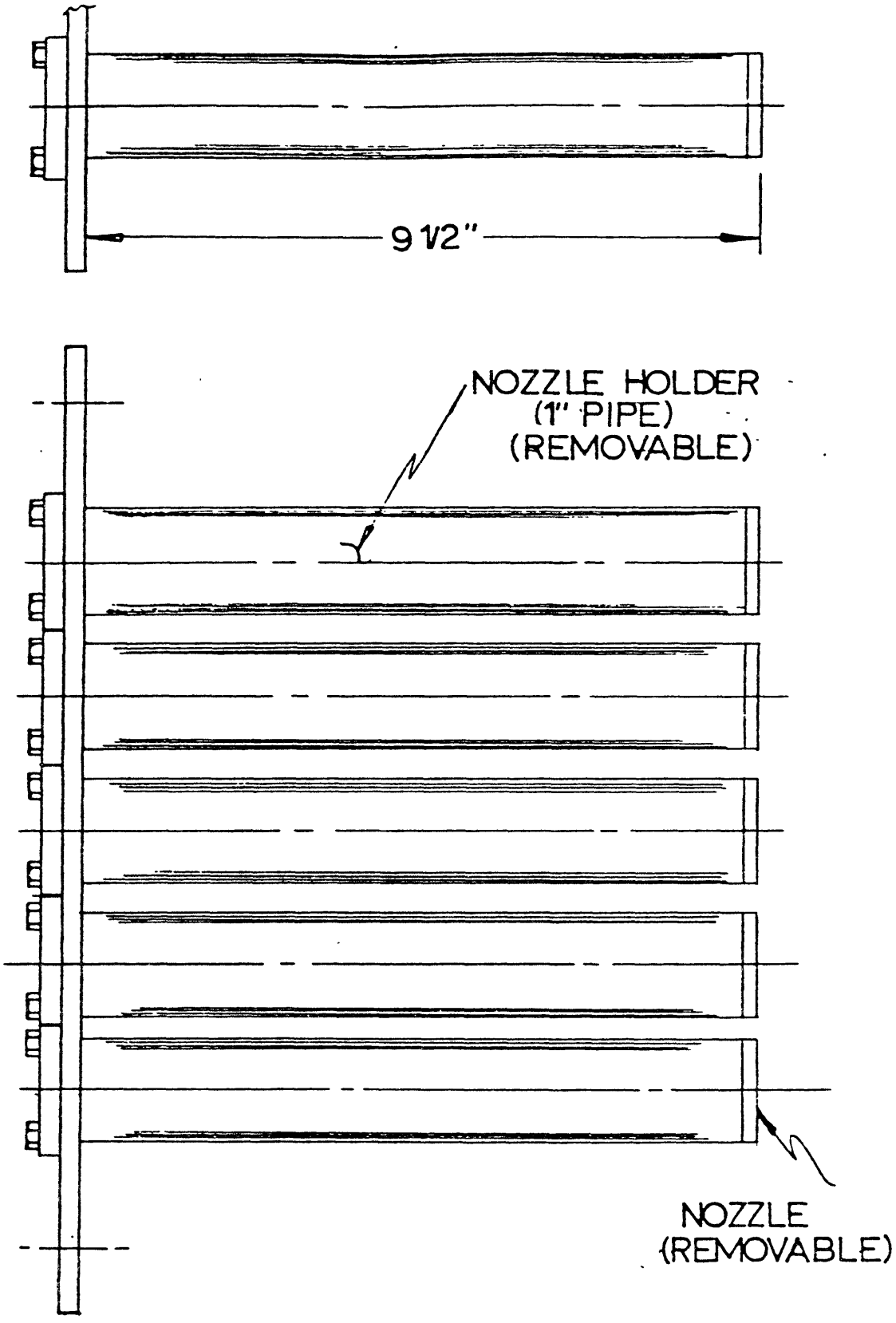

Figure 39 --

NOZZLE ASSEMBLY

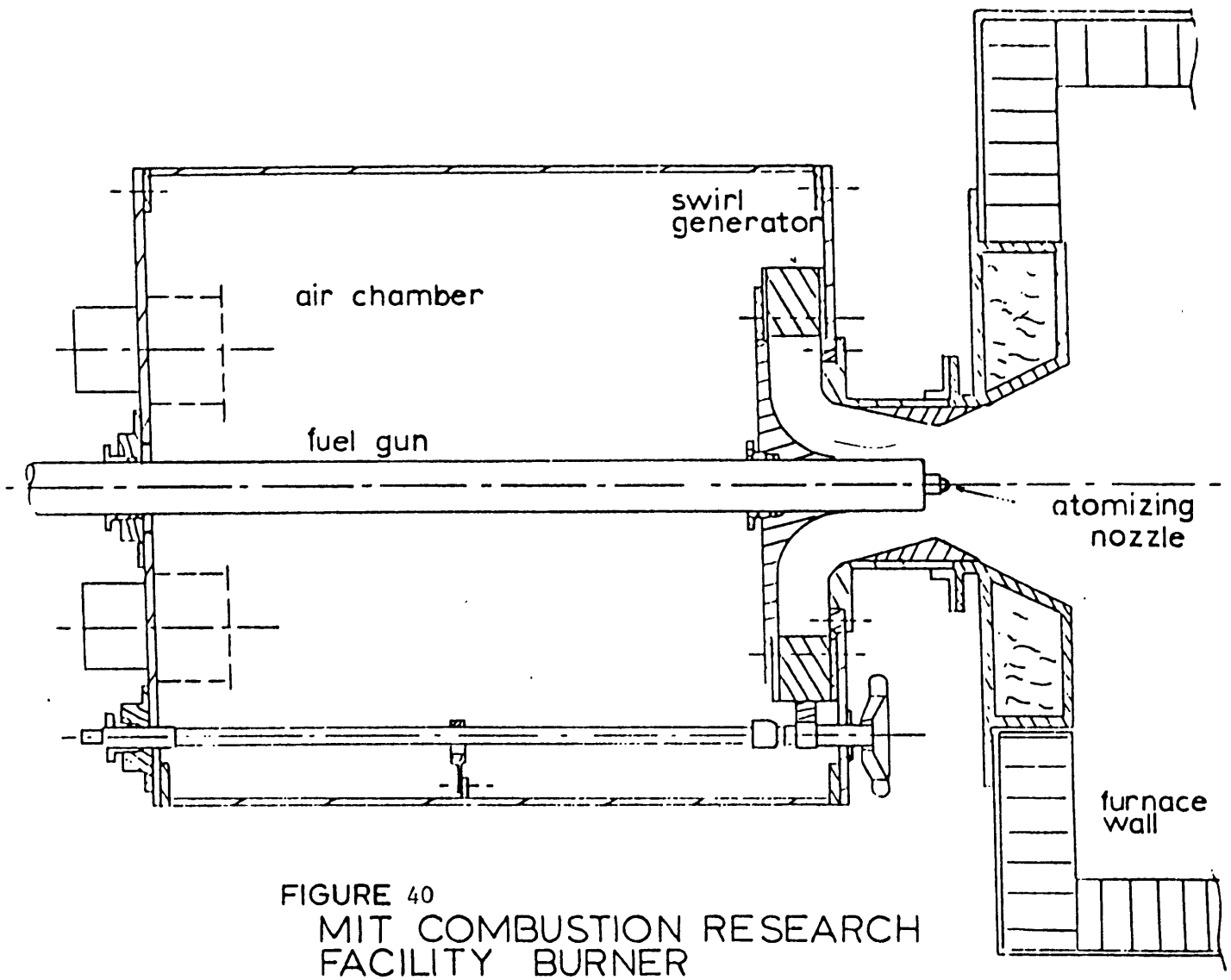

FIGURE 40
MIT COMBUSTION RESEARCH
FACILITY BURNER

of secondary stage injection air velocities was 20-200 m/sec which is one to two orders of magnitude greater than the mean axial velocity within the furnace for the range of staging conditions investigated. These design conditions were chosen to ensure adequate mixing of the primary zone exhaust gases with secondary zone injection air.

Throughout all of the staged combustion experiments the location of the secondary zone air injection was maintained constant at 8.5 ft from the exit plane of the burner.

In order to maintain flame stability and fuel/air mixing patterns in the early stages of the primary zone it was necessary to maintain burner throat air velocities within the range 20-40 m/sec throughout the staged combustion experiments. This was achieved by the insertion of a convergent-divergent nozzle in the burner throat, as shown in Figure 40.

The objective of this series of staged combustion experiments was to investigate the influence of primary stage or burner fuel equivalence ratio ϕ_b, atomizer type, air preheat, swirl number, and residence time on NO_x emissions. In addition, it was decided to obtain axial profiles of NO_x, CO_2, O_2, CO and temperature together with overall solids emission for selected flames. These data greatly assist in the interpretation and understanding of the NO_x formation and destruction processes occurring in staged combustion systems, and help provide a more detailed understanding of the flame processes than the simple input-output type of study.

The approach taken was to obtain axial flame profiles for the minimum and maximum staging conditions i.e., $\phi_b = 1.08$ and $\phi_b = 1.9$ respectively with $\phi_{overall} = 0.95$ (5% XS air). In addition single point measurements of

NO_x, CO_2, O_2, CO and temperature were made on the furnace axis at four intermediate staging conditions. Flue gas composition was monitored continuously for all staging conditions. A total of 32 flames have been investigated to determine the effects of the staging conditions i.e., ϕ_b, atomizer type, air preheat, swirl number, and residence time on overall NO_x emission and flame characteristics. Table 8 lists the values of the input parameters used in these studies.

A typical set of data obtained from a staged combustion test is presented in Figures 41-43, in which the measured axial profiles of temperature, NO_x, CO_2, O_2, CO are shown. These data were obtained using the pressure jet nozzle with air preheat temperature at 500° F and a burner swirl number of 0.4.

Figure 41 shows the axial temperature distribution for both the minimum and maximum staging conditions, i.e., overall fuel equivalence ratio $\phi_o = 0.95$, and burner equivalence ratios of ϕ_b of 1.15 and 2.05 respectively. The minimum staging condition exhibits an axial temperature profile which decreases steadily from a maximum close to the burner in a similar manner to the unstaged profiles shown in Figure 33, both the peak flame temperature and the flue gas temperature are lower at the minimum staging conditions than in the single stage flame by approximately 100° C. There is, however, a significant difference in the region of interaction of the secondary zone air jets, with a pronounced 'dip' in the temperature profile of the minimally staged flame. The maximum staging condition ($\phi_b = 2.05$, $\phi_o = 0.95$) exhibits a considerably different temperature profile, with a characteristic M-shape. The peak flame temperature in the primary

TABLE 8

A LIST OF THE FLAMES ALONG WITH VALUES OF THEIR RESPECTIVE INPUT VARIABLES THAT COMPRISE THE TWO-STAGE STUDY

Flame Number	CRF Run Number and Date		Atomizer Type	Air Temperature °K	Air Temperature °F	Swirl Number	Burner Fuel Equivalence Ratio
9	25a	8/8/79	pressure jet	533	500	0.53	1.15
10	25b	8/8/79	pressure jet	533	500	0.53	2.05
11	26a	8/9/79	pressure jet	533	500	0.53	1.18
12	26b	8/9/79	pressure jet	544	520	0.53	1.27
13	26c	8/9/79	pressure jet	544	520	0.53	1.47
14	26d	8/9/79	pressure jet	544	520	0.53	1.75
15	26e	8/9/79	pressure jet	544	520	0.53	1.88
16	26f	8/9/79	pressure jet	544	520	0.65	1.49
17	26g	8/9/79	pressure jet	544	520	1.17	1.51
18	26h	8/9/79	pressure jet	544	520	1.78	1.49
19	26i	8/9/79	pressure jet	544	520	2.7	1.45
20	27a	8/15/79	pressure jet	731	855	0.53	1.06
21	27b	8/15/79	pressure jet	750	890	0.53	1.31
22	27c	8/15/79	pressure jet	742	875	0.53	1.41
23	27d	8/15/79	pressure jet	742	875	0.53	1.75
24	27e	8/15/79	pressure jet	731	855	0.53	1.97

TABLE 8 : Continued

Flame Number	CRF Run Number and Date		Atomizer Type	Air Temperature °K	Air Temperature °F	Swirl Number	Burner Fuel Equivalence Ratio
25	18a	6/25/79	twin fluid	531	495	0.53	1.17
26	18b	6/25/79	twin fluid	531	495	2.7	1.17
27	18c	6/25/79	twin fluid	531	495	0.53	2.01
28	19a	6/26/79	twin fluid	744	880	0.53	1.12
29	19b	6/26/79	twin fluid	744	880	2.7	1.12
30	19c	6/26/79	twin fluid	744	880	0.53	1.70
31	31a	8/22/79	twin fluid	529	493	0.53	1.18
32	31b	8/22/79	twin fluid	531	495	2.7	1.19
33	31c	8/22/79	twin fluid	529	493	0.53	1.26
34	31d	8/22/79	twin fluid	531	495	0.53	1.42
35	31e	8/22/79	twin fluid	528	490	0.53	1.69
36	31f	8/22/79	twin fluid	529	493	0.53	1.77
37	31g	8/22/79	twin fluid	528	490	2.7	2.02
38	37a	10/15/79	twin fluid	300	80	0.53	1.48
39	37b	10/15/79	twin fluid	533	500	0.53	0.97
40	37c	10/15/79	twin fluid	533	500	0.53	1.29

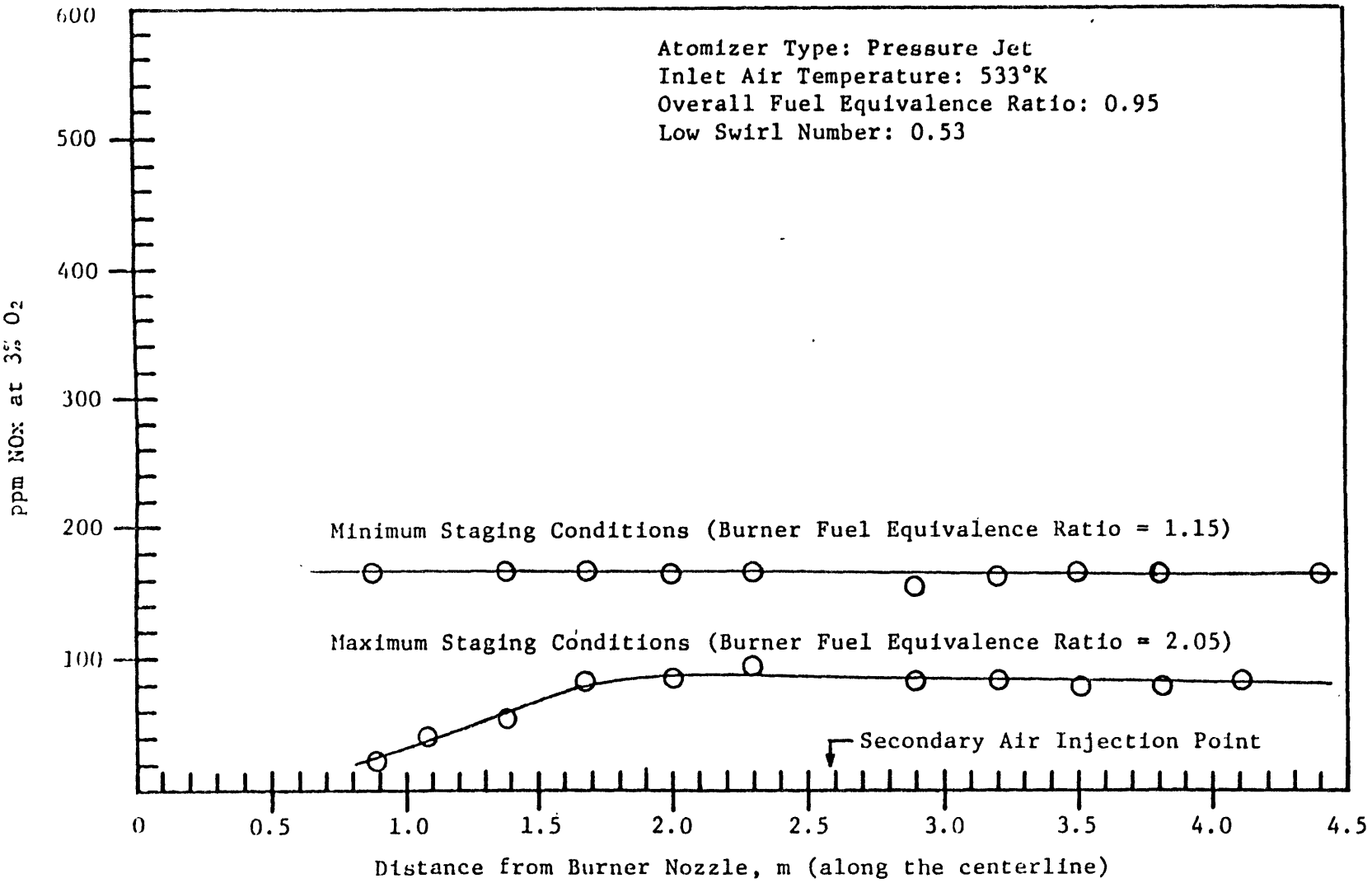

Figure 41 --Axial NOx concentration (ppm at 3% O_2) profiles, staged combustion study.

zone is seen to be shifted downstream from the burner exit nozzle. The measured peak temperature on the furnace axis at both the minimum and maximum staging condition is surprisingly close, $\sim 1450^{\circ}$ C. It is felt however, that this value is not indicative of peak flame temperatures which are known to occur off-axis in the earlier part of the flames.

The pronounced M-shaped axial temperature distribution also shows quite clearly that some back-mixing of injected secondary zone air is occurring, thus reducing the effective length of the primary zone. This back-mixing is thought to be due to the aerodynamics of the horizontally opposed high-momentum secondary zone air jets which create a local stagnation point at the position of impingement resulting in a reverse flow of air in this region. The maximum staging condition produces very high jet momentum levels in the secondary zone air injection jets, and the extent of back-mixing is greatest under these conditions.

The pronounced increase in temperature in the secondary zone under maximum staging conditions is to be expected since the heat release rate from the unburnt fuel carried over from the primary zone is well in excess of the local rate of heat loss. The final exhaust gas temperature from the secondary zone at maximum staging is seen to be higher by $\sim 200^{\circ}$ C than under minimum staging conditions.

Figure 42 shows the corresponding NO_x profiles at minimum and maximum staging conditions obtained with the pressure jet nozzle, low air preheat and low swirl number. The flat NO_x profile obtained at minimum staging indicates that most of the NO_x, both thermal-NO_x and fuel-NO_x, is formed very early in the flame. Furthermore, there is a negligible change in

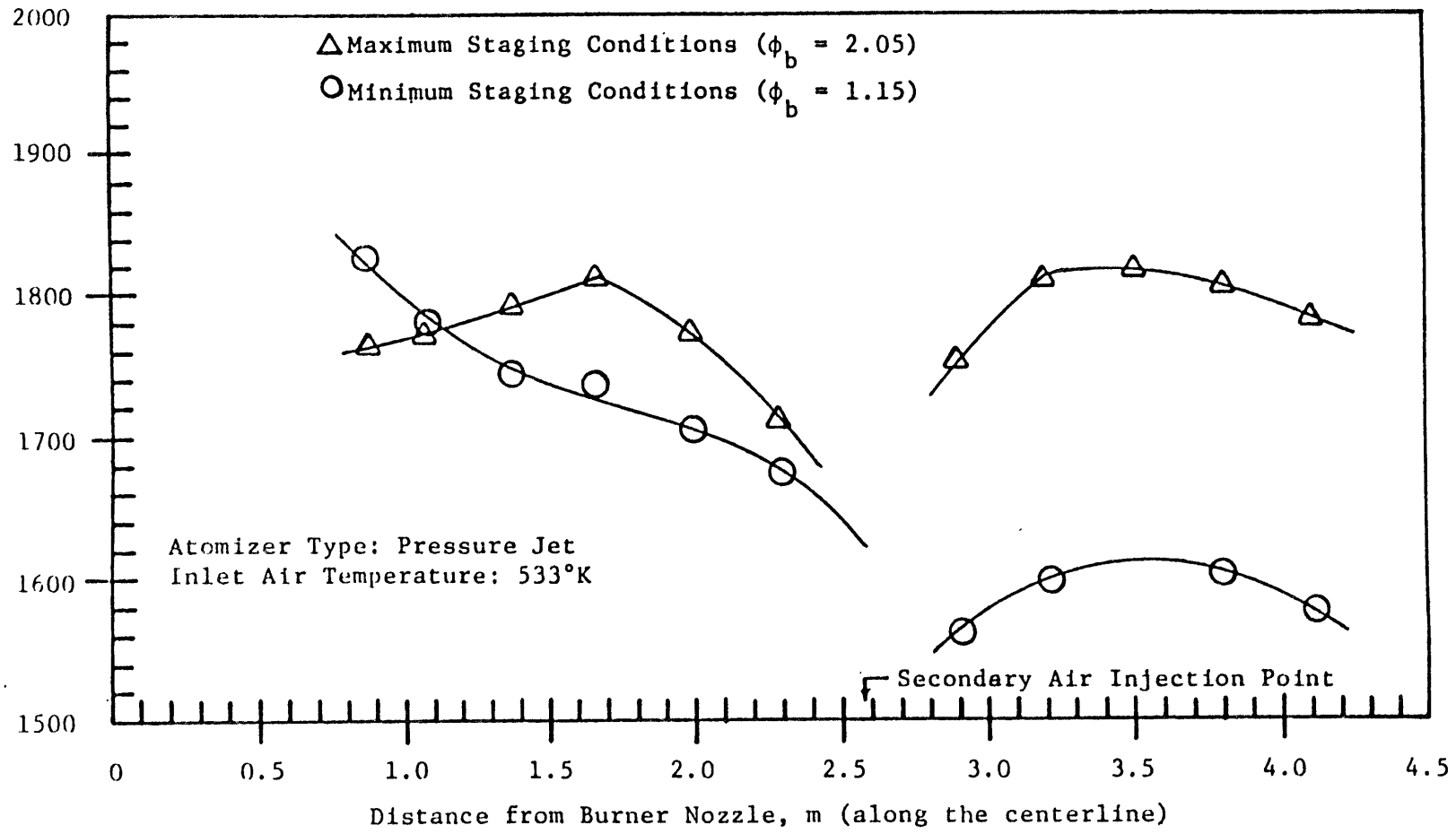

Figure 42 --Axial temperature profiles, staged combustion study.

NO_x concentration after injection of the small amount of secondary zone air, indicating that no further thermal-NO_x is produced in the locally oxidizing atmosphere. This observation is entirely consistent with the very slight temperature increase seen in Figure 41, in the secondary zone air injection region.

The axial NO_x profile obtained under maximum staging conditions exhibits an increase in NO_x level along the flame in the primary zone. The peak NO_x level in this region is seen to coincide with the position of the peak axial temperature and it is not clear what the relative contributions of thermal-NO_x and fuel-NO_x are in this region. However, there is a significant reduction in NO_x level ($\sim$40%) at the end of the primary zone compared to the minimum staging condition. This reduction is very likely due to the reduced conversion of fuel-N to NO_x in the fuel-rich primary zone. The observation that the NO_x level does not increase after the injection of secondary zone air confirms that all of the available fuel-N has been transformed in the primary zone and in addition that local flame temperatures in the secondary zone do not exceed the critical level ($\sim$1800 K) for thermal NO_x formation. The reduction in NO_x emission of $\sim$40% at maximum staging conditions is considered to be significant and confirms the general trends indicated by the computer studies of both the equilibrium and kinetics of the NO_x formation reactions.

Figure 43 shows the corresponding axial profiles of O_2 and CO_2, which can be seen to be consistent with the overall stoichiometry of the minimum and maximum staging conditions. Of particular interest is the shift towards the burner of the peak O_2 level under maximum staging conditions

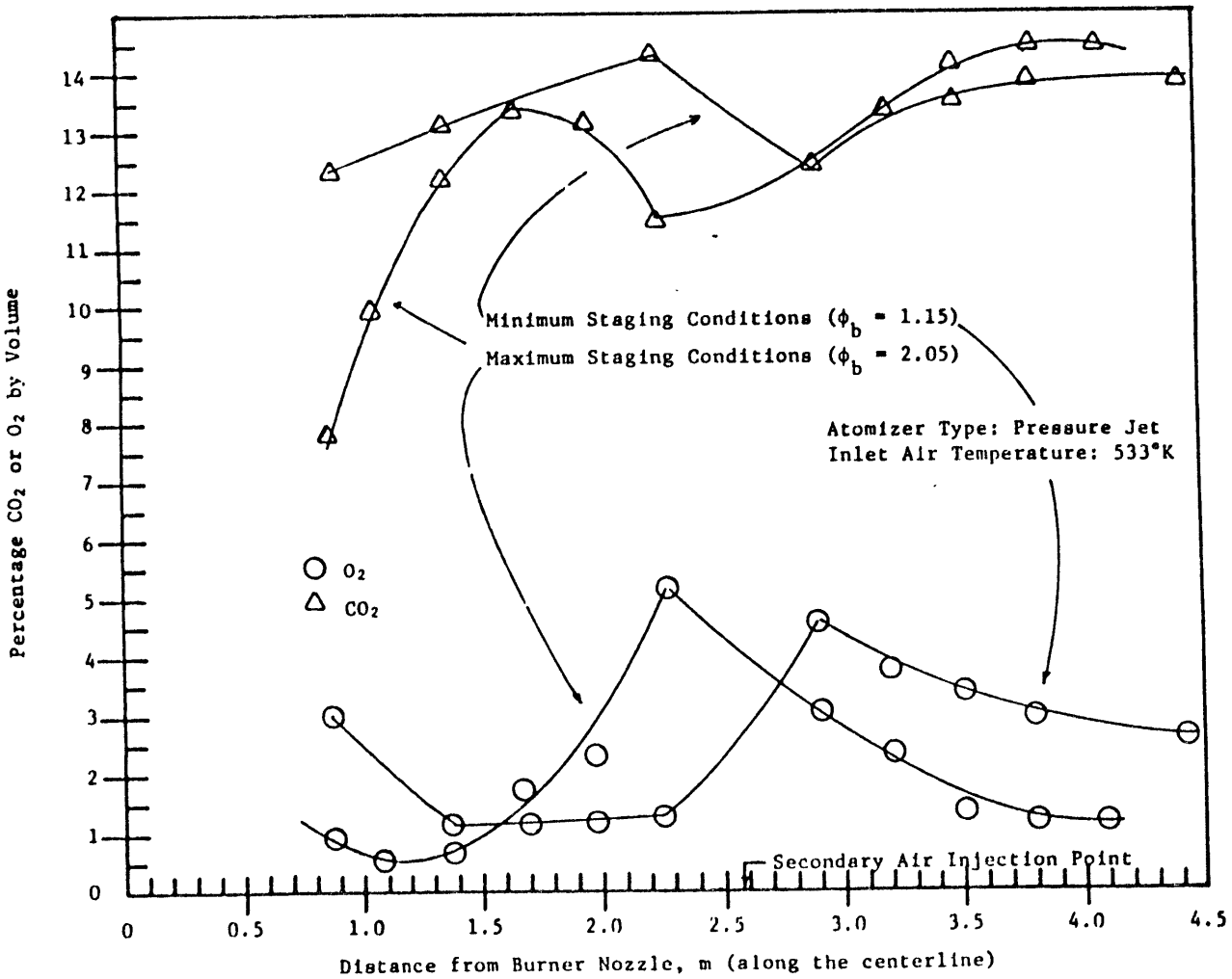

Figure 43 --Axial CO_2 and O_2 concentration profiles, staged combustion study.

as compared to minimum staging. This again confirms the conclusions drawn from the observed temperature profiles, that considerable back-mixing of secondary zone air is occurring at maximum staging conditions.

The effect of swirl number on the NO_x emissions from a staged flame obtained with a pressure jet nozzle and 500° F air preheat is shown in Figure 44. The staging conditions i.e., $\phi_o = 0.95$ and $\phi_b = 1.46$, were maintained constant and the swirl number varied by use of the variable swirl generator. Figure 44 shows that under these staging conditions, swirl number did not have a significant effect on NO_x emission. Only a slight decrease in NO_x ($\sim 10\%$) is observed for changes in swirl number from 0.4 to 2.7.

The influence of fuel atomizer type on the axial NO_x profile of a staged flame is shown in Figure 45. These profiles were obtained at under almost identical staging conditions. The pressure jet flame had $\phi_o = 0.95$ and $\phi_b = 2.05$ and the steam atomized flame had $\phi_o = 0.91$ and $\phi_b = 1.77$. The swirl number was 0.4 and the air preheat 500° F in both cases.

The measured NO_x emission from both of these flames does not differ significantly, being ~ 90 ppm in both cases. However, the axial NO_x profiles show a slight difference in shape, with the steam atomized flame exhibiting a slightly higher peak NO_x concentration at the exit of the primary zone. The flatter profile from the pressure jet flame indicates that atomization, mixing and subsequent fuel-N conversion is more complete than in the steam atomized flame. This is consistent with the higher momentum of the latter type flame which would tend to carry more unreacted fuel-N into the air-rich secondary stage. Figure 46 shows the effect of

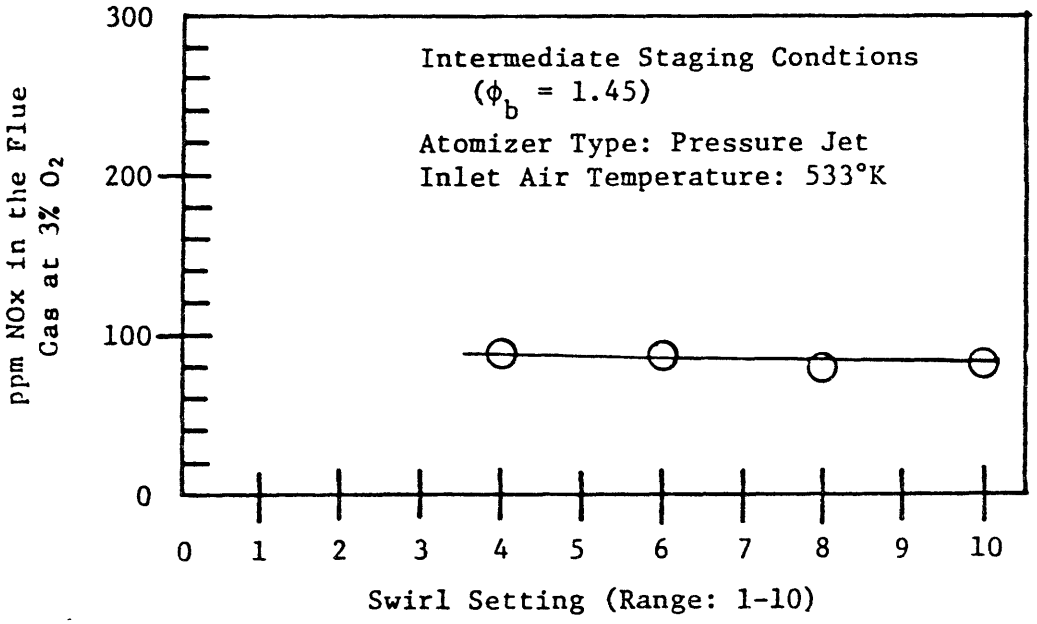

Figure 44 --An example of the effect of swirl on the flue gas NOx concentration during staged combustion.

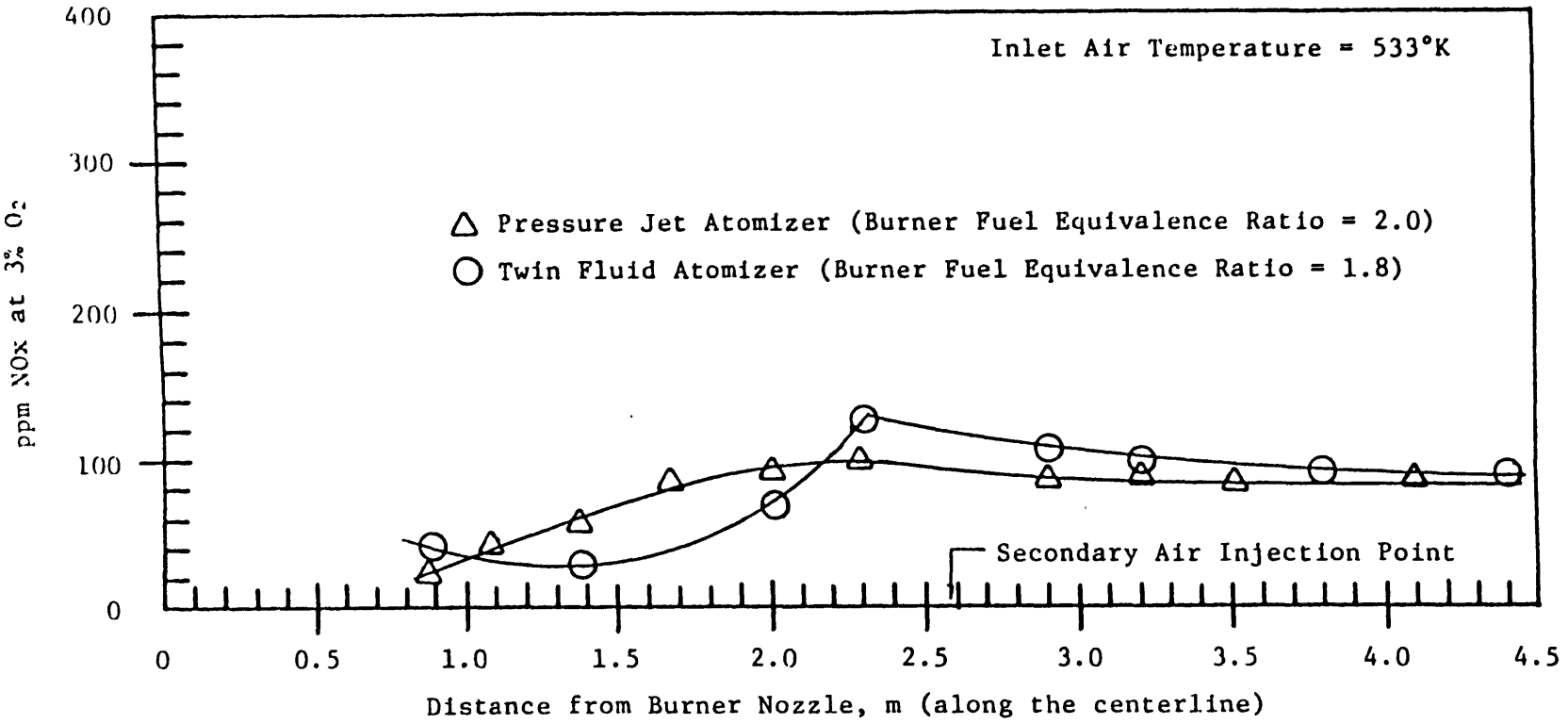

Figure 45 --An example of the effect of atomizer type on the NOx concentration profile (ppm at 3% O_2) during staged combustion.

air preheat on NO_x profiles of staged flames. Again the staging conditions were maintained almost identical for two pressure jet flames with a swirl number of 0.4. The high air preheat (800° F) flame had $\phi_o = 0.95$ and $\phi_b = 1.06$ and the low air preheat flame had $\phi_o = 0.95$ with $\phi_b = 1.15$. There is a slight increase in NO_x emission at the higher level of air preheat i.e., 175 ppm to 160 ppm. It is interesting to note that NO_x levels in the primary zone tend to be slightly lower in the high air preheat flame. This observation is consistent with the expected influence of temperature on the rates of reaction of the fuel-N conversion reaction in a fuel-rich first stage.

The significant effect of staging on NO_x emissions from the high-N fuel oil flames obtained with a pressure jet atomizer, 500° F air preheat and swirl number of 0.4 is illustrated in Figure 47. The axial NO_x profiles of single and two-stage flames are compared in Figure 47 which clearly shows that the highest NO_x emissions ($\sim$ 375 ppm) occurred with a high swirl number single-stage flame (i.e., short high intensity flame). The lowest NO_x emissions ($\sim$ 85 ppm) were obtained with a two-stage flame at maximum staging conditions ($\phi_o = 0.95$, $\phi_b = 2.05$). A four-fold reduction in NO_x emissions was obtained by staging the combustion process.

The influence of primary zone stoichiometry (ϕ_b) on NO_x emissions is shown in Figure 48. These data were obtained by adjusting the primary zone stoichiometry while maintaining the overall stoichiometry constant, using pressure jet atomization, a swirl number of 0.4 and air preheat of 500° F.

The strong effect of staging is again clearly shown. The NO_x emissions decrease steeply with increasing (ϕ_b) in the range of ϕ_b from

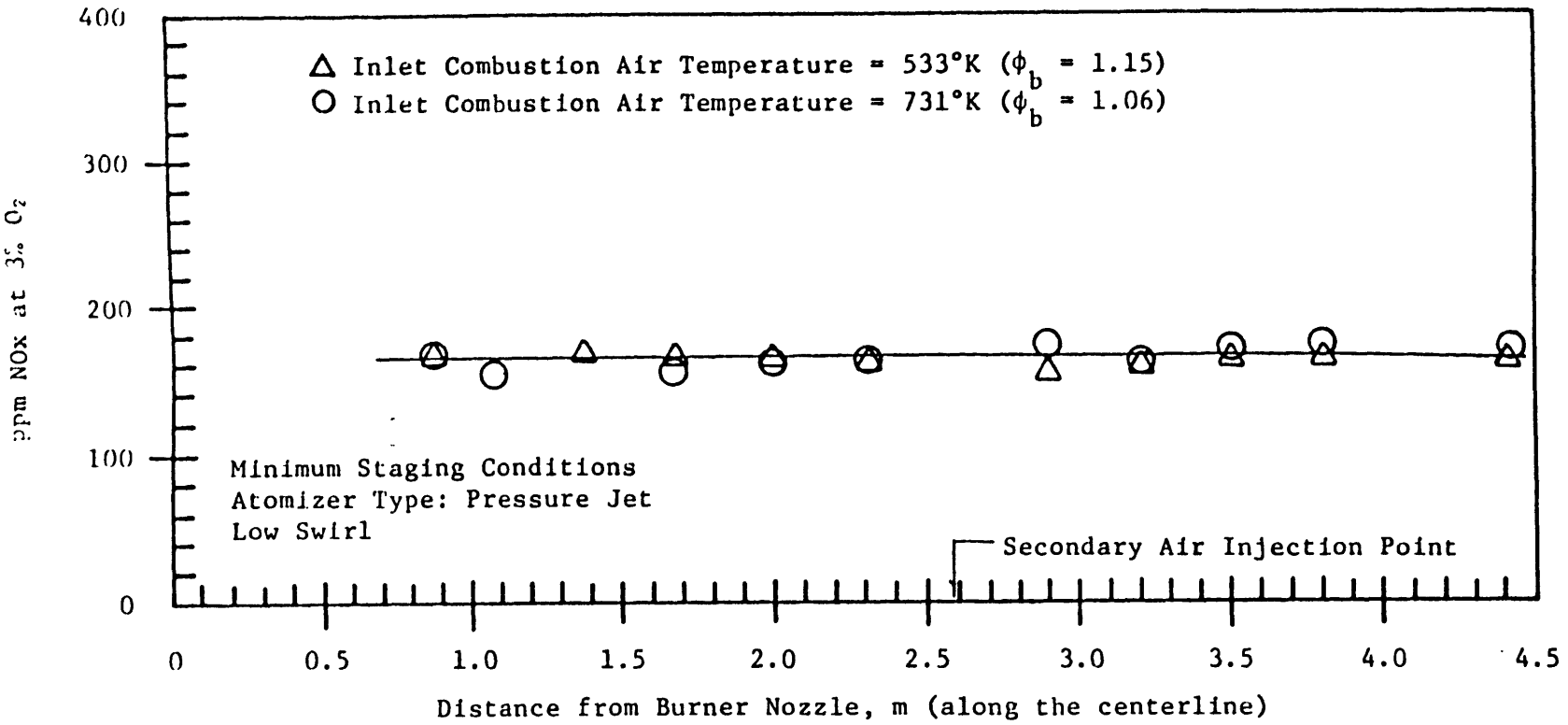

Figure 46 --An example of the effect of inlet combustion air temperature on the NOx concentration (ppm at 3% O_2) profile during staged combustion.

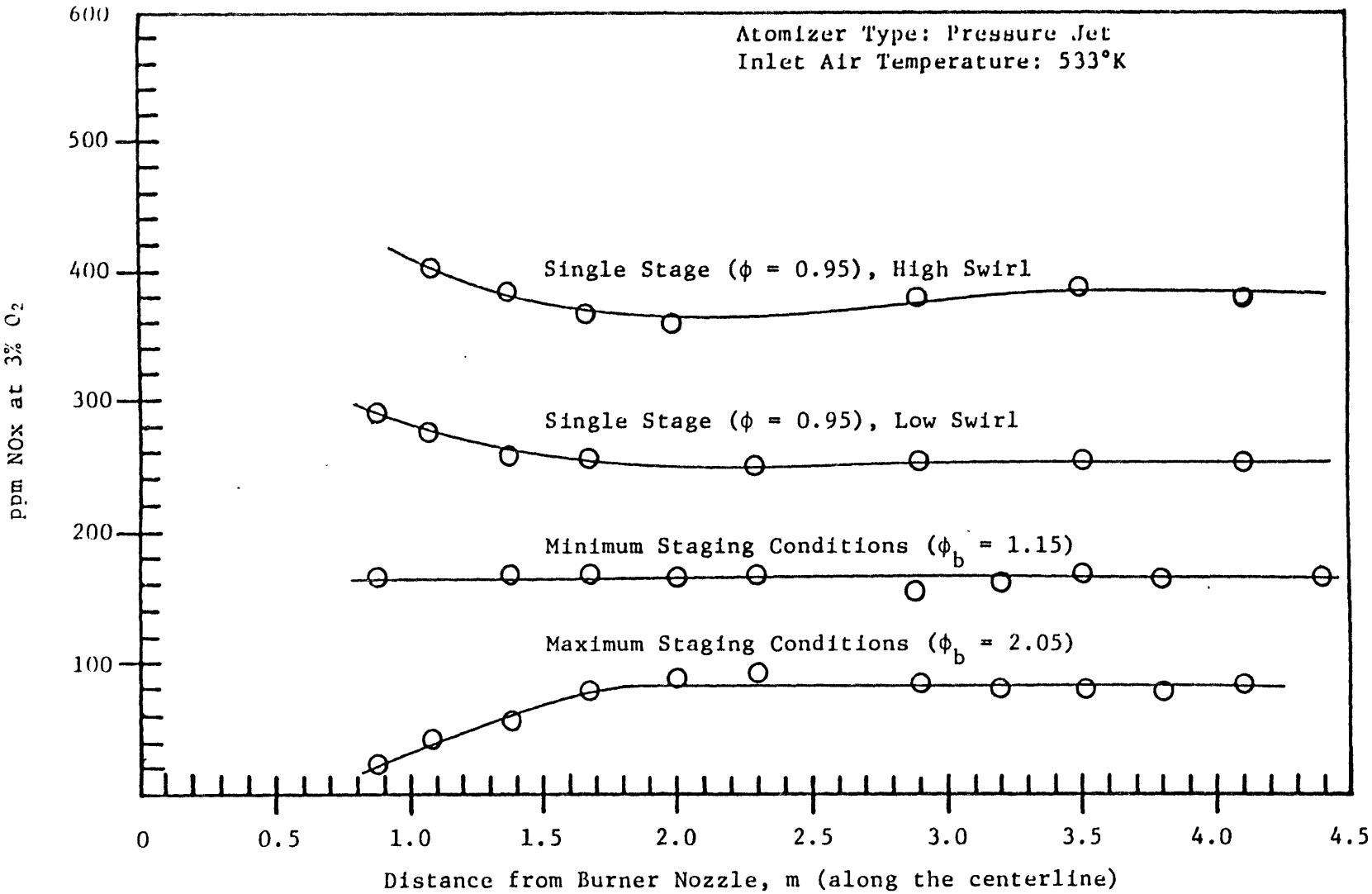

Figure 47 --Axial NOx concentration (ppm at 3% O_2) profiles, comparison between staged and unstaged conditions.

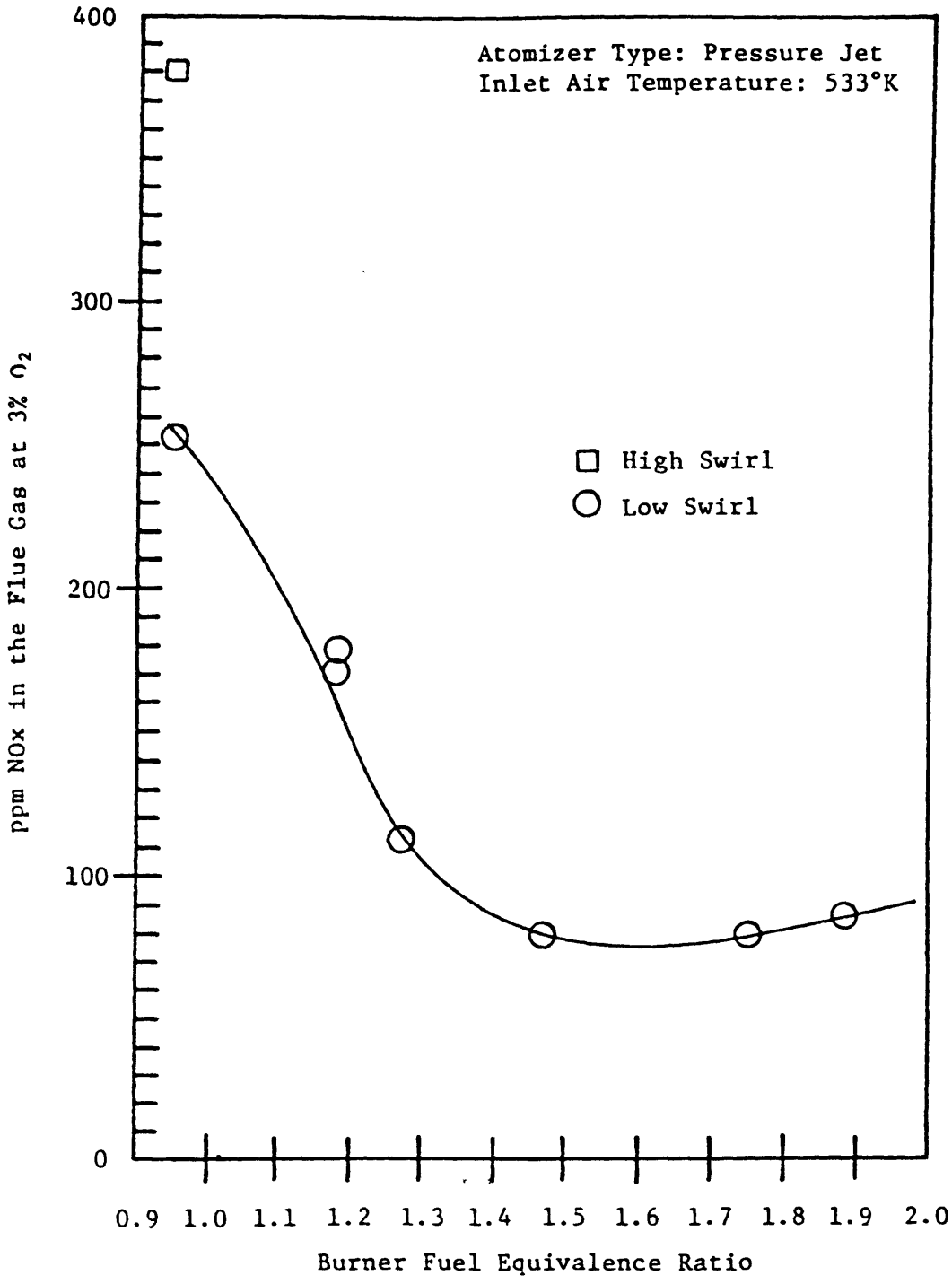

Figure 48 --NOx concentration (ppm at 3% O_2) in the flue gas as a function of burner fuel equivalence ratio.

0.95 - 1.3. The minimum NO_x emission is seen to occur at ϕ_b of 1.4 - 1.7, and a slight increase in NO_x emission is observed as increasingly fuel-rich conditions are experienced beyond ϕ_b of $\sim$1.6.

These experimental data are in very good agreement with the predictions of the simplified plug flow reactor model which accounts for the rates of both fuel-N and atmospheric nitrogen reactions under flame conditions. The predicted value of ϕ_b for minimum NO_x emissions under plug flow and adiabatic conditions with an air preheat of 500° F and a residence time of 4 seconds is 1.65.

3.2.1 Results of Parametric Study for the Effects of Air Preheat Temperature, Burner Air Swirl Number, Atomizer Type, Residence Time and Burner Fuel Equivalence Ratio on NO_x Emissions

The experimental data discussed in the preceding section consisted of a typical set of results obtained at maximum and minimum staging conditions using the pressure jet atomizer with constant burner swirl number, air preheat and residence time. Similar measurements were made on a 'y'-jet atomizer; two levels of air preheat, burner air swirl number and residence time were investigated for each atomizer type over a range of burner fuel equivalence ratios. The complete matrix of variables yielded 32 staged combustion experiments. The input conditions for each of these flames is listed in Table 8. The data obtained from these experiments are presented in graphical form in Figures 49 through 60 and Appendix C lists all of the data in tabular form. Because of the extensive amount of data obtained an averaging approach was employed to identify the relative importance of the above variables on NO_x emissions.

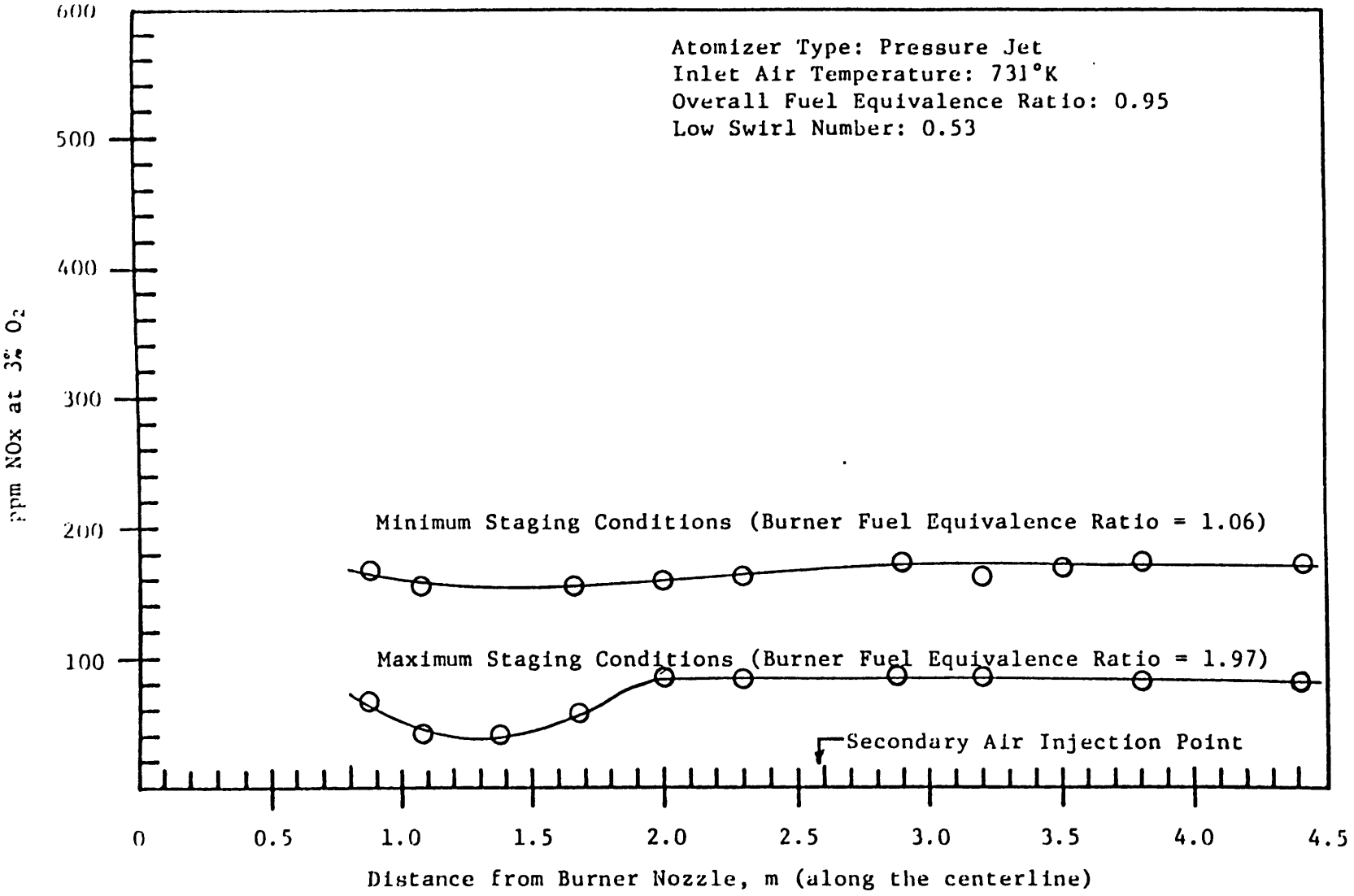

Figure 49 --Axial NOx concentration (ppm at 3% O_2) profiles, staged combustion study.

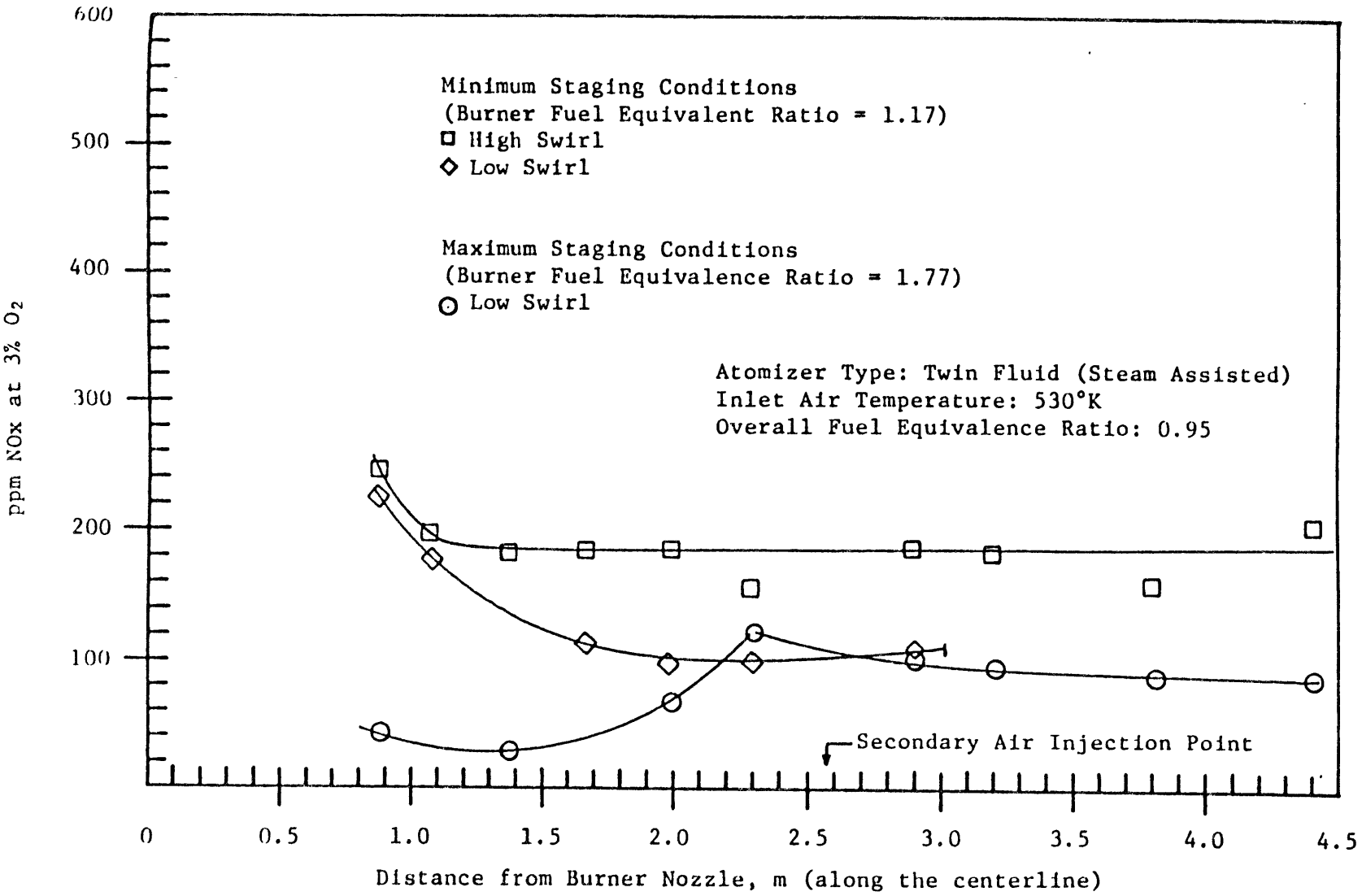

Figure 50 --Axial NOx concentration (ppm at 3% O_2) profiles, staged combustion study.

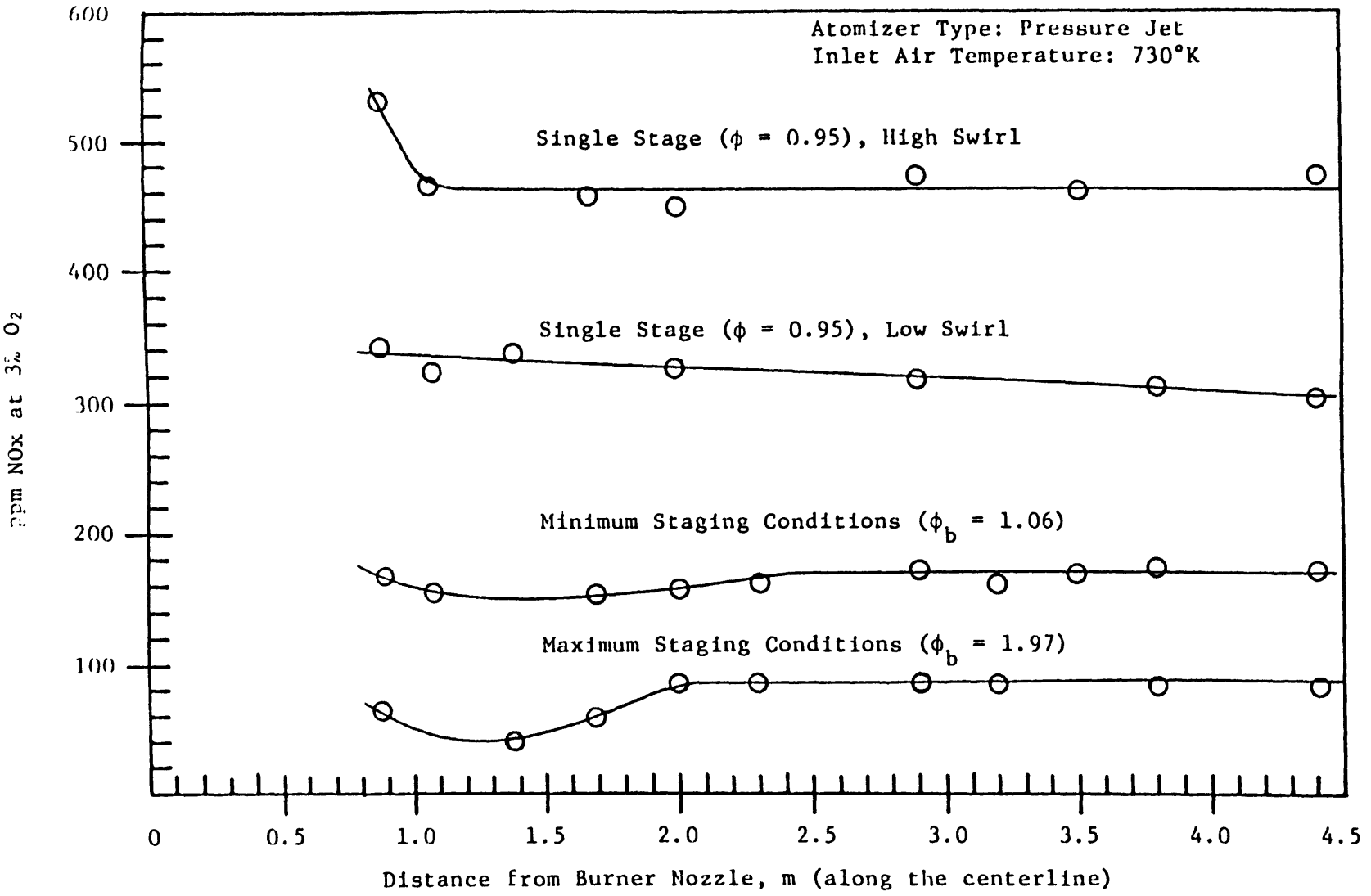

Figure 51 --Axial NOx concentration (ppm at 3% O_2) profiles, comparison between staged and unstaged conditions.

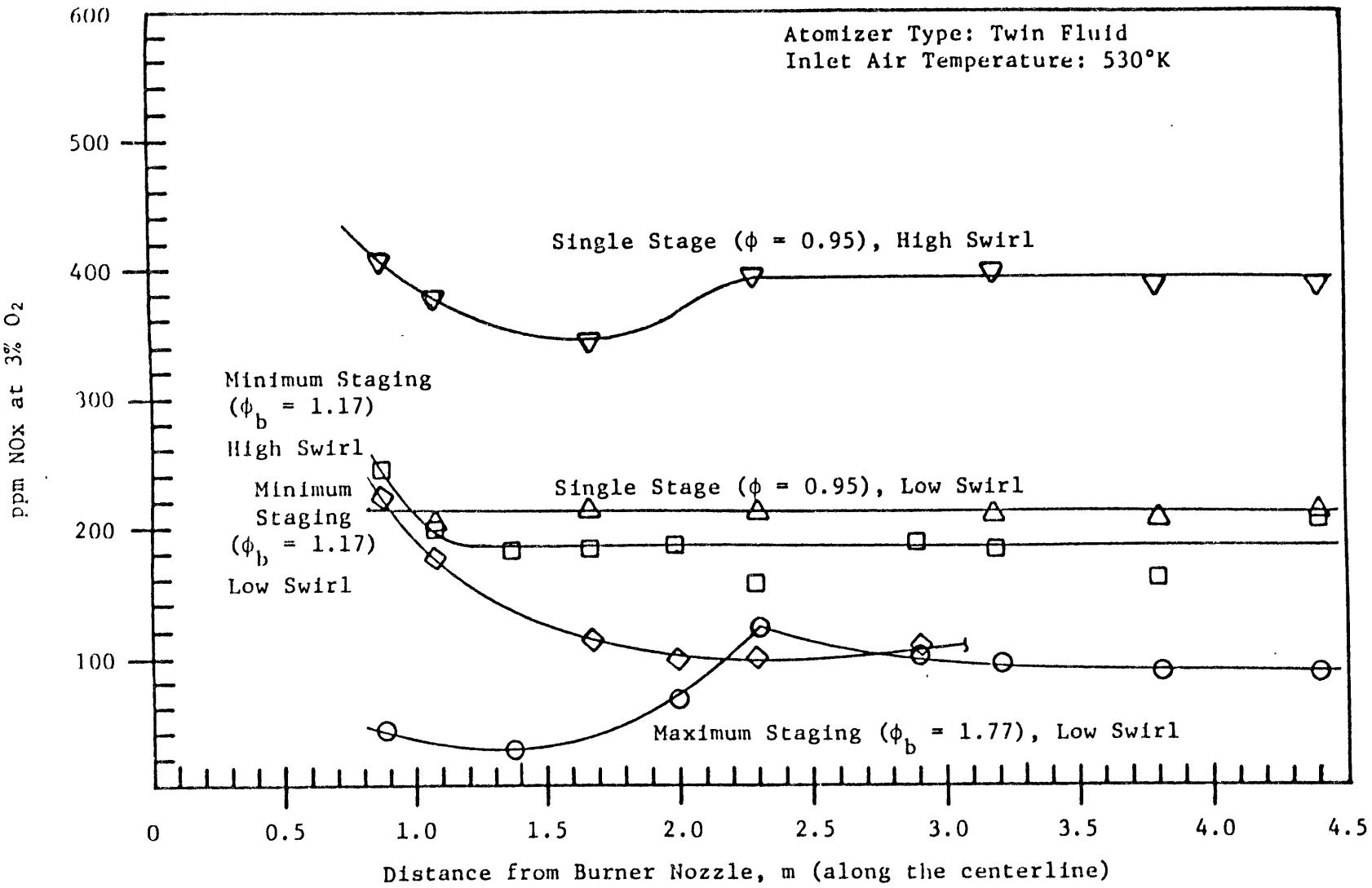

Figure 52 --Axial NOx concentration (ppm at 3% O_2) profiles, comparison between staged and unstaged conditions.

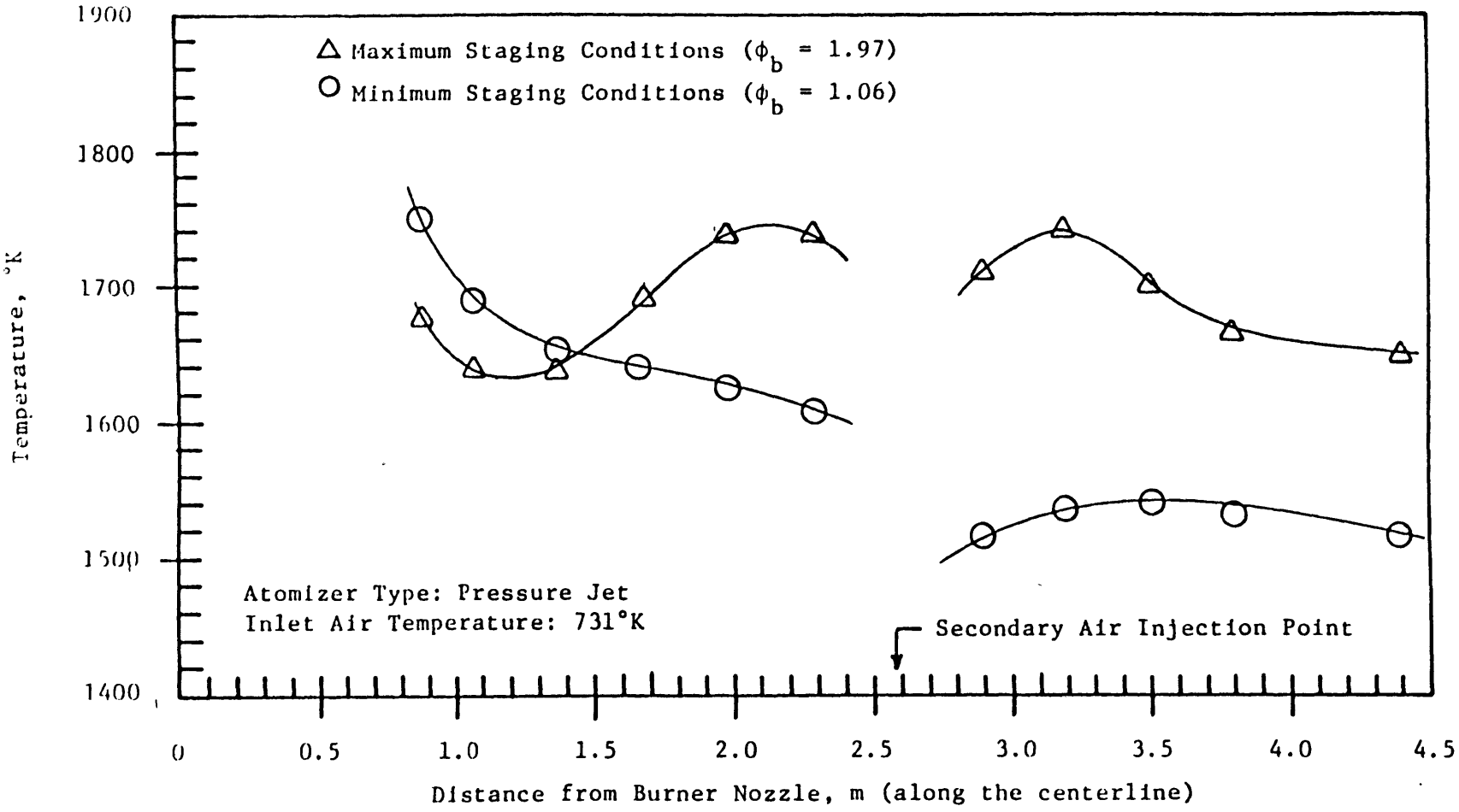

Figure 53 --Axial temperature profiles, staged combustion study.

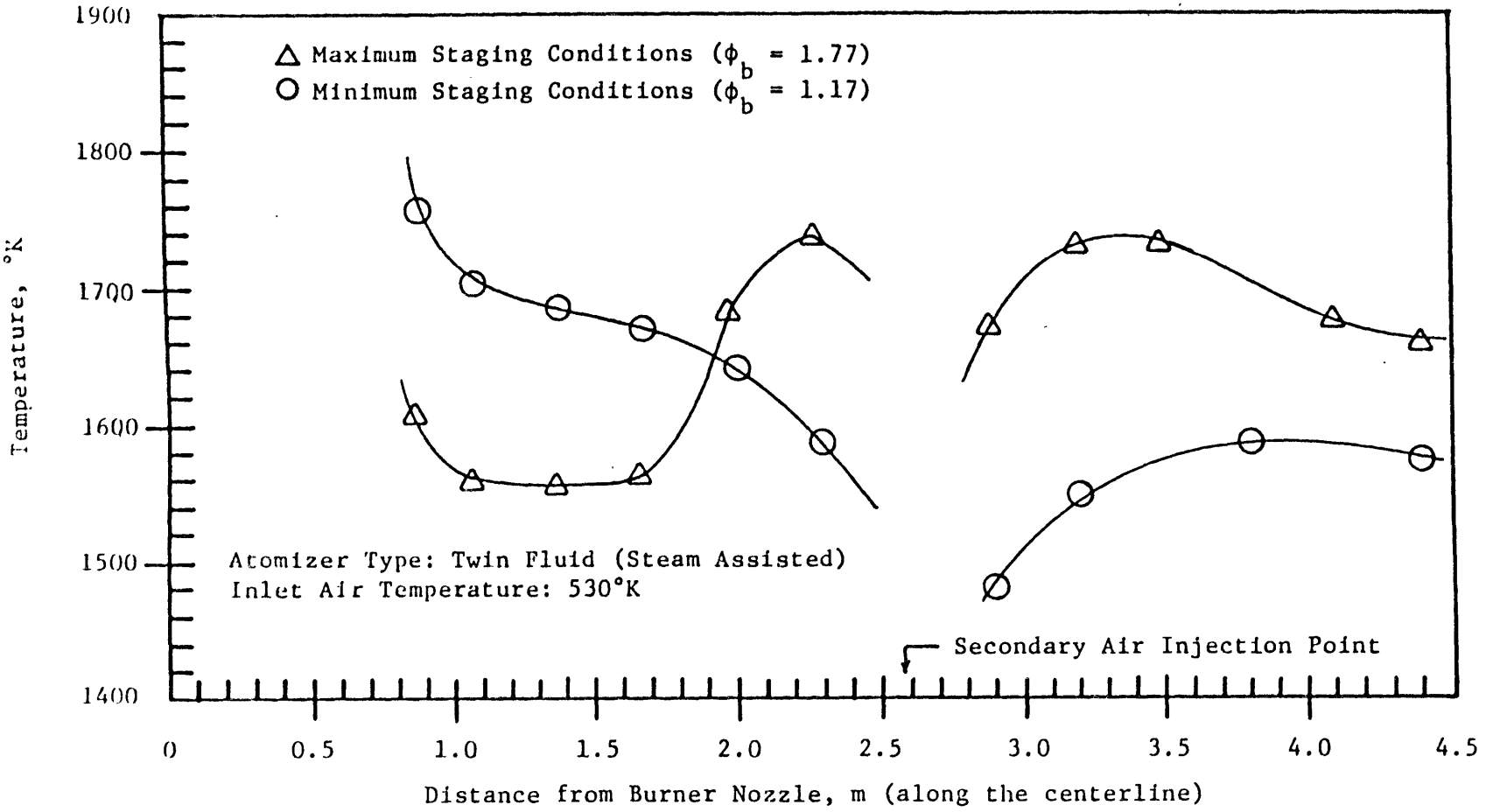

Figure 54 --Axial temperature profiles, staged combustion study.

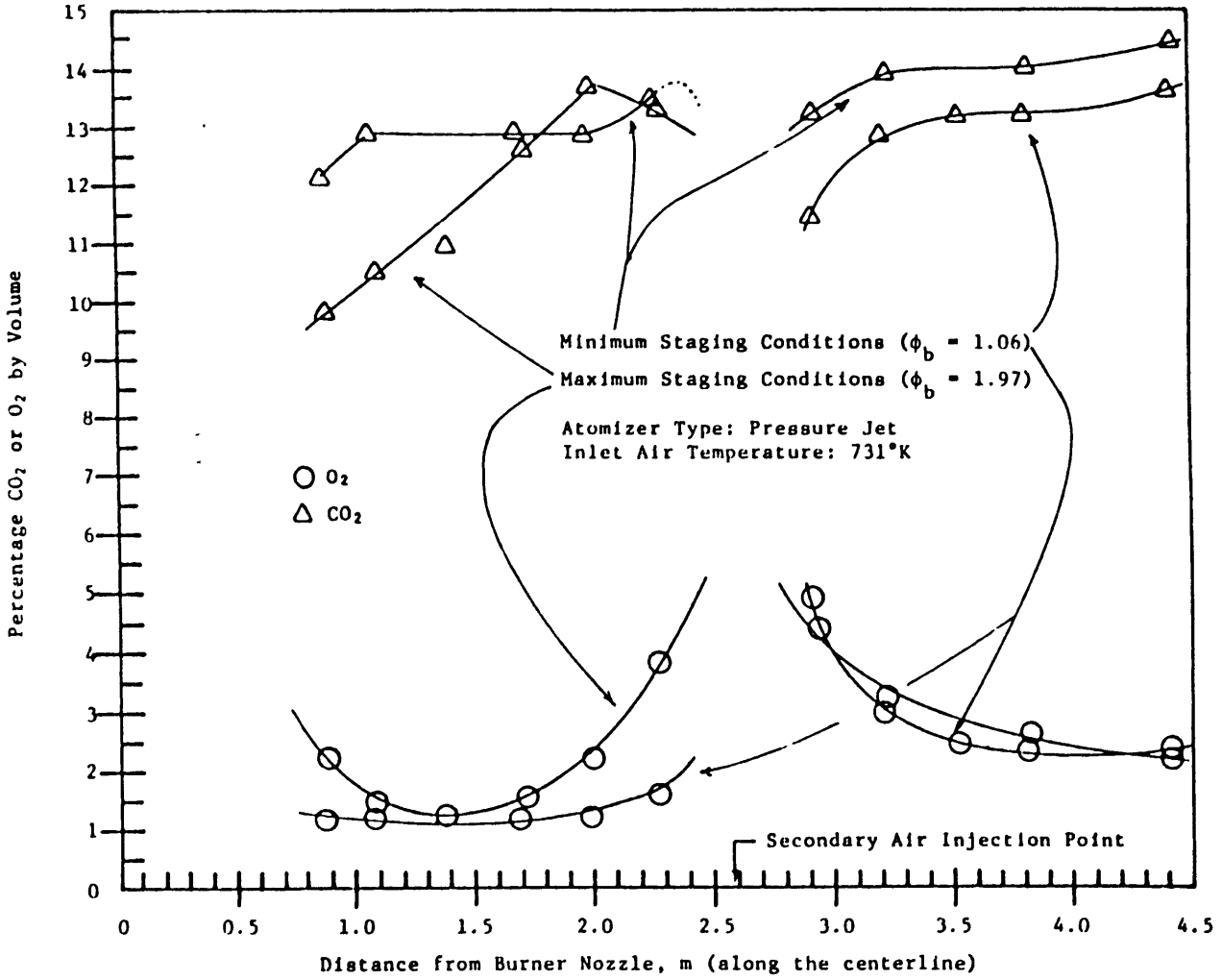

Figure 55 --Axial CO_2 and O_2 concentration profiles, staged combustion study.

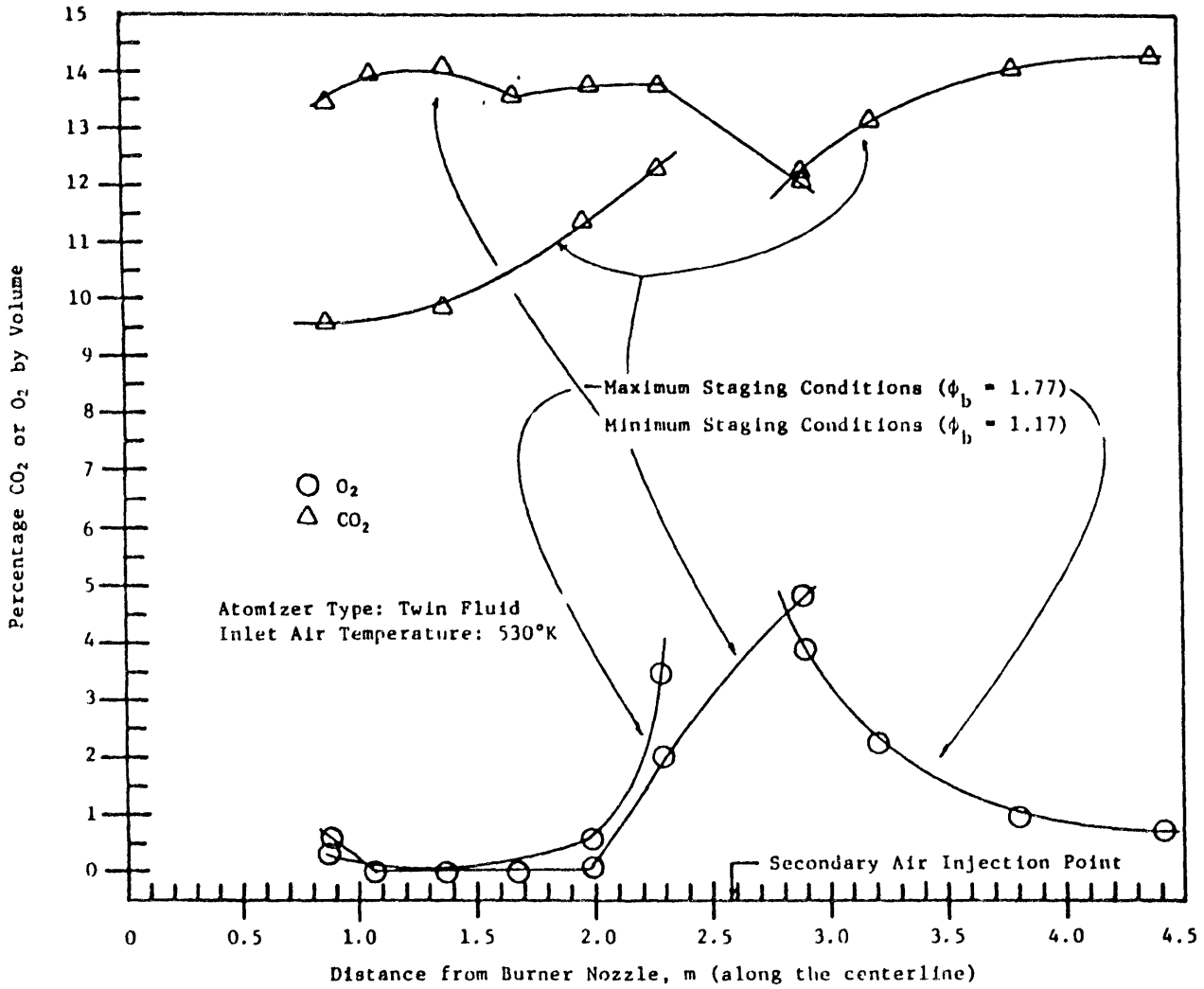

Figure 56 --Axial CO_2 and O_2 concentration profiles.

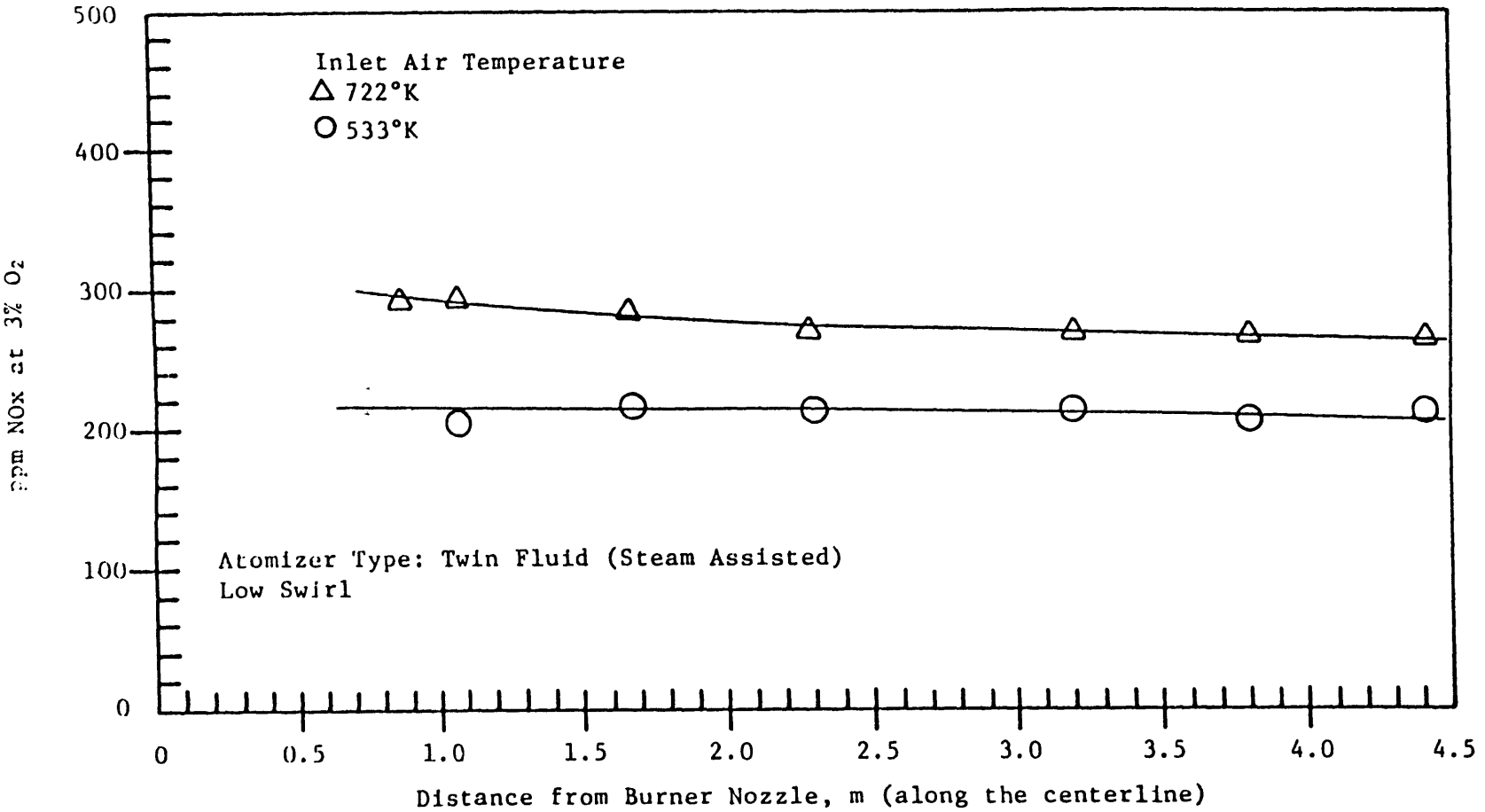

Figure 57 --An example of the effect of inlet combustion air temperature on the NOx concentration (ppm at 3% O_2) profile in conventional unstaged combustion.

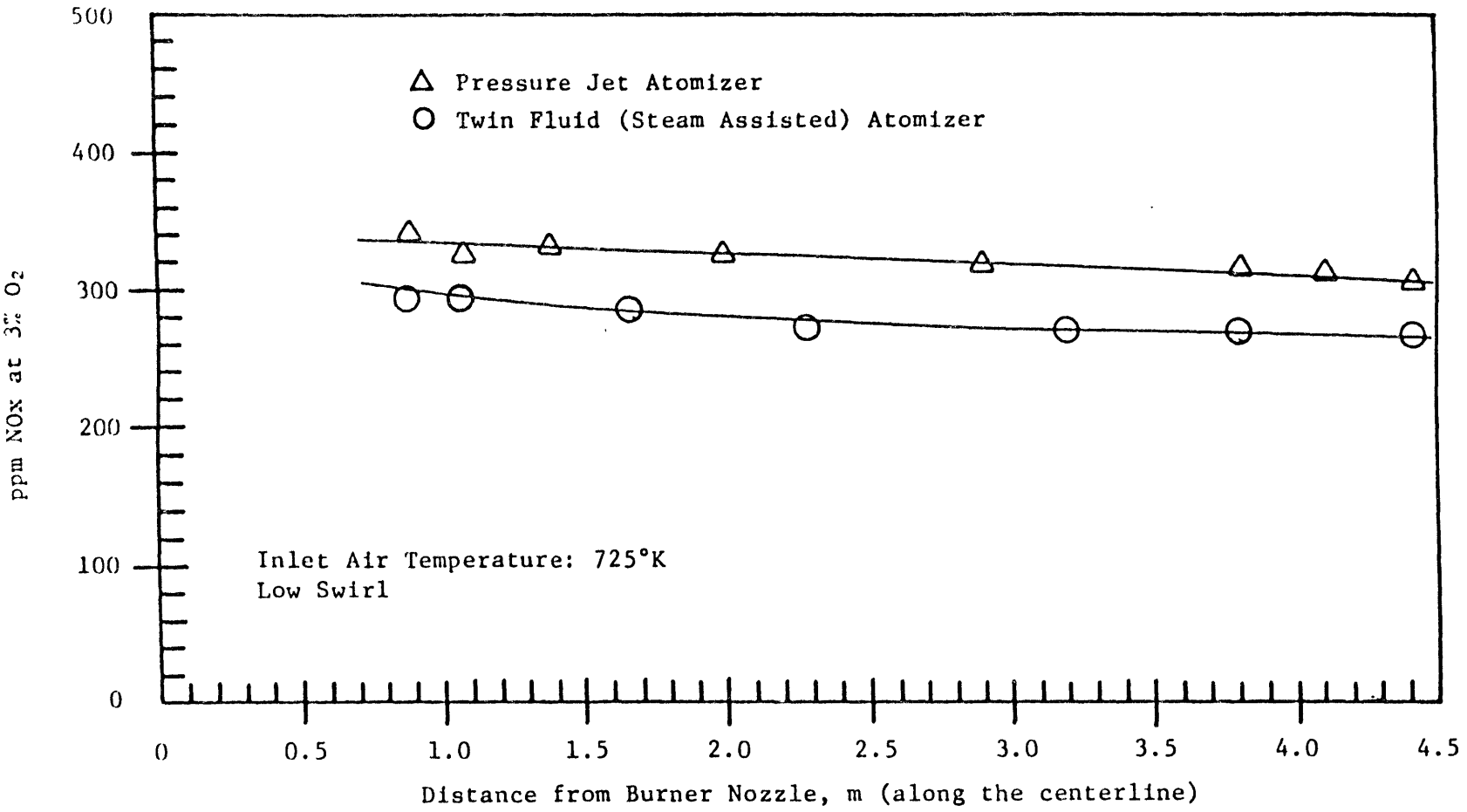

Figure 58 --An example of the effect of atomizer type on the NOx concentration (ppm at 3% O_2) profile in conventional unstaged combustion.

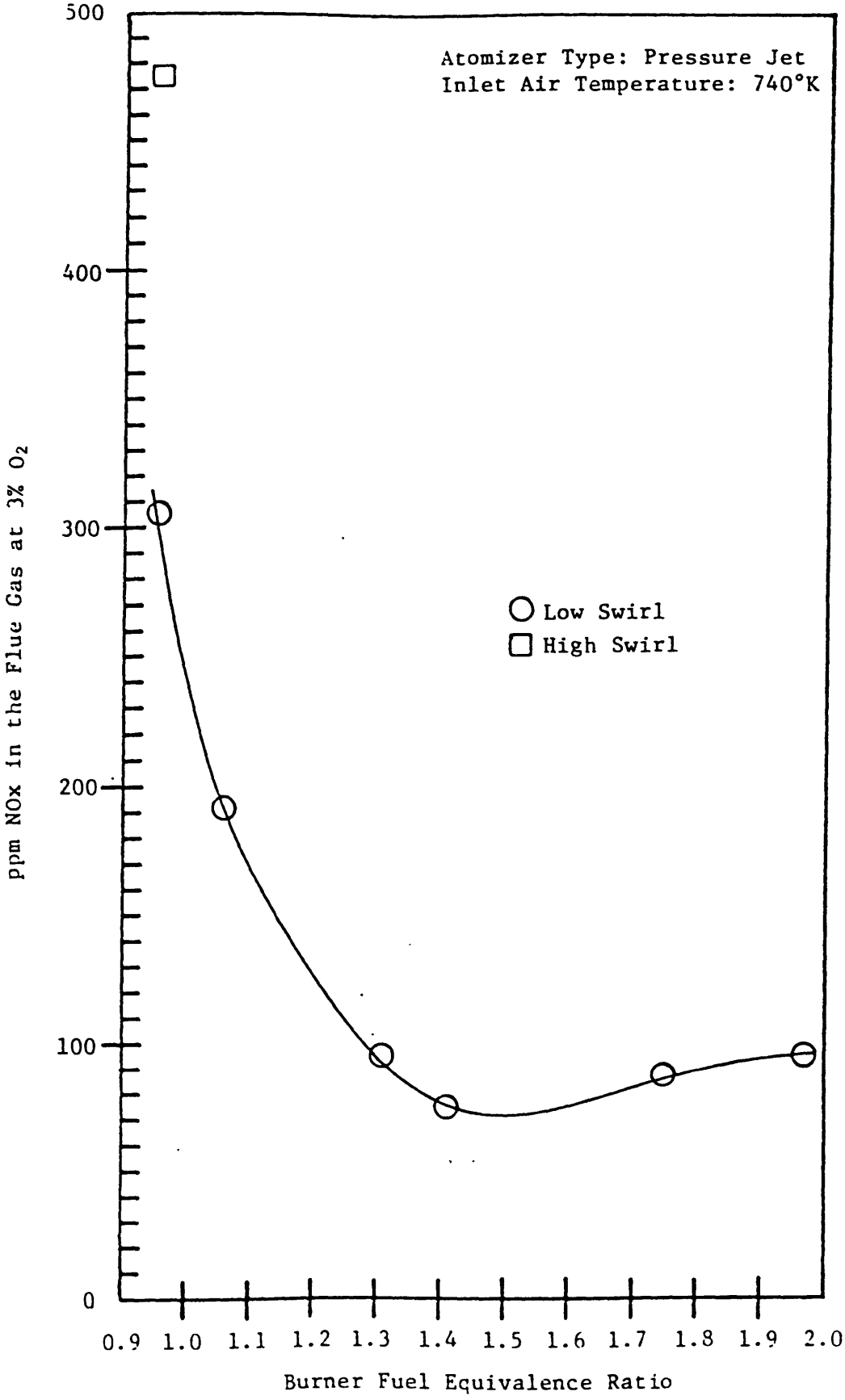

Figure 59 --NOx concentration (ppm at 3% O_2) in the flue gas as a function of burner fuel equivalence ratio.

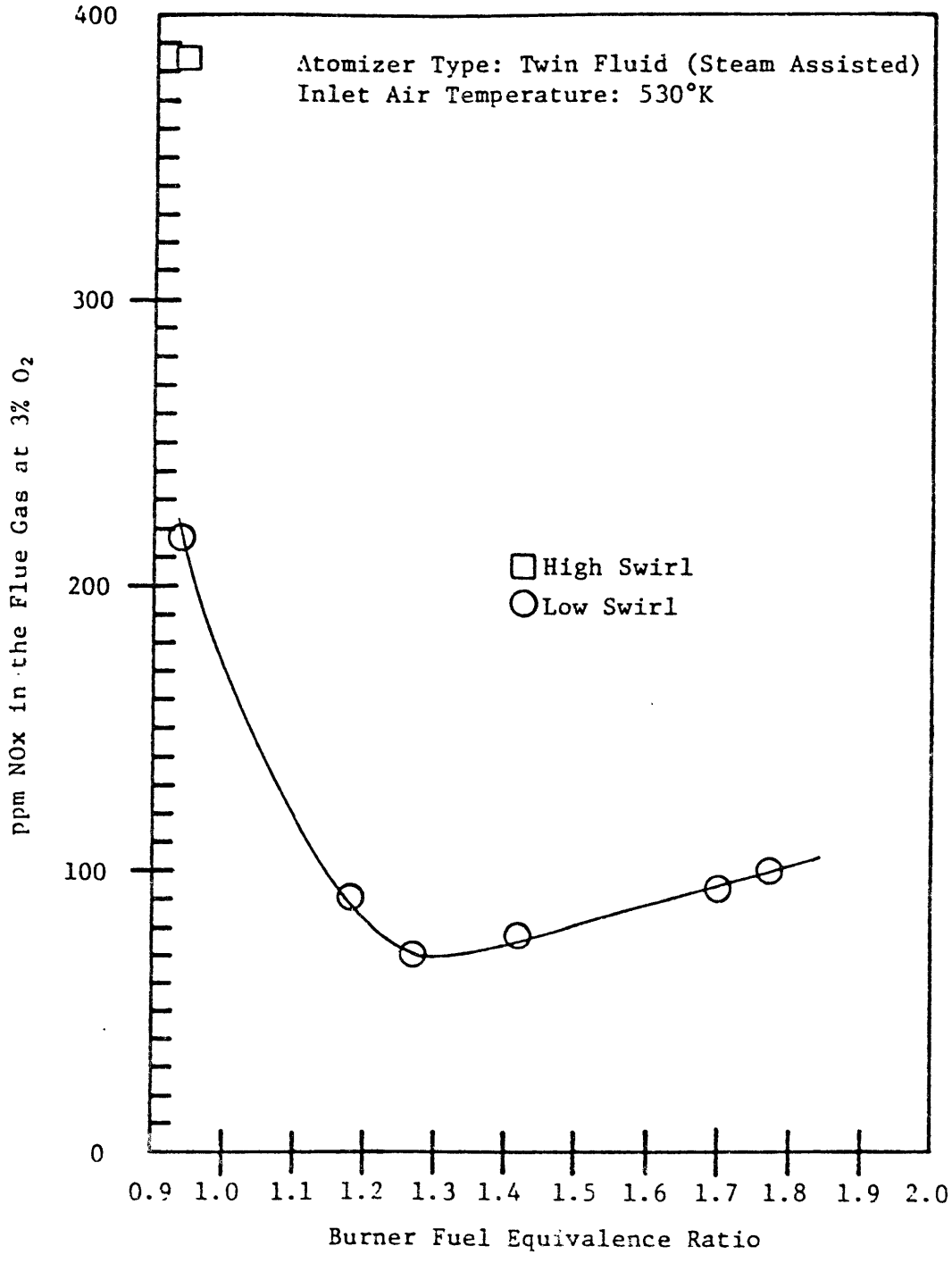

Figure 60 .--NOx concentration (ppm at 3% O_2) in the flue gas as a function or burner fuel equivalence ratio.

Both the experimental data and the theoretical model indicate that NO_x emission is a strong function of burner fuel equivalence ratio. Hence plots were made of ppm NO_x in the flue gas versus the burner fuel equivalence ratio (ϕ_b), in which the indicated NO_x emission for a given ϕ_b actually represented an average of all the available data over the individual variations in NO_x emissions for two out of the three variables. Thus, three graphs were formed; one in which the effect of inlet air temperature was examined, where variations in NO_x emissions due to changes in swirl and atomizer type was averaged; a second where the effect of swirl was examined and the variations in NO_x emission due to the other two variables, air preheat and atomizer type were averaged; and a third in which the effect of atomizer type was similarly examined. The graphs from this study are discussed in this section; a summary of this averaging study, presented in the form of a table, may be found in Appendix D. Shown in this table are the individual values of NO_x emission levels used in this study.

3.2.2 Inlet Combustion Air Temperature

Figures 31 and 57 are examples of the effect of combustion air temperature upon NO_x emission from the experimental combustor when it is fired in a conventional unstaged mode. Both figures demonstrate that there is an overall increase in NO_x emissions at higher inlet combustion air temperatures. The higher air preheat has the effect of increasing the combustion temperature which in turn enhances the formation of thermal NO_x, particularly in those portions of the flame where peak temperatures of $1800^{o}K$ are approached and exceeded. The higher combustion temperatures may also enhance the conversion efficiency of the fuel-nitrogen

to NO_x. It should be pointed out, though, that under unstaged firing conditions, the effect of temperature (in the neighborhood of 1800° K and above), is much greater on the direct oxidation of N_2 to NO_x (the formation of thermal NO_x) than on the conversion of fuel-nitrogen to NO_x (Sarofim, Pohl, and Taylor, 1978). Hence there is reason to believe that the observed increase in overall NO_x emissions with increasing air preheat (see Figures 31 and 57) is primarily due to increased thermal NO_x formation. However, further experimentation is required, perhaps with low nitrogen-content fuel oils, to fully verify this conclusion.

Figure 46 is an example of the effect of air temperature upon the axial NO_x profile in a fully-staged combustion condition. As can be seen, the effect is negligible. More will be said about this result after the effects of swirl upon NO_x emission have been discussed.

Figure 61 is a result of the averaging study described earlier, and consists of an examination of the effect of inlet air temperature upon averaged NO_x emissions at various burner fuel equivalence ratios. The "error bars" represent the spread (high and low values) of the individual data over which the averages were taken. Figure 61 reaffirms the trends indicated by the individual examples of Figures 31, 46 and 57. At the preheat levels investigated (533° K and 730° K), this variable has a substantial effect only on NO_x levels in the flue gas under conventional, unstaged conditions ($\phi_b = 0.9 - 1.0$) and under weakly-staged ($\phi_b = 1.0 - 1.2$) conditions. As the combustor is made to operate in a fully-staged mode ($\phi_b > 1.2$), the effect of inlet air temperature (in the range of 298° K - 730° K), upon NO_x emissions becomes negligible.

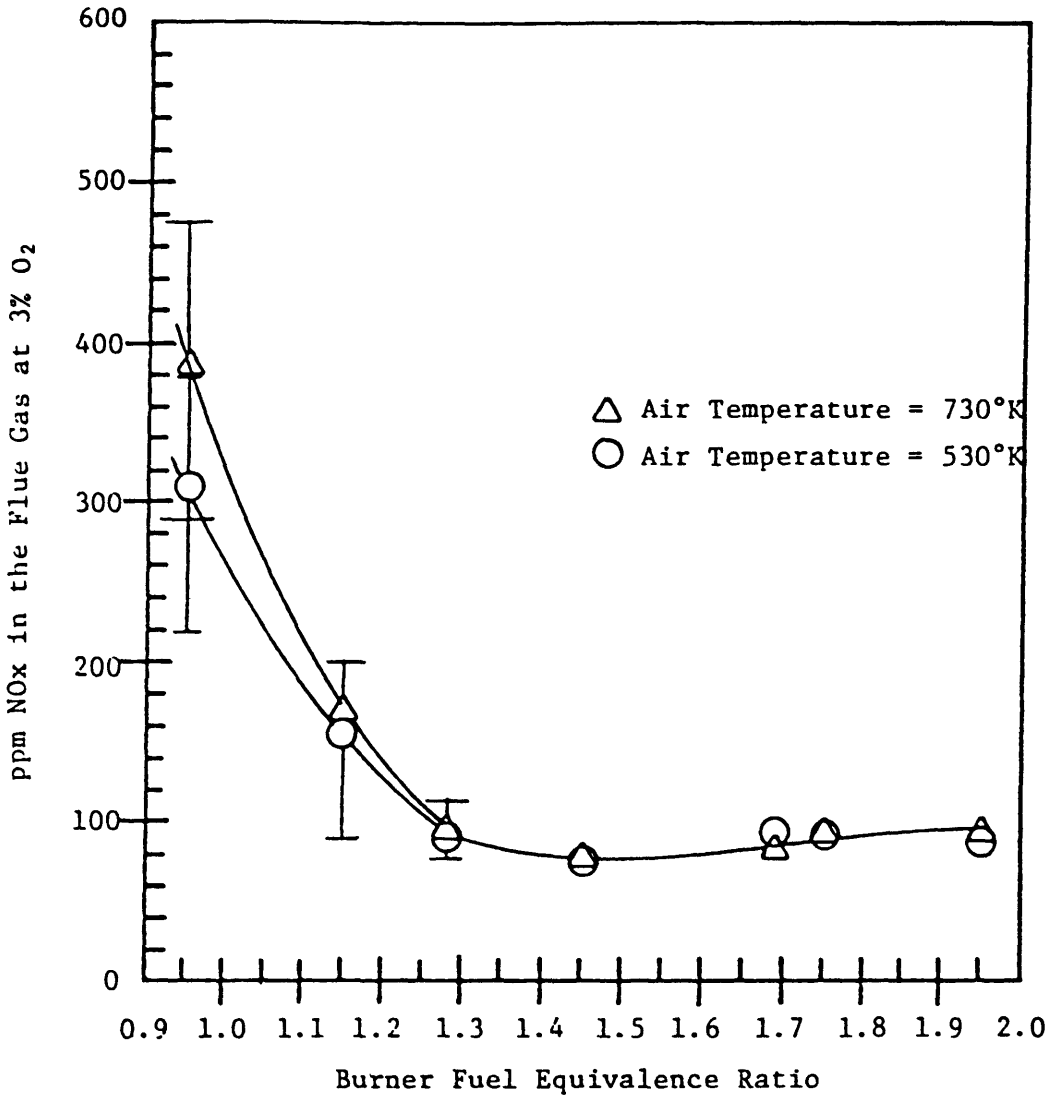

NOTE: Variations in NOx concentrations at a given fuel equivalence ratio due to other variables are averaged.

Figure 61 --NOx concentration (ppm at 3% O_2) in the flue gas as a function of burner fuel equivalence ratio; examination of the effect of inlet combustion air temperature.

3.2.3 Degree of Swirl

Examples from various experimental runs of the effect of swirl upon the axial NO_x profiles in the case of single-stage firing are shown in Figures 26 to 29. These figures show that increases in degree of swirl lead to higher NO_x emission levels. Increasing the degree of swirl has the effect of increasing the intensity of fuel-air mixing. This has the effect of increasing both fuel and thermal NO_x formation due to effects upon local fuel-air stoichiometry and combustion temperature in the flame. Increases in fuel NO_x formation are primarily brought about by the increased oxygen availability that accompanies high-intensity mixing under overall fuel-lean conditions. Increases in thermal NO_x are primarily the result of increased combustion temperature. Further experimentation is required to determine the relative degree to which fuel NO_x and thermal NO_x are affected by increases in degree of swirl (e.g., by comparisons between fuel oils having different nitrogen contents).

Figure 44 is an example of the effect of swirl upon NO_x emissions at a fully-staged condition. The effect of swirl in the ranges investigated,* $S = 0.53$ to 2.7, is seen to be negligible.

Figure 62 presents data that come from the averaging study, and give further support to trends in the effect of swirl upon NO_x emissions

---

* As the swirl number is decreased below 0.53 to 0, an increase in NO_x emissions is observed, perhaps due to poor separation of stages (i.e., unburnt fuel carryover to the 2nd stage) and to poor mixing in the fuel-rich stage. At such low swirl conditions the flame front is blown significantly downstream from the nozzle, and the flame tends to become unstable. For reasons of flame stability the swirl number was generally maintained at a value no lower than 0.5 during the course of the experiments.

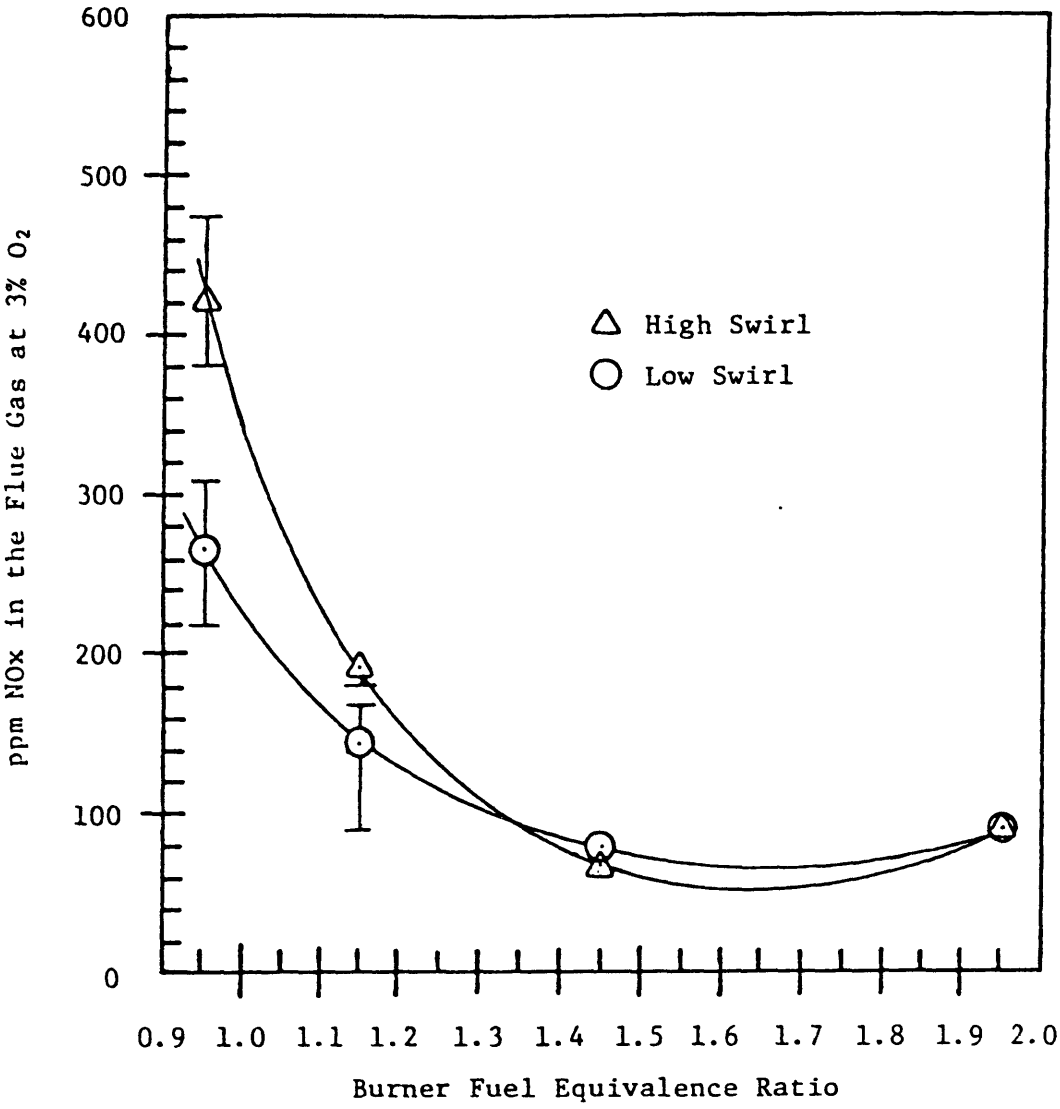

NOTE: Variations in NOx concentrations at a given fuel equivalence ratio due to other variables are averaged.

Figure 62 --NOx concentration (ppm at 3% O_2) in the flue gas as a function of burner fuel equivalence ratio; examination of the effect of swirl.

observed in the individual examples of Figures 26-29 and 44. The degree of swirl is seen to have a noticeable effect on NO_x emissions only under unstaged and weakly-staged conditions ($\phi_b < 1.2$). Under fully-staged conditions ($\phi_b > 1.2$), this effect becomes negligible ($S = 0.53$ to 2.7).

3.2.4 Atomizer Type

Figures 30 and 58 show the effect of atomizer type upon the axial NO_x concentration profiles for a number of unstaged flames. These figures demonstrate that NO_x formation is somewhat lower in the case of a twin-fluid atomizer than that of a pressure jet atomizer. The axial momentum of the fuel jet spray delivered by a twin-fluid atomizer is considerably higher than that of a pressure jet atomizer. Visual observation of the flames represented in Figures 30 and 58 confirms this: the steam-atomized flames were considerably longer than those that were pressure-atomized. As discussed in Chapter 1, delayed, slower, fuel-air mixing, which is characteristic of longer turbulent diffusion flames, results in lower NO_x emissions, due to the occurrence of lower local oxygen concentrations and lower peak temperatures where combustion occurs within the flame. With these observations in mind, the results shown in Figures 30 and 58 are understandable and to be expected.

Figure 45 gives an example of the effect of atomizer type upon the axial NO_x profile for a staged flame. Differences in NO_x concentrations due to use of either a twin-fluid atomizer or a pressure jet are quite small. Theoretically, a twin-fluid atomizer would be expected to have just the opposite effect upon NO_x emission in the case of a staged flame,

as in that of an unstaged flame. The higher axial momentum of the fuel spray delivered by a twin-fluid atomizer would be expected under some circumstances (e.g., a short primary zone), to result in carry-over of fuel droplets directly into the fuel-lean stage. Such an occurrence would partially defeat the purpose of the staged combustion process, since some of the fuel would be combusted under fuel lean conditions. The NO_x profiles shown in Figure 45 appear to confirm this reasoning; the NO_x concentrations upon entering the second stage are slightly higher for the twin field atomizer. However, as stated earlier, the difference is small, and further experimentation would be required, perhaps with a shorter first stage, to confirm this interpretation of the data. These slight differences as shown by the profiles in Figure 45 might alternately be attributed to differences in peak combustion temperatures achieved upon introduction of the secondary air into the combustor.

Figure 63 is a result of the averaging study described earlier, and is an examination of the effect of atomizer type upon averaged flue gas NO_x levels at different burner fuel equivalent ratios. The trends shown in Figure 63 are consistent with the discussion above concerning individual examples shown in Figures 30, 45 and 58.

3.2.5 Residence Time

Table 9 consists of a list of values for residence times in the M.I.T. CRF combustor, in terms of seconds per meter, for different burner fuel equivalence ratios and combustion temperatures. These values are based upon chemical equilibrium combustion calculations of the volume of combustion gas produced per kilogram of fuel input, and upon total inputs

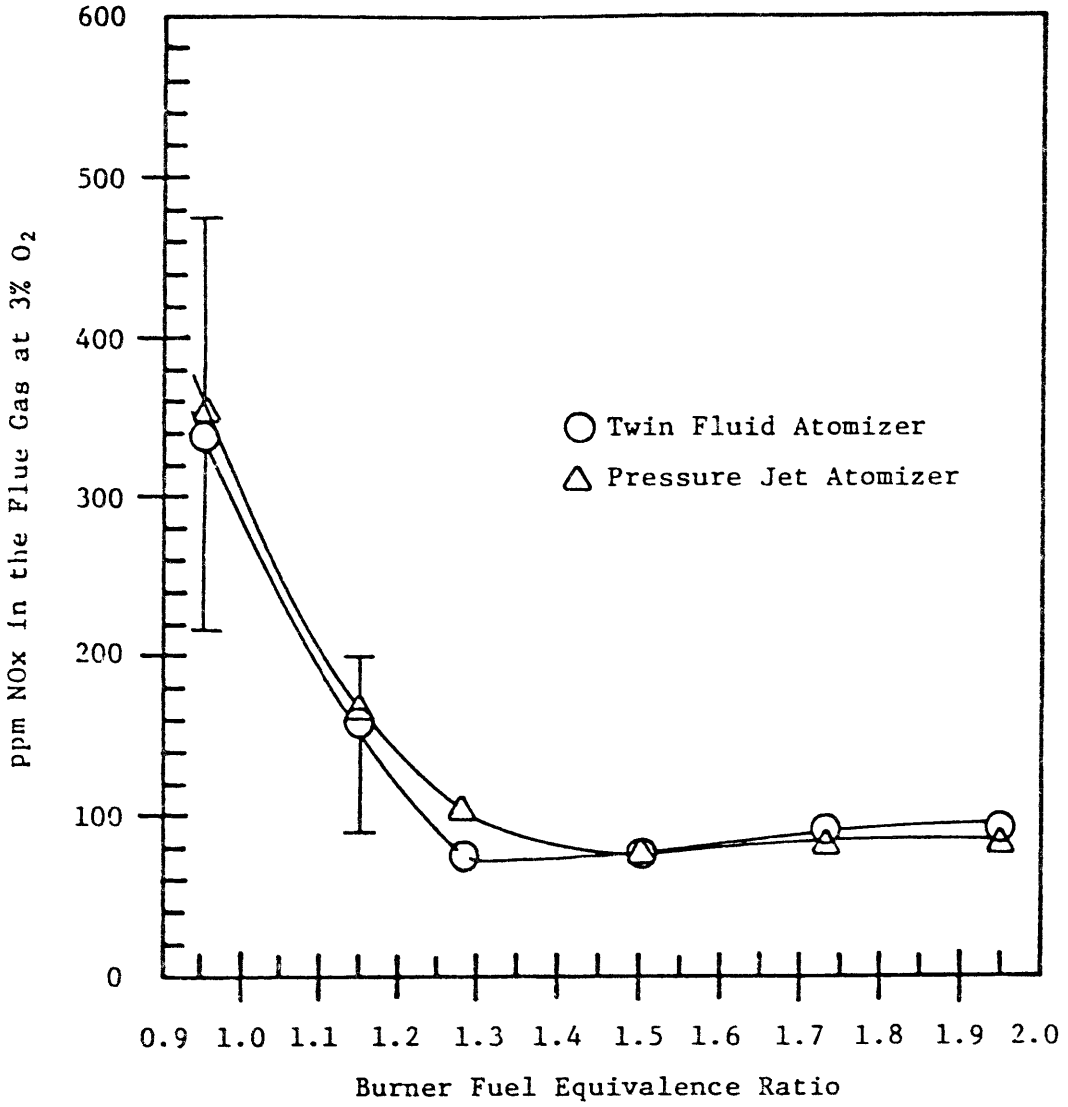

NOTE: Variations in NOx concentrations at a given fuel equivalence ratio due to other variables are averaged.

Figure 63 --NOx concentration (ppm at 3% O_2) in the flue gas as a function of burner fuel equivalence ratio; examination of the effect of atomizer type.

TABLE 9

RESIDENCE TIMES IN THE M.I.T. CRF FURNACE

Seconds per Meter

Fuel Equivalence Ratio	Combustion Temperature, °K					
	1400	1500	1600	1700	1800	1900
Basis: 83 kg/hr Fuel Input						
0.80	0.9118	0.8512	0.7979	0.7510	0.7092	0.6717
0.85	0.9662	0.9017	0.8454	0.7956	0.7513	0.7116
0.90	1.0200	0.9520	0.8925	0.8400	0.7932	0.7512
0.95	1.0736	1.0020	0.9394	0.8841	0.8348	0.7906
1.00	1.1269	1.0517	0.9859	0.9277	0.8758	0.8291
1.05	1.1683	1.0904	1.0223	0.9621	0.9086	0.8607
1.10	1.2087	1.1281	1.0576	0.9954	0.9401	0.8905
1.15	1.2481	1.1649	1.0921	1.0278	0.9707	0.9195
1.20	1.2865	1.2007	1.1257	1.0594	1.0006	0.9479
1.25	1.3240	1.2357	1.1585	1.0903	1.0297	0.9755
1.30	1.3606	1.2699	1.1905	1.1205	1.0582	1.0024
1.40	1.4312	1.3358	1.2523	1.1786	1.1131	1.0545
1.50	1.4986	1.3987	1.3113	1.2341	1.1655	1.1041
1.60	1.5630	1.4588	1.3676	1.2872	1.2156	1.1516
1.70	1.6246	1.5163	1.4215	1.3379	1.2634	1.1969
1.80	1.6836	1.5713	1.4731	1.3864	1.3094	1.2404
2.00	1.7942	1.6746	1.5699	1.4775	1.3954	1.3219
Basis: 143 kg/hr Fuel Input						
0.80	0.5297	0.4941	0.4631	0.4359	0.4116	0.3899
0.85	0.5608	0.5234	0.4907	0.4618	0.4361	0.4134
0.90	0.5920	0.5526	0.5180	0.4876	0.4604	0.4360
0.95	0.6231	0.5816	0.5452	0.5131	0.4865	0.4589
1.00	0.6544	0.6104	0.5722	0.5385	0.5083	0.4812
1.05	0.6781	0.6329	0.5934	0.5584	0.5274	0.4996
1.10	0.7016	0.6548	0.6139	0.5777	0.5457	0.5169
1.15	0.7244	0.6761	0.6339	0.5966	0.5634	0.5337
1.20	0.7467	0.6969	0.6534	0.6149	0.5808	0.5502
1.25	0.7685	0.7172	0.6724	0.6328	0.5977	0.5662
1.30	0.7897	0.7371	0.6910	0.6504	0.6142	0.5818
1.40	0.8307	0.7753	0.7269	0.6841	0.6461	0.6121
1.50	0.8698	0.8118	0.7611	0.7163	0.6765	0.6408
1.60	0.9073	0.8467	0.7938	0.7471	0.7056	0.6684
1.70	0.9429	0.8801	0.8251	0.7765	0.7334	0.6947
1.80	0.9772	0.9120	0.8550	0.8047	0.7600	0.7200
1.90	1.0099	0.9426	0.8837	0.8317	0.7855	0.7441
2.00	1.0414	0.9720	0.9112	0.8576	0.8099	0.7673

Note: Combustion of high nitrogen No. 6 fuel oil. Both temperature and dissociation taken into account.

of 83 kg/hr and 143 kg/hr, respectively. Flames 1 to 38 listed in Tables 6 and 8 are based upon a fuel input of approximately 83 kg/hr, and flames 39 and 40 upon an input of 143 kg/hr. The values presented in Table 9 may be used to obtain approximate estimes of residence times of the combustion mixture in the entire length of the combustion chamber for unstaged flames, and in the fuel-rish first stage for the staged flames. For example, temperatures of the unstaged flames varied between 1500 K and 1800 K, the combustion chamber length was approximately 4.6 m and the fuel equivalence ratio was about 0.95. Hence average residence times for the unstaged flames varied roughly between 3.8 and 4.6 seconds at a fuel input of 83 kg/hr. The primary zone of the staged flames was approximately 2.6 m long. Residence times in the primary zone at minimum staging conditions (ϕ_b - 1.1) varied between 2.4 and 2.8 seconds, and for minimum staging conditions (ϕ_b = 2.0) between 3.6 and 4.1 seconds, at a firing rate corresponding to 83 kg/hr.

Data on the effect of residence time upon NO_x emissions is limited. As evident from the discussion above, fuel input was maintained at primarily one value, 83 kg/hr, and the length of the primary zone in the case of the two-stage studies was left constant at 2.6 m. Flames 39 and 40 in Table 8 represent the only experiments carried out, in which the residence times were substantially changed. NO_x emissions from these flames are presented in Table 10 along with values from other flames for comparison. It appears that the increased firing rate and lowering of residence times have only a small effect upon the NO_x emissions of the flames. Roughly a 20 ppm increase in NO_x emission levels was observed. However, interpretation of the data is complicated by the fact that flame temperatures were higher. For example, in the case of flame 40,

higher primary zone temperatures may have accelerated the rates of the fuel-nitrogen reactions and therefore may have tended to lower the overall NO_x emission. The shorter primary zone residence time, on the other hand, may have offset the effect of the higher temperatures, the final outcome thus being, as shown in Table 10, little different from a similar flame based upon a lower fuel input.

It is concluded that the problem in interpretation of flame 40 as compared to flame 33 (see Table 10) is one of determining the degree to which each of the variables, residence time and temperature, has an effect on overall NO_x emission levels. The problem arises out of the fact that both tend to have opposite effects on the final outcome. Further experimentation is required in which residence time and primary zone temperature are varied separately by means of proper manipulation of firing rates (fuel input), and the physical length of the fuel-rich primary zone, so as to properly ascertain the individual effects of these two variables on NO_x emissions.

3.2.6 Burner Fuel Equivalence Ratio

Figures 47, 51 and 52 are direct comparisons of axial NO_x profiles under staged and unstaged conditions, and they dramatically demonstrate the effectiveness of the staged combustion strategy in reducing NO_x emissions. NO_x emissions are shown experimentally to be reduced by 3 to 5 times; the theoretical studies indicate a much greater potential with proper optimization of combustion variables.

The experimental results show that the most important variable in the staged combustion process from the standpoint of lowering NO_x emissions is

TABLE 10

COMPARISON BETWEEN NO_x EMISSIONS FROM FLAMES
BASED ON DIFFERENT FIRING RATES

Flame Number	CRF Run Number and Date		Fuel Input kg/hr	Atomizer Type	Air Temperature °K	Swirl Number	Burner Fuel Equivalence Ratio	NO_x Emission (ppm NO_x in the Flue Gas at 3% O_2)
6	29b	8/20/79	85.3	Twin Fluid	533	0.53	0.94	217
33	31c	8/22/79	83.8	Twin Fluid	529	0.53	1.26	73
39	37b	10/15/79	142.4	Twin Fluid	533	0.53	0.87	238
40	37c	10/15/79	143.2	Twin Fluid	533	0.53	1.29	90

the burner fuel equivalence ratio. Figures 48, 59 and 60 show the effect of burner fuel equivalence ratio upon NO_x emissions at different inlet air temperatures and with use of different atomizer types. NO_x emissions drop sharply as burner fuel equivalence ratio is increased from 0.95 to 1.1, then passes through a minimum, and finally increases slightly at burner fuel equivalence ratios greater than 1.6.

Most of the data displayed in Figures 48, 59 and 60 were taken at a low swirl condition (i.e., a swirl number equal to 0.53). Included, however, are NO_x emissions data for a high swirl condition ($S = 2.7$), at conventional unstaged conditions ($\phi_b = 0.95$), for the purpose of demonstrating the worst possible (i.e., the highest), NO_x emission levels that could be achieved in the CRF combustor. As indicated in discussions earlier, the difference in NO_x emissions at a high swirl condition becomes negligible at fuel equivalence ratios greater than 1.2.

The experimental results shown in Figures 48, 59 and 60 substantiate trends shown by the theoretical studies. The experimental data verify that there is indeed an optimum value for the fuel equivalence ratio in the fuel-rich, first stage, at which the resulting NO_x level in the flue gas exiting the combustor is at a minimum due to destruction of NO_x and conversion of fuel nitrogen to N_2 in the first stage. The data indicate an optimum burner fuel equivalence ratio between 1.4 and 1.7, as compared to 1.6 and 1.8 predicted by the theoretical studies. Differences in values of the optima are thought to be due to generally lower temperatures in the real combustor resulting from heat losses, and to delayed fuel-air mixing effects which are not accounted for in the simple reactor model employed in the theoretical studies.

3.2.7 Particulate Emission

A limited number of measurements were made to determine the concentrations of particulates in the flue gases, for both staged and unstaged flames. The data obtained on solids emissions from staged and unstaged flames are shown in Table 11. These data were obtained from single point measurements taken in the flue gas, using a water-cooled solids sampling probe system which collects the solids in a sintered bronze thimble-type filter. This sampling system is designed primarily for in-flame measurement where particulate concentrations are quite high, and long sampling periods were required to measure the extremely low particulate concentration reported in Table 11.

It can be seen from Table 11 that particulate emissions were very low, at least an order of mangnitude below existing emission standards, under both staged and unstaged conditions. No major differences are observed between staged and unstaged flames and the only parameter which appears to have any significant effect on particulate concentration in the flue gas is swirl number, at high air preheat temperatures. This observation reflects the influence of fuel spray/combustion air interaction and mixing on particulate emission, i.e. at high swirl levels and high burner throat air velocities (due to air preheat level) a mismatch can be expected between the fuel spray and the air flow resulting in poor mixing and increased particulate formation.

It was concluded that the high velocity, transverse air jets, which deliver the secondary stage air were instrumental in achieving efficient mixing in the fuel-lean stage. At the high temperatures prevailing in

TABLE 11

SOLIDS EMISSIONS DATA FROM STAGED AND UNSTAGED FLAMES

Flame Type	Flame Conditions					Flame #	Solids lb/10^6 Btu
	ϕ_b	ϕ_b	Nozzle	S	Air Preheat		
Unstaged	0.95	0.95	Steam	2.7	800° F	7	.005
Unstaged	0.95	0.95	Steam	0.4	800° F	8	.008
Unstaged	0.95	0.95	Steam	2.7	500° F	5	.004
Unstaged	0.95	0.95	Steam	0.4	500° F	6	.004
Staged	1.97	0.95	Pressure Jet	2.7	800° F	20	.005
Staged	1.97	0.95	Pressure Jet	0.4	800° F	21	.008
Staged	1.15	0.95	Pressure Jet	0.4	500° F	9	.001
Staged	2.05	0.05	Pressure Jet	0.4	500° F	10	.001
Staged	1.10	0.95	Steam	0.4	500° F	31	.004

this region, carbon burnout is extremely rapid, of the order of 100 msecs.

Conclusions

A systematic experimental study has been carried out on the conversion of fuel-nitrogen in single stage and two stage combustion of a 0.7% N content heavy fuel oil using the M.I.T. Combustion Research Facility. The experiments were guided by results of kinetic model calculations of the fuel-N conversion to NO_x and N_2 respectively. Results of the experiments show that staged combustion can effectively reduce NO_x emission without excessive emission of carbonaceous particulates. It is shown that in agreement with theoretical model predictions, an optimum range of fuel equivalence ratios $\phi_{opt} \simeq 1.4 - 1.8$, exists for the fuel rich stage. Under close control of the mixing and flame temperatures in both the fuel rich and lean stages, NO_x (at 3% O_2) emission levels of 80 ppm could be achieved with no visible emission of soot. Of the other variables tested in the experiments, the degree of swirl in the burner had insignificant effect, for stable flames, under staged combustion conditions; higher swirl degrees giving slightly lower NO_x emissions for first stage fuel equivalence ratios $\phi > 1.5$. Under single stage combustion, reduced intensity of mixing brought about by a lower degree of swirl in the combustion air decreased the NO_x emission level from about 400 ppm at S = 2.7 to 250 ppm at S = 0.53. NO_x emissions increased stepwise for both staged and unstaged flames when the swirl number was reduced below the critical level needed to maintain a stable flame, i.e. under "lifted-flame" conditions.

Air preheat, the effect of which was studied at three levels: 293 K, 500 K and 730 K, was expected to be a significant factor in fuel-N conversion in the fuel rich stage but this was not borne out by experiment, most likely because the experimental temperature range (1000 to 1900 K) was too low to illustrate this theoretically predicted temperature effect.

Experiments carried out under conditions of reduced residence time in the combustor showed only slight increase in NO_x emission.

The results obtained from the theoretical and experimental studies showed that in general terms no fundamental limitations exist which would preclude low NO_x and particulates emission from high nitrogen content liquid fuel flames. Information obtained from this study may be used as a technical basis for the development and design of burners and boiler furnaces. In particular, the optimum concentrations and temperature histories of the fuel which have been identified in these investigations may provide guidance for the flow and mixing pattern, the quality of fuel atomization, the use of air preheat and the combination of heat extraction and fast secondary air admixing needed in full scale boiler plant for the control of NO_x and particulates emission.

However it should be appreciated that the very low NO_x and particulates emission levels obtained in these studies are due primarily to the close controls over the combustion process which can be obtained using the MIT-CRF. While the combustion conditions are representative of those in full scale plants, such controls, particularly the high velocity secondary air jets, may not be economically feasible for utility size boilers. Consequently the main value of the results presented in this report are in their potential application to the development of a design strategy and the absolute values of NO_x emissions reported may be regarded as lower bounds for emission.

Acknowledgement

Special thanks go to Mr. Barry Taylor, graduate student, Chemical Engineering Department, MIT, for the assistance and information he has given in connection with the equilibrium and chemical kinetics computer program used in this study. The kinetics scheme employed in this computer program was developed by Mr. Taylor.

The authors gratefully acknowledge the assistance of Jon E. Haebig of Gulf Research and Development Company in making available the specially prepared experimental No. 6 fuel oil.

References

1. B.S. Haynes, "Production of Nitrogen Compounds from Molecular Nitrogen in Fuel-Rich Hydrocarbon-Air Flames", Fuel, 56, 199, April, 1977.

2. J.M. Levy, J.P. Longwell, and A.F. Sarofim, Conversion of Fuel-Nitrogen to Nitrogen Oxides in fossil Fuel Combustion: Mechanistic Considerations. Report to Energy and Environmental Research Corporation (EER) by MIT Energy Laboratory, October 1, 1977 - April 30, 1978

3. A.F. Sarofim, J.H. Pohl, and B.R. Taylor, Strategies for Controlling Nitrogen Oxide Emissions During Combustion of Nitrogen-Bearing Fuels. AIChE Symposium Series 175 Volume 74, 1978, p. 67.

APPENDIX A

MIT COMBUSTION RESEARCH FACILITY (CRF)

The schematic arrangement of the experimenal plant is shown in Figure A-1 The furnace and the systems for the storage, metering, feeding and controlling fuels, the pumping, preheating, metering of the combustion air and that for cleaning and pumping the combustion products are represented in Figures A-2 through A-7 respectively.

The Fuel System

1. Fuel Oils

The fuel oil is pumped along a 100-ft long, steam-heated supply line into either of two storage tanks (2000 gallons capacity each). In the tanks the oil can be maintained at a temperature adequate for pumping (e.g., 100-150°F for heavy fuel oils) by two heaters in each tank. The tanks have temperature and level controls. Excess fuel during filling is dumped through a pressure-relief valve into a dump tank.

The oil is pumped to a 300-gallon day tank where it can be maintained at about 150°F temperature.

A fuel preparation system filters the oil and heats it to the final temperature necessary for satisfactory atomization. Provision is made for the mixing and emulsification of fuel oils and for their injection through the burner at controlled flow rates and temperature. The excess fuel fed through the oil preparation system is recirculated to the day tank.

2. Natural Gas

Natural gas is supplied to the air preheater, the afterburner and also to the main burner of the experimental furnace. Provision is made for the mixing of the natural gas with diluents (CO_2, N_2) for reducing its calorific value if required for experimental purposes. The gas from high pressure mains is distributed to the three supply lines at controlled flow rates and pressures as shown in the drawing.

3. Solid Fuels/Slurries

In the second stage of its development, the experimental plant will be provided with a pulverized coal storage metering and feeder assembly as shown schematically in Figure A-3. This system is in procurement.

The Air Supply System

1. The Combustion Air

The combustion air is supplied by a fan capable of delivering 3500 SCFM against 80 in WG pressure. The air can be preheated in an externally-fired air preheater, up to 500°C (900°F). The preheated air can then be divided into two separately metered branches for introduction to the burner as primary and secondary air flows.

2. Oxygen

Oxygen is supplied both to the burner for oxygen enrichment of the combustion air and to the natural gas-oxygen burner used in the afterburner assembly.

3. Pressurized Air

Pressurized air is available for air-atomization of liquid fuels.

4. Steam

Steam is available for heating the oil transport lines and the tanks and also for steam atomization of liquid fuels. The regulated pressure of the heating steam is measured. Both the flow rate and temperature of the super-heated steam used for atomization can be recorded.

The Gas Exhaust and Cooling Water System

1. The Gas Chamber

The pressure in the experimental furnace is maintained close to the atmospheric pressure by the balanced operation of the forced draft and induced draft fans. The combustion products pass from the experimental section of the furnace into the afterburner section where the gas temperature is raised to about 1200 ^{o}C and the oxygen concentration increased by a natural gas-oxygen burner so that submicron size soot particles can be burned completely. Downstream of the afterburner section the combustion products are cooled by water spray to 200 ^{o}C. The gas vapor mixture then enters a wet scrubber which removes inorganic particles in excess of 1 μm size with an overall efficiency $\geq$ 90%. An induced draft fan propels the gases through the stack.

2. The Cooling Water System

The cooling water system is used to cool the one-foot wide sections of the experimental furnace. The cooling water is circulated in a closed loop cooled by river water in a heat exchanger. The individual furnace sections are instrumented for the measurement of the water flow rate and the temperature rise of the cooling water so as to enable sectional heat balances of the furnace to be calculated. The furnace sections are provided with a high temperature alarm system for their protection against dry-out.

3. Tap Water Supply

The tap water supply is available for the emulsifier, for the probes' cooling water, for the spray that cools the exhaust gases before entrance to the scrubber and for the scrubber.

Control and Interlock System

A comprehensive automatic control and interlock system is used for the safe light up shut off and operation of the experimental plant.

Measurements - Instrumentation

Probe and optical measurements are made within the flames and at the furnace walls. Time average gas temperatures are measured by suction pyrometers and time average velocities with water cooled impact probes capable of measuring axial, radial and tangential velocity components at points in the flame. Gas and solid samples are taken from the same points in the flame for chemical analyses.

Laser-droppler velocimetry is used for the measurement of the spatial distribution of time-resolved velocities in the furnace, and laser-diffraction and multi-flash photographic methods employed for determining particle and droplet size distributions in the flame.

The furnace sections are of two types of water-cooled inside walls or of refractory-lined inside walls. Wall temperatures are measured at several points in each section. The total heat transfer from the flame to the furnace is determined by using conductivity plug type heat flow meters and the radiative heat transfer contribution by using hemispherical type hollow ellipsoidal radiometers, both at the furnace wall. Flame emissivities are determined optically according to the Schmidt method using total radiation pyrometers.

All measured variables are displayed at the control panel after transduction to their electrical analogs and these electrical analogs are used as the inputs to manual or, in some cases automatic control loops; a data acquisition computer system based on a PDP11/60 machine common to several facilities in the building is used to log all data. The system permits quasi real-time processing of the data with comparisons between model predictions and current experimental results.

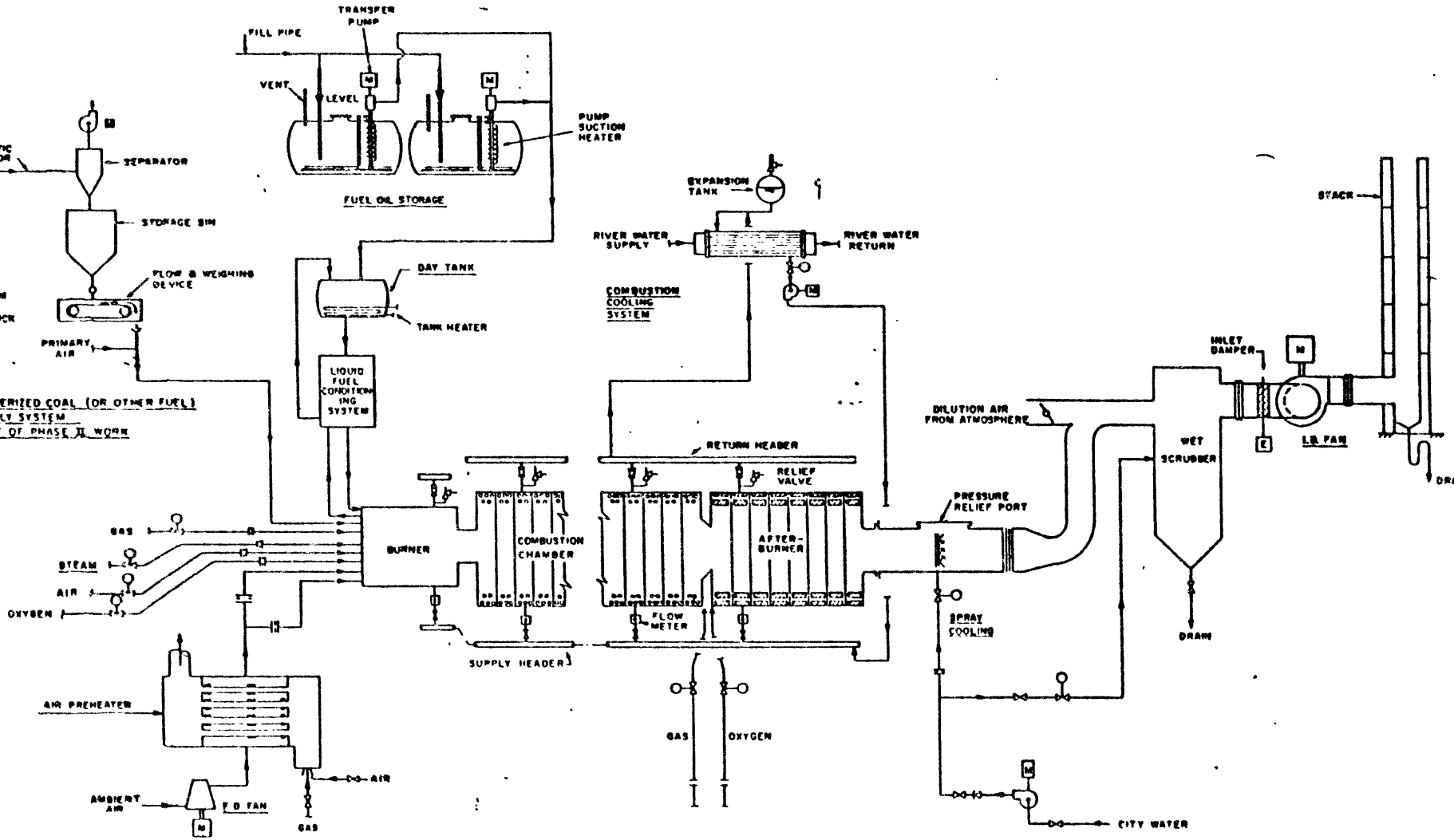

Figure A-1 MIT COMBUSTION RESEARCH FACILITY

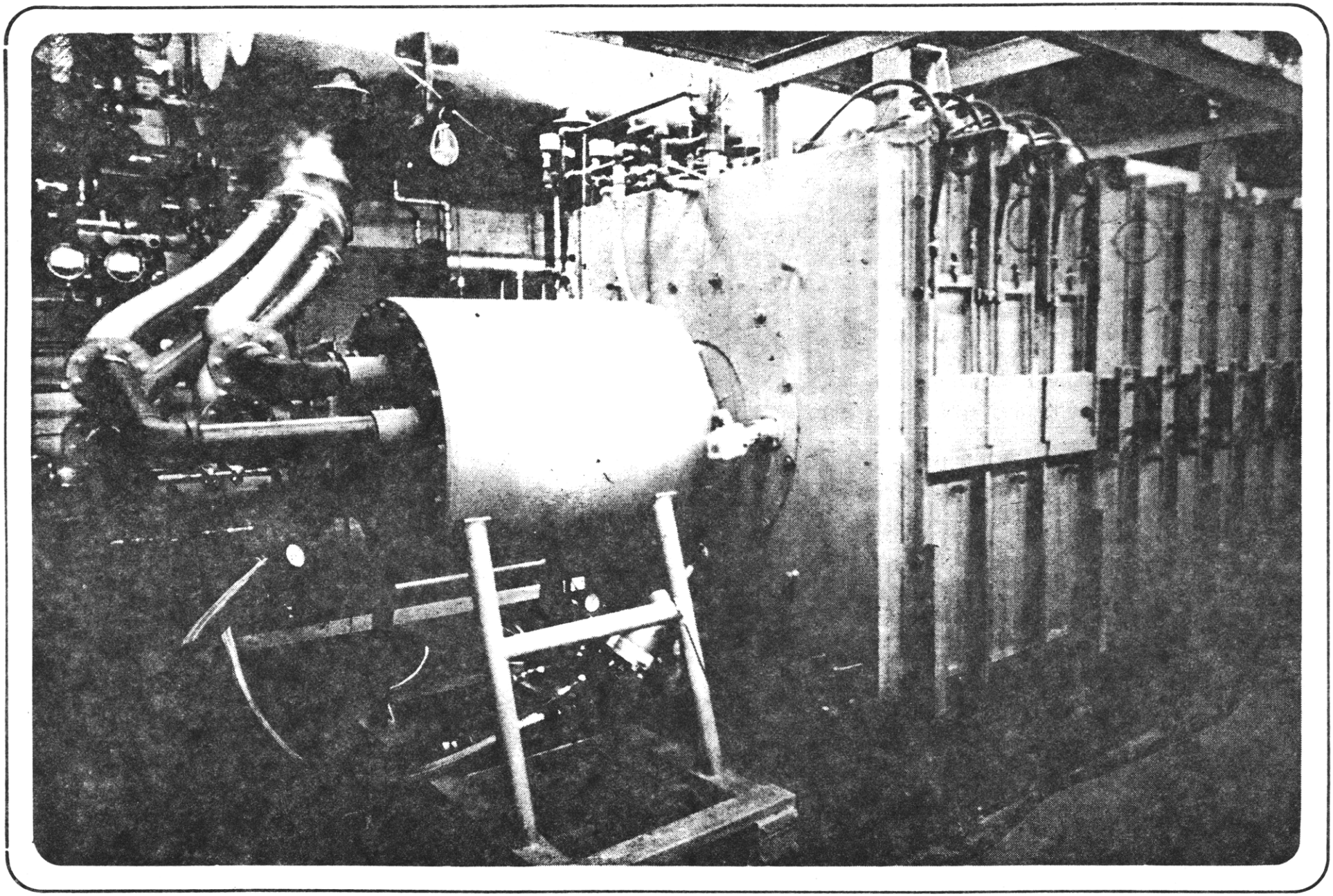

Figure A-2. View of Multi-Fuel Swirl Burner in MIT CRF.

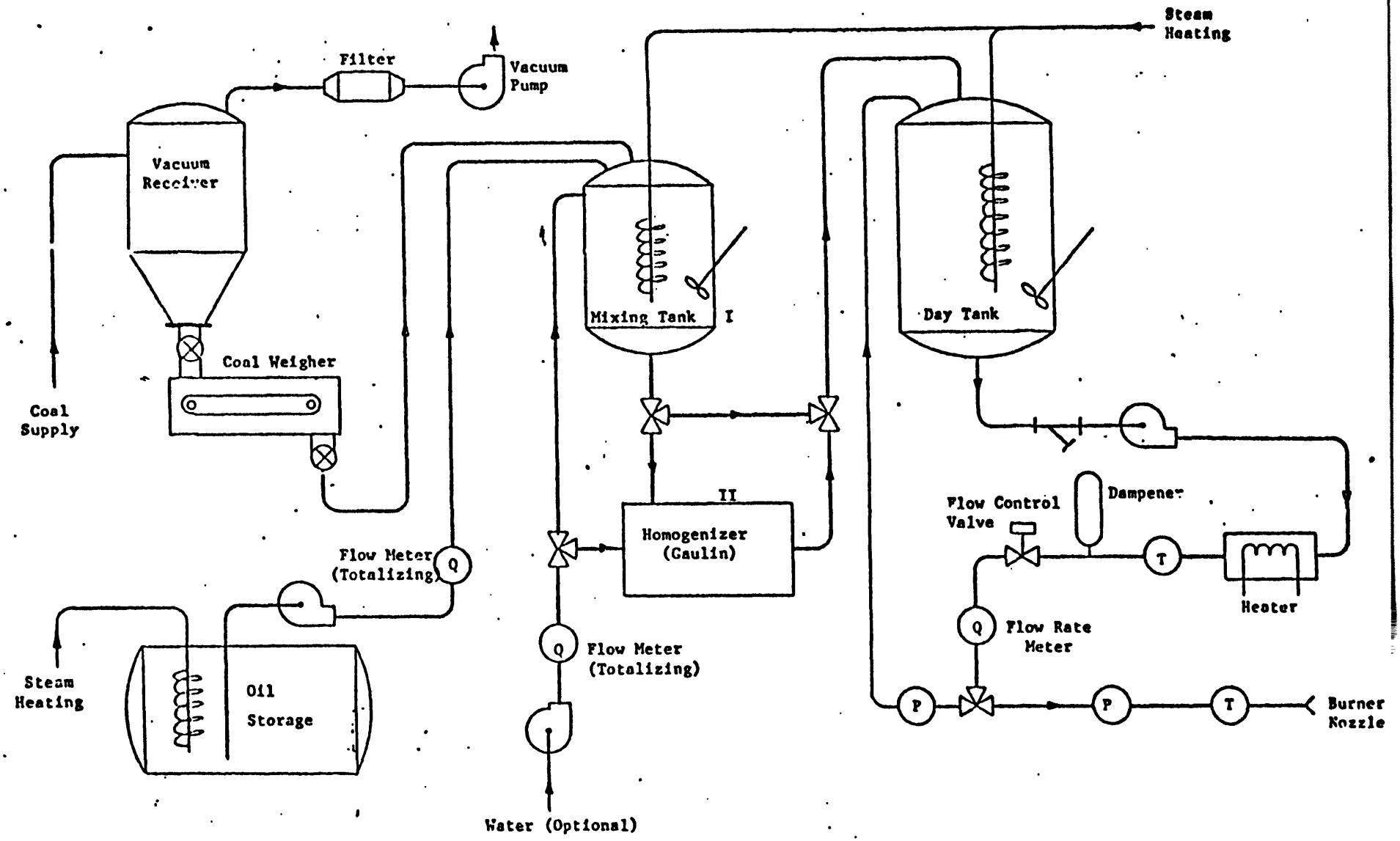

Figure A-1 COM Preparation and Handling Systems.

I - Conventional Mixing Tank
II - Mechanical Homogenization (Gaulin)

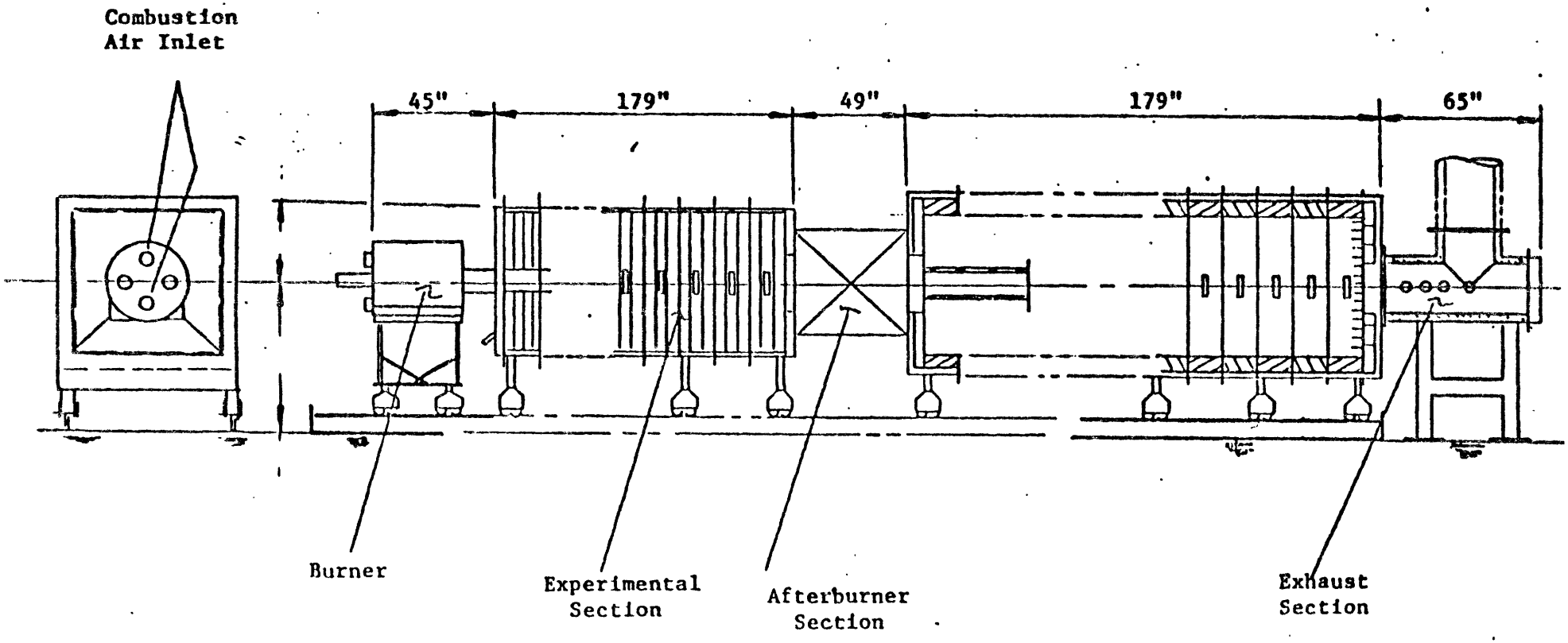

Figure A-4. Furnace Assembly

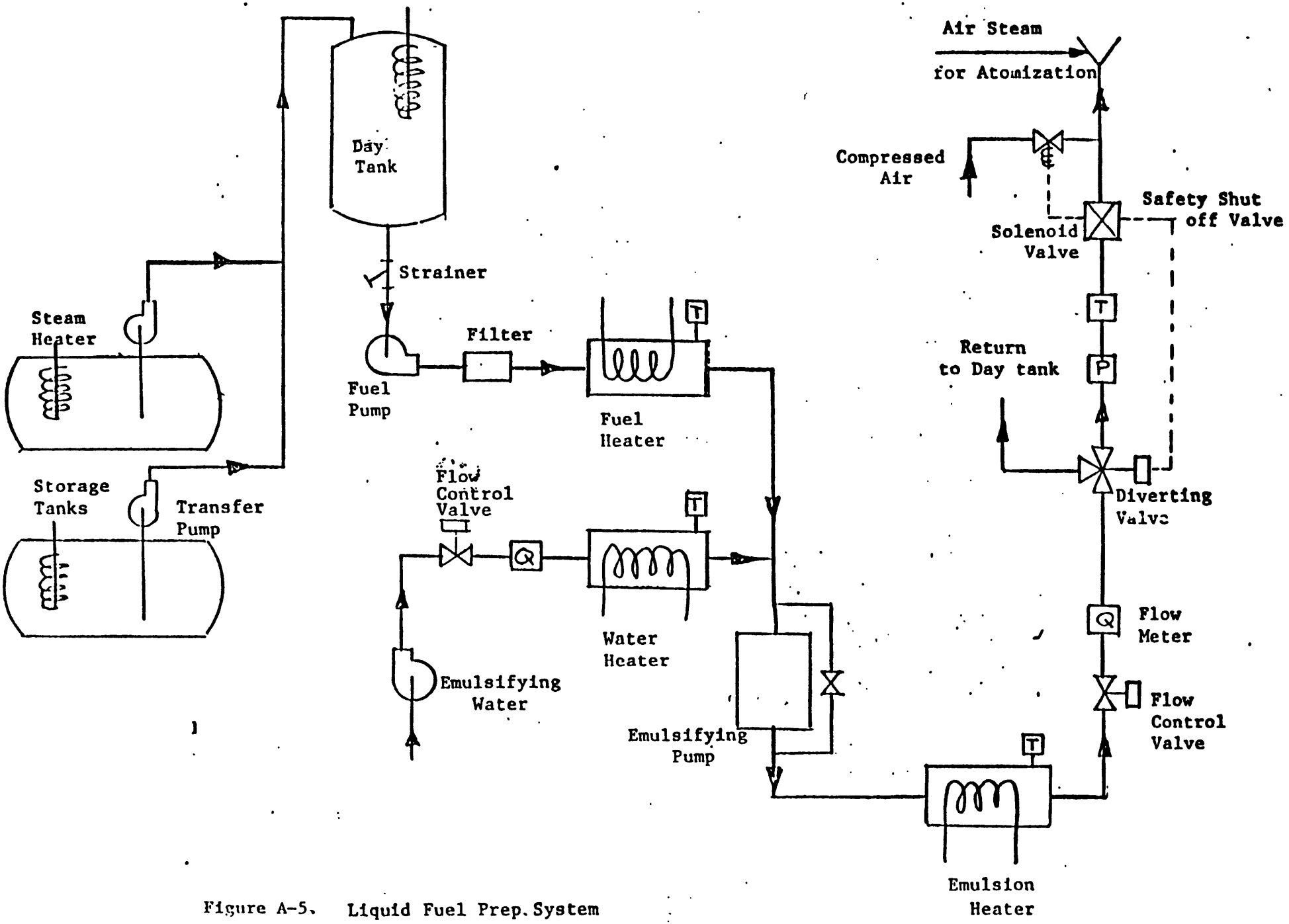

Figure A-5. Liquid Fuel Prep. System

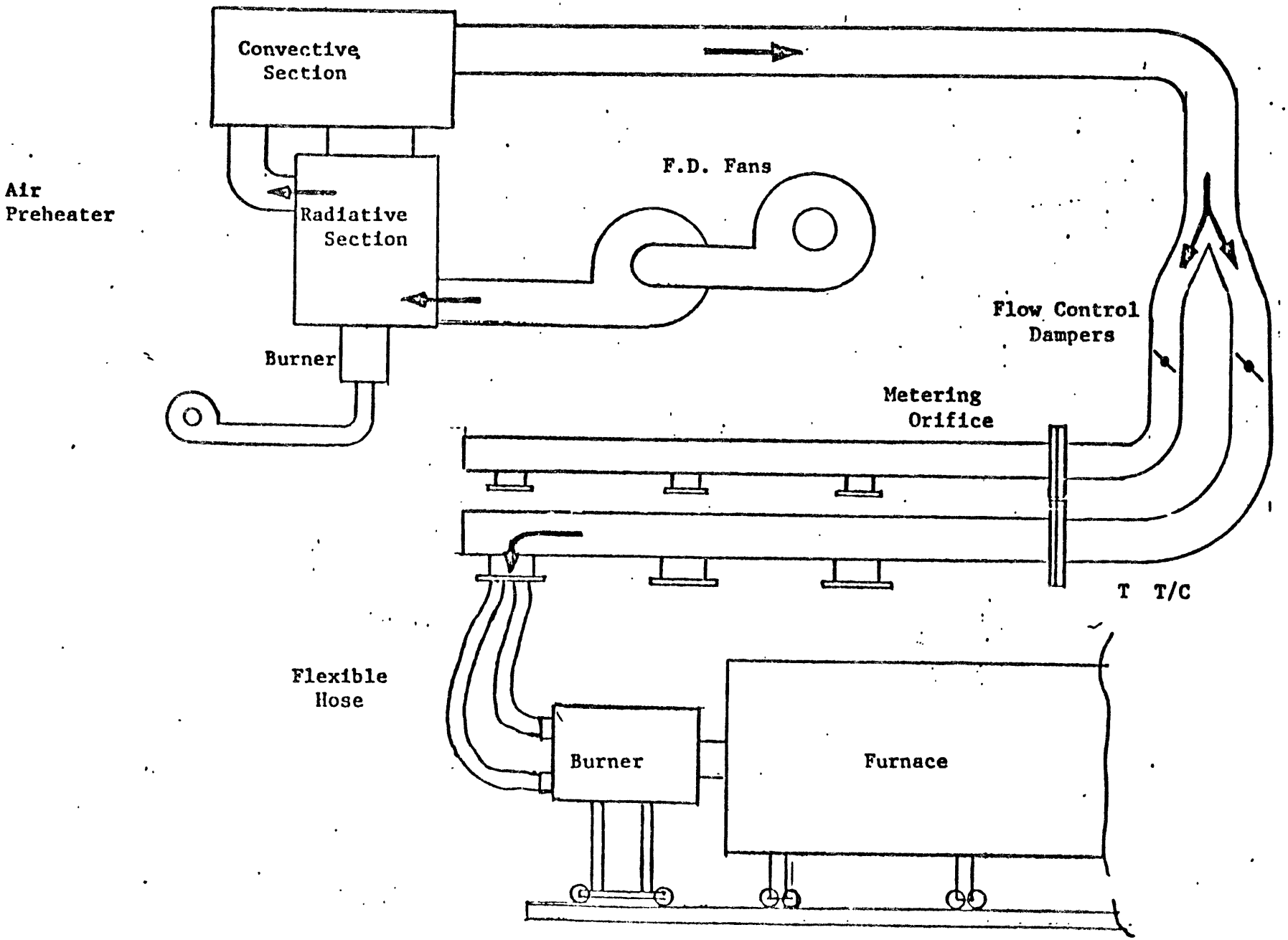
Convective Section
Air Preheater
Radiative Section
F.D. Fans
Flow Control Dampers
Burner
Metering Orifice
T T/C
Flexible Hose
Burner
Furnace

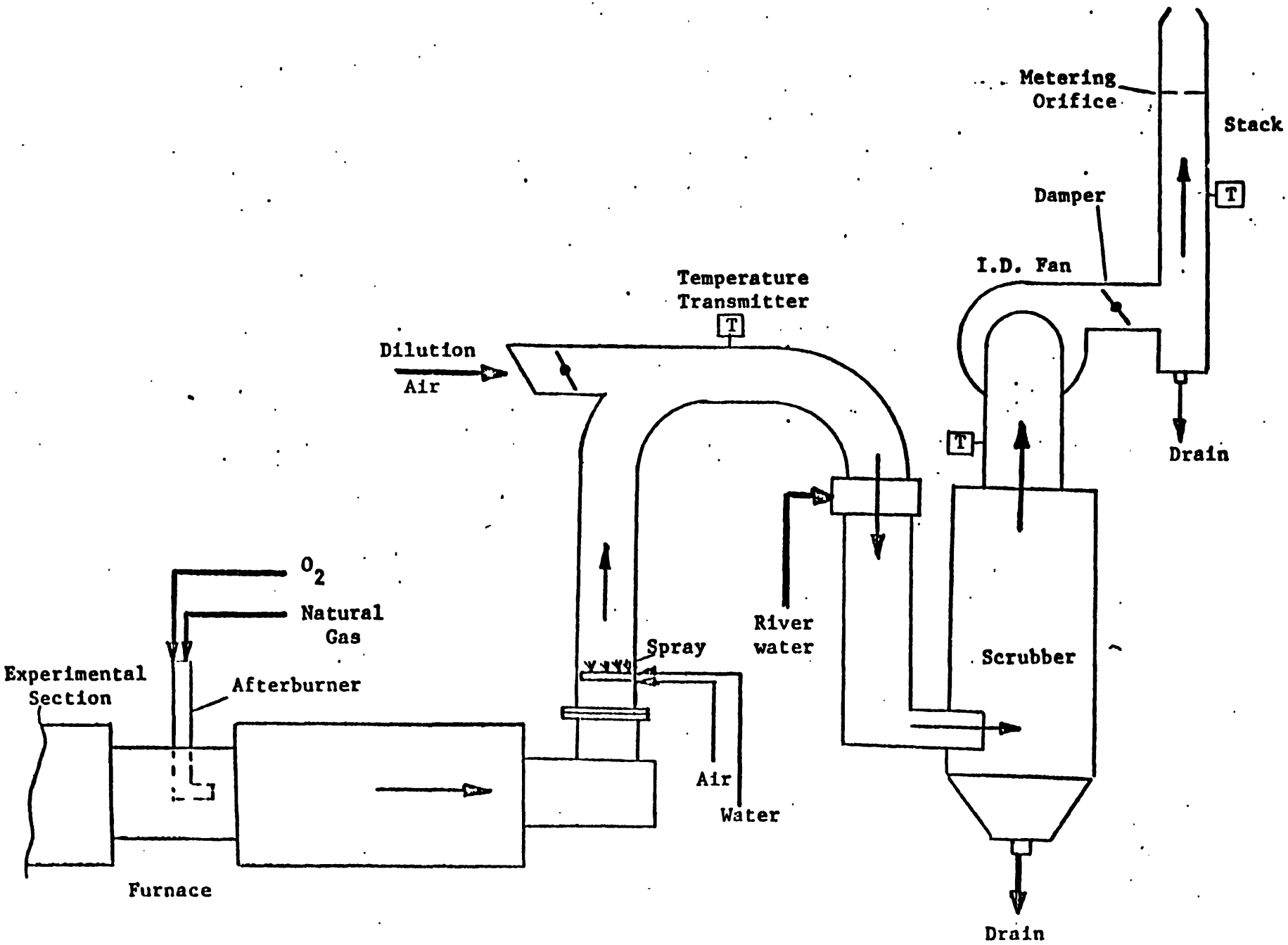

Figure A-7. 3 Exhaust System

APPENDIX B

TABULATED DATA FROM THE EXPERIMENTAL STUDIES

1) Experimental and Operating Data, Unstaged Flames (1-8), Tables B-1a-b.

2) Experimental and Operating Data, Staged Flames (9-40), Tables B-2a-b.

3) Gas Composition and Temperature Measurements, Flames 1-40, Table B-3.

TABLE B.1a

COMBUSTION RESEARCH FACILITY OPERATING AND EXPERIMENTAL DATA,
FLAMES 1-8; HIGH NITROGEN NO. 6 FUEL OIL;
UNSTAGED, CONVENTIONAL FLAMES

Flame Number	CRF Run Number	Overall Fuel Equivalence Ratio	Swirl		Atomizer Type
			Swirl Setting	Swirl Number	
1	21a	.97	10	2.7	Pressure Jet
2	21b	.97	3	.42	Pressure Jet
3	24a	.97	10	2.7	Pressure Jet
4	24b	.97	3	.42	Pressure Jet
5	29a	.93	10	2.7	Twin Fluid
6	29b	.93	3.5	.53	Twin Fluid
7	30a	.93	10	2.7	Twin Fluid
8	30b	.93	3.5	.53	Twin Fluid

TABLE B.1b

COMBUSTION RESEARCH FACILITY OPERATING AND EXPERIMENTAL DATA,
FLAMES 1-8; HIGH NITROGEN NO. 6 FUEL OIL;
UNSTAGED, CONVENTIONAL FLAMES

Flame Number	CRF Run Number	Combustion Air Temperature		Fuel Oil Temperature		Combustion Air Flow Rate		Fuel Flow Rate	
		°K	°F	°K	°F	$\frac{kg}{hr}$	$\frac{lbs}{min}$	$\frac{kg}{hr}$	$\frac{lbs}{min}$
1	21a	533	500	376	217	1179	43.34	83.01	3.050
2	21b	533	500	376	217	1179	43.34	83.01	3.050
3	24a	728	850	375	215	1188	43.66	83.01	3.050
4	24b	728	850	375	215	1188	43.66	83.01	3.050
5	29a	533	500	369	204	1271	46.72	85.27	3.133
6	24b	533	500	369	204	1271	46.72	85.27	3.133
7	30a	722	840	381	225	1260	46.31	84.70	3.113
8	30b	722	840	381	225	1260	43.31	84.70	3.113

TABLE B.2a

COMBUSTION RESEARCH FACILITY OPERATING AND EXPERIMENTAL DATA, FLAMES 9-40; HIGH NITROGEN NO. 6 FUEL OIL; STAGED FLAMES

Flame #	CRF Run #	Burner Fuel Equivalence Ratio	Overall Fuel Equivalence Ratio		Swirl		Atomizer Type	Staging Air Injection Point (Distance from Nozzle, m)
			From Fuel & Air Flows	From Flue Gas O_2 Analysis	Swirl Setting	Swirl #		
9	25a	1.15	0.950	.95	3.5	0.53	Pressure Jet	2.59
10	25b	2.05	0.996	.95	3.5	0.53	Pressure Jet	2.59
11	26a	1.18	0.994	.93	3.5	0.53	Pressure Jet	2.59
12	26b	1.27	0.983	.95	3.5	0.53	Pressure Jet	2.59
13	26c	1.47	0.980	.94	3.5	0.53	Pressure Jet	2.59
14	26d	1.75	0.980	.95	3.5	0.53	Pressure Jet	2.59
15	26e	1.88	0.930	.94	3.5	0.53	Pressure Jet	2.59
16	26f	1.49	0.992	.96	4.0	0.65	Pressure Jet	2.59
17	26g	1.51	0.997	.95	6.0	1.17	Pressure Jet	2.59
18	26h	1.49	0.980	.97	8.0	1.78	Pressure Jet	2.59
19	26i	1.45	0.970	.96	10.0	2.70	Pressure Jet	2.59
20	27a	1.06	0.933	.95	3.5	0.53	Pressure Jet	2.59
21	27b	1.31	0.975	.93	3.5	0.53	Pressure Jet	2.59
22	27c	1.41	0.937	.96	3.5	0.53	Pressure Jet	2.59
23	27d	1.75	0.955	.95	3.5	0.53	Pressure Jet	2.59
24	27e	1.97	0.964	.95	3.5	0.53	Pressure Jet	2.59
25	18a	1.17	0.960		3.5	0.53	Twin Fluid	2.59
26	18b	1.17	0.960		10.0	2.70	Twin Fluid	2.59
27	18c	2.01	0.880	.89	3.5	0.53	Twin Fluid	2.59
28	19a	1.12	0.960		3.5	0.53	Twin Fluid	2.59
29	19b	1.12	0.960		10.0	2.70	Twin Fluid	2.59
30	19c	1.70	0.830	.91	3.5	0.53	Twin Fluid	2.59
31	31a	1.18	1.010	.97	3.5	0.53	Twin Fluid	2.59
32	31b	1.19	1.000	.95	10.0	2.70	Twin Fluid	2.59
33	31c	1.26	0.950	.96	3.5	0.53	Twin Fluid	2.59
34	31d	1.42	0.960	.96	3.5	0.53	Twin Fluid	2.59
35	31e	1.69	0.950	.96	3.5	0.53	Twin Fluid	2.59
36	31f	1.77	0.910	.96	3.5	0.53	Twin Fluid	2.59
37	31g	2.02	1.000	.94	10.0	2.70	Twin Fluid	2.59
38	37a	1.48	0.860	.93	3.5	0.53	Twin Fluid	2.59
39	37b	0.97	0.870		3.5	0.53	Twin Fluid	2.59
40	37c	1.29	0.940	.94	3.5	0.53	Twin Fluid	2.59

TABLE B.2b

COMBUSTION RESEARCH FACILITY OPERATING AND EXPERIMENTAL DATA, FLAMES 9-40; HIGH NITROGEN NO. 6 FUEL OIL; STAGED FLAMES

Flame #	CRF Run #	Combustion Air Temperature °K	Combustion Air Temperature °F	Fuel Oil Temperature °K	Fuel Oil Temperature °F	Burner (Primary) Air Flow Rate kg/hr	Burner (Primary) Air Flow Rate lbs/min	Staging (Secondary) Air Flow Rate kg/hr	Staging (Secondary) Air Flow Rate lbs/hr	Fuel Flow Rate kg/hr	Fuel Flow Rate lbs/hr
9	25a	533	500	367	200	1006	36.97	210	7.73	83.63	3.073
10	25b	533	500	367	200	551	20.25	584	21.46	81.62	2.999
11	26a	533	500	365	197	1006	36.97	188	6.91	85.73	3.150
12	26b	544	520	369	204	932	34.23	273	10.02	85.46	3.140
13	26c	544	520	371	207	803	29.50	401	14.74	85.46	3.140
14	26d	544	520	372	209	661	24.27	516	18.96	82.28	3.060
15	26e	544	520	379	223	610	22.43	623	22.90	82.71	3.039
16	26f	544	520	377	218	775	28.46	384	14.12	83.01	3.050
17	26g	544	520	377	219	759	27.88	395	14.51	83.01	3.050
18	26h	544	520	371	207	755	27.73	395	14.51	81.38	2.990
19	26i	544	520	366	199	796	29.24	393	14.44	83.55	3.070
20	27a	731	855	369	205	1080	39.80	147	5.41	82.90	3.046
21	27b	750	890	374	213	871	32.00	302	11.10	82.57	3.034
22	27c	742	875	371	207	814	29.90	410	15.07	82.57	3.034
23	27d	742	875	374	213	654	24.02	544	19.99	82.60	3.035
24	27e	731	855	367	200	560	20.59	585	21.51	79.74	2.930
25	18a	531	495	352	173	979	35.96	211	7.75	82.60	3.035
26	18b	531	495	352	173	979	35.96	211	7.75	82.60	3.035
27	18c	533	500	352	173	570	20.95	733	26.93	82.60	3.035
28	19a	744	880	357	183	1030	38.00	178	6.54	83.63	3.073
29	19b	744	880	357	183	1030	38.00	178	6.54	83.63	3.073
30	19c	744	880	357	183	673	24.74	696	25.57	82.33	3.025
31	31a	533	500	370	206	948	34.85	172	6.32	81.40	2.991
32	31b	531	495	373	211	981	36.06	189	6.95	85.17	3.130
33	31c	529	493	373	212	912	33.50	309	11.34	83.80	3.079
34	31d	531	495	372	210	830	30.48	405	14.88	85.27	3.133
35	31e	528	490	373	211	690	25.37	533	19.59	84.18	3.093
36	31f	529	493	373	212	652	23.95	613	22.52	83.20	3.057
37	31g	528	490	372	209	584	21.45	584	21.44	85.27	3.133
38	37a	300	80	362	192	749	27.53	558	20.51	80.18	2.946
39	37b	533	500	368	203	2025	74.39	254	9.31	142.40	5.232
40	37c	533	500	373	211	1539	56.53	570	20.95	143.20	5.261

TABLE B.3

COMBUSTION RESEARCH FACILITY EXPERIMENTAL DATA; HIGH NITROGEN NO. 6 FUEL OIL;
GAS COMPOSITION AND TEMPERATURE MEASUREMENTS, FLAMES 1-40

Distance From Burner Nozzle (m)	Distance From Furnace Wall (m)	% CO_2 by Volume	% O_2 by Volume	CO ppm by Volume	NOx ppm by Volume	Lbs NO_2 / MM BTU	ppm NOx at 3% O	Temperature °K
		(as measured at the experimental conditions)						
Flame 1, CRF #21a								
1.07	.20	13.4	1.8	700-800	425	.506	395	1823
	center	13.8	1.4	150-300	440	.515	402	1783
	.75	—	—	—	—	—	—	1803
1.37	.20	13.5	1.0	300-450	415	.478	373	1798
	center	13.5	1.1	0	425	.492	384	1743
	.67	—	—	—	—	—	—	1748
1.675	.20	13.8	1.0	220	420	.486	380	1745
	center	13.8	1.2	0	405	.470	367	1733
	.75	—	—	—	—	—	—	1728
1.98	.20	13.8	1.0	220	400	.461	360	—
	center	14.0	1.0	150	400	.461	360	—
2.285	.20	—	—	—	—	—	—	—
	center	—	—	—	—	—	—	1703
	.75	—	—	—	—	—	—	1706
2.89	.20	13.6	1.2	0	420	.488	381	—
	center	13.6	1.2	0	420	.488	381	1668
3.505	.20	13.6	1.0	0	425	.490	383	1643
	.30	—	—	—	—	—	—	1648
	.50	—	—	—	—	—	—	1643
	center	13.6	1.1	0	430	.498	389	1643
	.75	—	—	—	—	—	—	1643
4.11	.20	13.6	1.2	0	420	.488	381	1612
	.30	—	—	—	—	—	—	1613
	.50	—	—	—	—	—	—	1613
	center	13.6	1.2	0	420	.488	381	1608
	.75	—	—	—	—	—	—	1611
Flame 2, CRF #21b								
0.87	.30	—	—	—	—	—	—	1758
	.40	—	—	—	—	—	—	1803
	.50	—	—	—	—	—	—	1828
	center	12.6	1.9	4000-5000	310	.374	292	1833
	.75	—	—	—	—	—	—	1814
1.07	.30	—	—	—	—	—	—	1776
	.40	—	—	—	—	—	—	1798
	.50	—	—	—	—	—	—	1811
	center	12.8	1.6	2700-3300	300	.355	277	1813
	.75	—	—	—	—	—	—	1793
1.37	.30	—	—	—	—	—	—	1768
	.40	—	—	—	—	—	—	1786
	.50	—	—	—	—	—	—	1791
	center	12.8	1.6	900-1650	280	.332	259	1786
1.675	.30	—	—	—	—	—	—	1763
	.40	—	—	—	—	—	—	1770
	.50	—	—	—	—	—	—	1768
	center	13.1	1.4	400-600	280	.328	256	1765
	.75	—	—	—	—	—	—	1758
2.285	.20	—	—	—	—	—	—	1713
	.30	—	—	—	—	—	—	1718
	.50	—	—	—	—	—	—	1713
	center	13.7	1.0	0-150	278	.320	250	1713
	.75	—	—	—	—	—	—	1708
2.890	.20	—	—	—	—	—	—	1658
	.30	—	—	—	—	—	—	1663
	.50	—	—	—	—	—	—	1618
	center	13.4	1.2	0	280	.325	254	1633
	.75	—	—	—	—	—	—	1653
3.505	.20	13.4	1.4	0	270	.316	247	1606
	.30	13.4	1.3	[illegible]	270	.316	247	1613

NOTE: The axial centerline is approximately 0.[illegible] m from the furnace side wall

TABLE B.3: Continued

Distance From Burner Nozzle (m)	Distance From Furnace Wall (m)	% CO_2 by Volume (as measured at the experimental conditions)	% O_2 by Volume (as measured at the experimental conditions)	CO ppm by Volume (as measured at the experimental conditions)	NOx ppm by Volume (as measured at the experimental conditions)	Lbs NO_2 / MM BTU	ppm NOx at 3% O_2	Temperature °K
Flame 2, CRF #21b: Continued								
3.505	.50	13.4	1.3	0	270	.316	247	1625
(con'd.)	center	13.4	1.4	0	280	.328	256	1623
	.75	--	—	--	--	--	—	1623
4.11	.20	13.7	1.2	0	280	.325	254	1586
	.30	13.7	1.2	0	280	.325	254	1592
	.50	13.7	1.2	0	280	.325	254	1596
	center	13.4	1.1	0	280	.325	253	1593
	.675	13.7	1.1	0	280	.324	253	1592
Flame 4, CRF #24b								
0.87	center	13.7	1.0	>5000	380	.438	342	1851
1.07	center	13.9	1.0	>5000	360	.415	324	1837
1.37	center	14.4	1.2	1400-2100	370	.431	337	1815
1.675	center	--	—	—	—	—	—	1779
1.98	center	14.5	1.2	300-900	360	.419	327	1755
2.285	center	--	—	--	--	—	—	1736
2.89	center	14.4	1.2	0	350	.408	319	1676
3.2	center	--	—	--	--	—	--	1657
3.505	center	--	—	--	--	—	—	1640
3.81	center	14.4	1.0	0	350	.403	315	1631
4.11	center	14.4	1.1	0	350	.405	316	1613
4.415	center	14.3	1.0	0	340	.392	306	1602
Flame 3, CRF #24a								
0.87	center	13.7	2.7	300	540	.678	530	1823
1.07	center	14.4	1.3	0	510	.597	466	1748
1.37	center	--	—	--	--	--	--	1722
1.675	center	14.4	1.3	0	500	.586	458	1710
1.98	center	14.4	1.0	0	500	.576	450	1700
2.285	center	--	--	--	—	--	—	1692
2.89	center	14.4	1.2	0	520	.606	474	1662
3.20	center	--	—	--	--	--	—	1653
3.505	center	14.4	1.1	0	510	.591	462	1639
3.81	center	--	—	--	--	—	—	1626
4.11	center	—	—	--	--	—	—	1617
4.415	center	14.4	1.4	0	520	.609	476	1609
Flame 5, CRF #29a								
0.87	center	14.0	2.4	0	420	.521	407	1848
1.07	center	14.2	2.0	50-150	400	.485	379	1713
1.37	center	--	—	--	--	—	—	1684
1.675	center	14.8	1.3	0-150	380	.445	348	1674
1.98	center	—	--	--	--	--	--	1654
2.285	center	14.6	1.25	0	435	.507	396	1630
2.89	center	—	—	--	--	--	--	1622
3.20	center	14.6	1.25	0	440	.512	400	1617
3.505	center	--	—	--	--	--	--	1607
3.81	center	14.6	1.4	0	425	.498	389	1598
4.11	center	--	—	--	—	—	--	1589
4.415	center	14.5	1.3	0	425	.498	389	1582
flue	center	14.5	1.4	0	420	.492	384	--

TABLE B.3: Continued

Distance From Burner Nozzle (m)	Distance From Furnace Wall (m)	% CO_2 by Volume	% O_2 by Volume	CO ppm by Volume	NOx ppm by Volume	Lbs NO_2 / MM BTU	ppm NOx at 3% O_2	Temperature °K
		(as measured at the experimental conditions)						
Flame 6, CRF #29b								
0.87	center	--	--	--	--	--	--	1767
1.07	center	11.6	2.0	>5000	240	.259	202	1761
1.37	center	--	--	--	--	--	--	1738
1.675	center	14.0	1.0	3000-4000	240	.276	216	1723
1.98	center	--	--	--	--	--	--	1703
2.285	center	15.0	0.8	550-1650	240	.273	213	1682
2.89	center	--	--	--	--	--	--	1643
3.2	center	15.0	0.8	550-1650	240	.273	213	1682
3.505	center	--	--	--	--	--	--	1602
3.81	center	15.0	0.5	0-550	235	.263	206	1585
4.415	center	15.0	0.8	0-300	240	.273	213	1541
flue	center	14.9	1.1	0	240	.278	217	--
Flame 7, CRF #30a								
0.87	center	13.3	2.2	550	480	.589	460	1845
1.07	center	14.2	2.0	150	500	.606	474	1773
1.37	center	--	--	--	--	--	--	1738
1.675	center	14.0	1.3	150	490	.574	449	1723
1.98	center	--	--	--	--	--	--	1708
2.285	center	14.6	0.8	0-1050	465	.530	414	1695
2.89	center	--	--	--	--	--	--	1667
3.20	center	14.9	0.6	300-900	450	.507	396	1646
3.505	center	--	--	--	--	--	--	1627
3.81	center	14.6	0.8	0	470	.535	418	1618
4.11	center	--	--	--	--	--	--	1604
4.415	center	14.9	0.8	0	490	.558	436	1586
flue	center	14.9	0.8	0	520	.592	463	--
Flame 8, CRF #30b								
0.87	center	13.3	1.4	>5000	320	.375	293	1815
1.07	center	14.0	1.5	4000-5000	320	.379	296	1771
1.37	center	--	--	--	--	--	--	1753
1.675	center	14.4	1.2	900-1650	315	.366	286	1710
1.98	center	--	--	--	--	--	--	1680
2.285	center	14.4	1.1	300	300	.347	271	1673
2.89	center	--	--	--	--	--	--	1633
3.2	center	14.4	1.0	0	300	.346	270	1611
3.505	center	--	--	--	--	--	--	1599
3.81	center	14.7	1.0	0	300	.346	270	1582
4.11	center	--	--	--	--	--	--	1566
4.415	center	14.4	1.1	0	295	.342	267	1551
flue	center	14.4	1.0	0	320	.369	288	--
Flame 9, CRF #25a								
0.87	center	12.4	2.0	4000-5000	175	.212	166	1725
1.07	center	--	--	--	--	--	--	1681
1.37	center	13.2	0.2	>5000	215	.216	169	1643
1.675	center	--	0.2	>5000	215	.216	169	1631
1.98	center	--	0.2	>5000	210	.211	165	1603
2.285	center	14.4	0.3	--	205	.214	167	1570
2.89	center	12.4	3.6	--	150	.199	155	1460
3.2	center	13.3	2.8	--	163	.207	162	1498
3.505	center	13.6	2.4	--	173	.215	168	--
3.81	center	13.9	2.0	--	175	.212	166	1499
4.11	center	--	--	--	--	--	--	1470
4.415	center	13.9	1.6	0	179	.211	165	--

TABLE B.3: Continued

Distance From Burner Nozzle (m)	Distance From Furnace Wall (m)	% Co_2 by Volume	% O_2 by Volume	CO ppm by Volume	NOx ppm by Volume	Lbs NO_2 / MM BTU	ppm NOx at 3% O_2	Temperature °K
		(as measured at the experimental conditions)						
				Flame 10, CRF #25b				
0.87	center	7.8	1.0	>5000	35	.030	23	1664
1.07	center	10.0	0.6	>5000	58	.053	41	1673
1.37	center	12.3	0.7	>5000	72	.071	55	1693
1.675	center	13.4	1.8	>5000	90	.108	84	1713
1.98	center	13.2	2.3	>5000	90	.111	87	1676
2.285	center	11.5	5.2	>5000	83	.122	95	1613
2.89	center	12.5	3.1	>5000	83	.107	84	1653
3.2	center	13.4	2.4	>5000	84	.104	81	1712
3.505	center	14.2	1.4	>5000	86	.101	79	1717
3.81	center	14.5	1.2	600-2650	86	.1	78	1706
4.11	center	14.5	1.2	900-2150	90	.105	82	1682
				Flame 11, CRF #26a				
flue	center	14.0	1.8	0	190	.230	180	—
flue	center	14.0	1.3	0	180	.218	170	--
1.675	center	--	--	--	--	--	--	1653
4.415	center	--	--	--	--	--	--	1493
				Flame 12, CRF #26b				
flue	center	14.7	1.1	0	125	.145	113	--
1.675	center	--	--	--	--	--	--	1639
4.415	center	--	--	--	--	--	--	1572
				Flame 13, CRF #26c				
flue	center	14.7	1.2	0	88	.102	80	—
1.675	center	--	--	--	--	--	--	1636
4.415	center	--	--	--	--	--	--	1591
				Flame 14, CRF #26d				
flue	center	14.3	1.2	0	88	.102	80	—
1.675	center	--	--	--	--	--	--	1648
4.415	center	--	--	--	--	--	--	1617
				Flame 15, CRF #26e				
flue	center	14.0	1.3	0	95	.111	87	--
1.675	center	--	--	--	--	--	--	1691
4.415	center	--	--	--	--	--	--	1652
				Flame 16, CRF #26f				
flue	center	14.3	1.0	0	88	.101	79	--
				Flame 17, CRF #26g				
flue	center	14.3	1.1	0	85	.0985	77	--

TABLE B.3: Continued

Distance From Burner Nozzle (m)	Distance From Furnace Wall (m)	% CO_2 by Volume	% O_2 by Volume	CO ppm by Volume	NOx ppm by Volume	Lbs NO_2 / MM BTU	ppm NOx at 3% O_2	Temperature °K
		(as measured at the experimental conditions)						
Flame 18, CRF #26h								
flue	center	14.6	0.65	0-900	78	.088	69	--
Flame 19, CRF #26i								
flue	center	14.6	0.95	0-700	78	.09	71	--
Flame 20, CRF #27a								
0.87	center	12.1	0.2	>5000	220	.214	167	1748
1.07	center	12.9	0.2	>5000	203	.2	156	1688
1.37	center	--	--	--	--	--	--	1652
1.675	center	12.9	0.2	>5000	200	.2	156	1641
1.98	center	1.9	0.2	>5000	205	.205	160	1622
2.285	center	13.5	0.6	>5000	205	.209	163	1605
2.89	center	11.5	3.9	0-400	165	.223	174	1512
3.2	center	12.9	2.0	0-250	178	.216	163	1533
3.505	center	13.2	1.5	0-550	185	.219	171	1539
3.81	center	13.2	1.4	0-550	190	.223	174	1528
4.415	center	13.6	1.4	0-100	188	.221	172	1515
flue	center	13.9	1.3	0	210	.246	192	--
Flame 21, CRF #27b								
flue	center	13.6	1.6	0	103	.121	95	--
1.675	center	12.3	0.2	>5000	115	.113	88	1663
4.415	center	13.5	1.4	560-2650	105	.123	96	1614
Flame 22, CRF #27c								
flue	center	14.0	1.0	0-255	83	.096	75	--
1.675	center	12.8	0.6	>5000	88	.087	68	1675
4.415	center	13.5	1.3	>5000	83	.097	76	1637
Flame 23, CRF #27d								
flue	center	14.0	1.1	0	98	.114	89	--
1.675	center	11.8	0.3	>5000	85	.082	64	1663
4.415	center	13.8	0.7	>5000	95	.108	84	1614
Flame 24, CRF #27e								
0.87	center	8.8	1.2	>5000	95	.085	66	1675
1.07	center	9.5	0.4	>5000	60	.054	42	1638
1.37	center	10.0	0.2	>5000	60	.055	43	1638
1.675	center	11.6	0.5	>5000	78	.075	59	1663
1.98	center	12.7	1.2	>5000	95	.111	86	1741
2.285	center	12.3	2.8	>5000	87	.111	86	1735
2.89	center	12.2	3.4	850-3300	85	.111	87	1712
3.2	center	12.9	2.2	850-2650	90	.111	86	1741
3.505	center	--	--	--	--	--	--	1698
3.81	center	13.0	1.6	550-4050	90	.107	83	1663
4.41	center	13.3	1.2	0-4050	90	.105	82	1648
flue	center	13.8	1.2	0-50	105	.122	95	--

TABLE B.3: Continued

Distance From Burner Nozzle (m)	Distance From Furnace Wall (m)	% CO_2 by Volume	% O_2 by Volume	CO ppm by Volume	NOx ppm by Volume	Lbs NO_2 / MM BTU	ppm NOx at 3% O_2	Temperature °K
		(as measured at the experimental conditions)						
				Flame 25, CRF #18a				
0.87	.20	12.6	2.8	>5000	260	.33	258	1623
	.30	12.7	1.0	>5000	280	.323	252	1728
	.40	13.1	0.6	>5000	280	.316	247	1756
	.50	13.4	0.7	>5000	270	.306	239	1753
	center	13.5	0.6	>5000	260	.293	229	1856
1.07	.20	13.8	0.4	>5000	230	.258	202	1623
	.50	14.0	0.0	>5000	220	.227	177	1733
	.55	—	—	—	—	—	—	1713
	center	14.0	0.0	>5000	220	.227	177	1703
1.37	.20	13.6	0.0	>5000	190	.194	152	1698
	.30	—	—	—	—	—	—	1688
	.45	13.5	0.0	>5000	180	.184	144	—
	.50	—	—	—	—	—	—	1683
	.55	14.1	0.0	>5000	200	.208	163	1688
	center	14.1	0.0	>5000	230	.239	187	1688
1.675	.40	—	—	—	—	—	—	1663
	.45	14.1	0.0	>5000	150	.156	122	—
	.50	13.8	0.0	>5000	145	.148	116	1658
	center	13.6	0.0	>5000	140	.143	112	1671
1.98	.35	14.0	0.0	>5000	125	.129	101	—
	.40	13.8	0.0	>5000	125	.128	100	1640
	.50	13.8	0.0	>5000	125	.128	100	1643
	center	13.8	0.1	>5000	125	.128	100	1641
2.285	.35	14.0	0.2	>5000	105	.116	91	—
	.40	14.0	0.1	>5000	110	.122	95	1543
	.50	14.0	1.2	>5000	105	.122	95	1573
	center	13.8	2.0	>5000	105	.127	99	1588
2.89	.35	11.9	4.6	300-1250	100	.141	110	—
	.40	12.1	4.6	0	100	.141	110	1533
	.50	11.9	4.6	0	100	.141	110	1493
	center	12.1	4.8	0	100	.143	112	1481
3.2	.30	—	—	—	—	—	—	1563
	.50	—	—	—	—	—	—	1547
	center	—	—	—	—	—	—	1548
3.81	.40	—	—	—	—	—	—	1587
	center	—	—	—	—	—	—	1586
4.415	.40	—	—	—	—	—	—	1577
	center	—	—	—	—	—	—	1573
				Flame 26, CRF #18b				
0.87	.20	13.1	0.6	>5000	275	.31	242	1733
	.30	13.9	0.2	>5000	300	.309	241	1773
	center	13.9	0.0	>5000	305	.314	245	1813
1.07	.20	13.9	0.0	>5000	250	.258	202	1695
	.30	13.9	0.0	>5000	240	.247	193	1693
	center	14.1	0.0	>5000	240	.246	192	1713
1.37	.20	14.0	0.0	>5000	230	.236	184	1678
	.30	14.0	0.0	>5000	230	.236	184	1681
	center	14.1	0.0	>5000	230	.236	184	1668
1.675	.20	14.1	0.0	>5000	220	.225	176	1668
	.30	14.1	0.0	>5000	220	.225	176	1663
	center	14.1	0.4	>5000	230	.236	184	1668
1.98	.20	14.1	0.0	>5000	210	.216	169	1663
	.30	14.1	0.0	>5000	210	.216	169	1648
	center	13.6	2.0	0-900	200	.242	189	1608
2.285	.20	13.9	1.3	900-2650	200	.234	183	1633
	.30	13.4	1.6	900-5000+	175	.207	162	—
	.40	—	—	—	—	—	—	1585
	center	12.0	3.7	150-1250	150	.2	156	1538
2.89	.20	10.9	4.7	0	160	.227	177	1513
	.30	11.3	5.3	0	160	.234	183	1498

TABLE B.3: Continued

Distance From Burner Nozzle (m)	Distance From Furnace Wall (m)	% CO_2 by Volume	% O_2 by Volume	CO ppm by Volume	NOx ppm by Volume	Lbs NO_2 / MM BTU	ppm NOx at 3% O_2	Temperature °K
		(as measured at the experimental conditions)						
				Flame 26, CRF #18b: Continued				
2.285	.40	—	—	--	—	—	—	1473
(con'd.)	center	10.8	5.8	0	160	.243	190	1483
3.2	.20	12.3	3.6	0	190	.251	196	1478
	.30	12.8	2.9	0	190	.242	189	--
	.40	—	--	--	--	--	—	1561
	center	12.8	2.6	0	190	.239	187	1573
3.81	.30	13.2	2.0	0	200	.242	189	1565
	center	13.6	1.4	0	180	.211	165	1579
4.415	.20	13.8	0.9	0	220	.252	197	1553
	.40	—	—	--	--	—	—	1553
	center	13.8	1.0	0	220	.253	198	1575
				Flame 27, CRF #18c				
1.07	center	11.0	0	>5000		.044	34.3	—
2.89	center	12.6	2.5	3300-4000		.124	97	—
flue	center	—	1.4	--	100			—
				Flame 28, CRF #19a				
0.87	.45	--	—	--	--	—	--	1777
	.50	--	--	--	--	—	—	1819
	center	10.9	2.0	>5000	230	.279	218	1830
1.07	.30	--	--	--	--	—	—	1766
	.40	--	--	--	--	—	--	1774
	.50	—	--	--	--	--	--	1785
	center	12.3	1.2	>5000	225	.261	204	1804
1.37	.30	--	--	--	--	--	--	1753
	.40	—	--	—	--	--	--	1766
	.50	—	—	--	--	—	—	1766
	center	13.4	0.4	>5000	215	.241	188	1777
1.675	.30	--	--	--	--	—	--	1740
	.40	14.0	0.0	>5000	175	.192	150	1741
	.50	—	--	--	—	--	—	1751
	center	13.9	0.0	>5000	200	.209	163	1747
1.98	.30	—	--	--	—	--	--	1717
	.40	--	—	--	—	—	—	1719
	center	14.0	0.0	>5000	190	.199	155	1720
2.285	.30	13.8	0.0	>5000	190	.198	155	1699
	.40	13.8	0.3	>5000	190	.210	164	1687
	center	13.8	0.8	>5000	190	.215	168	1675
2.89	.20	12.7	2.0	0-1700	160	.194	152	1649
	.30	12.6	2.5	0-2700	165	.205	160	1622
	.40	12.2	3.3	0-900	160	.208	163	1592
	.50	11.3	4.2	0-900	145	.199	155	1580
	center	11.3	4.6	0-900	145	.204	159	1580
3.2	.20	12.9	2.2	0-3300	160	.196	153	1650
	.30	12.7	2.4	0-2100	155	.192	150	1633
	.40	12.7	2.8	0-600	155	.197	154	1622
	center	12.7	2.8	0-900	150	.191	149	1619
3.505	.20	12.9	1.8	250-2100	165	.197	154	1585
	.30	12.9	1.8	0-600	165	.197	154	1596
	.40	12.9	1.9	0-900	165	.199	155	1636
	center	12.8	2.0	0-900	165	.2	156	1630
4.11	.20	12.9	1.8	0-1200	165	.197	154	1624
	.40	13.0	1.4	0-1450	165	.194	152	1620
	center	13.1	1.2	0-1200	165	.192	150	1612

TABLE B.3: Continued

Distance From Burner Nozzle (m)	Distance From Furnace Wall (m)	% CO_2 by Volume	% O_2 by Volume	CO ppm by Volume	NOx ppm by Volume	Lbs NO_2 / MM BTU	ppm NOx at 3% O_2	Temperature °K
		(as measured at the experimental conditions)						
				Flame 29, CRF #19b				
0.87	.45	--	--	--	--	--	--	1835
	.50	--	--	--	--	--	--	1808
	center	14.3	0.0	>5000	340	.355	277	1817
1.07	.30	--	--	--	--	--	--	1764
	.40	--	--	--	--	--	--	1751
	center	14.3	0.0	>5000	265	.277	216	1733
1.37	.30	--	--	--	--	--	--	1719
	.40	--	--	--	--	--	--	1713
	center	14.3	0.0	>5000	240	.25	195	1709
1.675	.30	--	--	--	--	--	--	1708
	.40	--	--	--	--	--	--	1706
	center	14.3	0.0	>5000	230	.24	188	1693
1.98	.30	--	--	--	--	--	--	1700
	.40	--	--	--	--	--	--	1706
	center	14.3	0.0	>5000	220	.23	180	1688
2.285	.30	--	--	--	--	--	--	1678
	.40	--	--	--	--	--	--	1673
	center	13.1	1.9	>5000	200	.241	188	1657
2.89	.20	12.8	3.0	0-2650	180	.23	180	1590
	.30	12.8	3.4	0-1250	165	.216	169	1567
	.40	12.6	3.9	0	165	.223	174	1550
	.50	11.8	4.2	0-15	160	.216	169	1564
	center	11.8	4.2	0-550	160	.216	169	1583
3.2	.30	--	--	--	--	--	--	1617
	.40	--	--	--	--	--	--	1611
	center	13.5	2.0	0-5000	190	.23	180	1608
3.505	.30	--	--	--	--	--	--	1620
	.40	--	--	--	--	--	--	1620
	center	14.0	1.4	0-550	220	.258	202	1614
4.11	.20	--	--	--	--	--	--	1601
	.40	--	--	--	--	--	--	1597
	center	14.0	0.8	0	220	.251	196	1595
				Flame 30, CRF #19c				
flue	center	13.5	2.0	0		.109	85	--
				Flame 31, CRF #31a				
flue	center	14.0	0.8	0-300	100	.114	89	--
				Flame 32, CRF #31b				
flue	center	13.8	1.2	0	200	.233	182	--
				Flame 33, CRF #31c				
flue	center	14.0	1.0	0	80	.092	72	--
1.675	center	11.8	0.1	>5000	80	.077	60	1639
4.415	center	13.8	1.2	0-1650	80	.093	73	1611

TABLE B.3: Continued

Distance From Burner Nozzle (m)	Distance From Furnace Wall (m)	% CO_2 by Volume	% O_2 by Volume	CO ppm by Volume	NOx ppm by Volume	Lbs NO_2 / MM BTU	ppm NOx at 3% O_2	Temperature °K
		(as measured at the experimental conditions)						
Flame 34, CRF #31d								
flue	center	13.8	1.0	0-300	85	.098	77	--
1.675	center	10.4	1.1	>5000	60	.059	46	1619
4.415	center	13.4	1.1	0-3300	80	.093	73	1645
Flame 35, CRF #31e								
flue	center	14.0	1.0	0-300	103	.119	93	--
1.675	center	9.3	0.2	>5000	37	.033	26	1589
4.415	center	14.4	0.5	0-2650	100	.112	88	1678
Flame 36, CRF #31f								
0.87	center	9.6	0.3	>5000	60	.054	42	1608
1.07	center	--	--	--	--	--	--	1560
1.37	center	9.9	0.1	>5000	40	.036	28	1559
1.675	center	--	--	--	--	--	--	1563
1.98	center	11.4	0.6	>5000	90	.086	67	1682
2.285	center	12.3	3.5	900-1650	120	.158	124	1738
2.89	center	12.3	3.9	900-1650	100	.135	106	1671
3.2	center	13.2	2.3	900-1650	100	.123	96	1730
3.505	center	--	--	--	--	--	--	1731
3.81	center	14.0	1.0	900-2650	100	.115	90	1696
4.11	center	--	--	--	--	--	--	1676
4.415	center	14.3	0.8	0-2650	100	.114	89	1661
flue	center	14.3	1.1	0	110	.127	99.5	--
Flame 37, CRF #31g								
flue	center	14.0	1.4	0.0	100	--	92	--
Flame 38, CRF #37a								
flue	center	13.0	1.5	0-600	105	.124	97	--
flue	center	13.3	1.4	0-600	100	.118	92	--
Flame 39, CRF #37b								
flue	center	13.3	1.5	0	255	.301	236	--
flue	center	13.3	1.4	1	260	.305	238	--
1.675	center	12.7	0.8	>5000	260	.296	231	--
2.285	center	--	--	--	--	--	--	1768
2.89	center	--	--	--	--	--	--	1614
3.2	center	--	--	--	--	--	--	1674
3.81	center	--	--	--	--	--	--	1705
4.11	center	12.4	2.9	300-1650	235	.299	233	1701
4.415	center	--	--	--	--	--	--	1702
Flame 40, CRF #37c								
flue	center	12.4	2.0	0-1650	95	.115	90	--
1.675	center	8.2	1.4	>5000	95	.112	87	--

APPENDIX C

TABULATION OF THE EXPERIMENTAL DATA

AVERAGING STUDY

1) Examination of the effect of atomizer type on NOx emissions, Table C.1.

2) Examination of the effect of inlet combustion air temperature on NOx emissions, Table C.2.

3) Examination of the effect of degree of air swirl on NOx emissions, Table C.3.

TABLE C.1

EXPERIMENTAL DATA AVERAGING STUDY; EXAMINATION OF THE EFFECT OF ATOMIZER TYPE ON FLUE GAS NOx LEVELS (VARIATIONS DUE TO OTHER VARIABLES--INLET AIR TEMPERATURE, DEGREE OF SWIRL—ARE AVERAGED); NOx IN THE FLUE GAS VERSUS FUEL EQUIVALENCE RATIO (NOx IN PPM AT 3% O_2)

Burner Fuel Equivalence Ratio	CRF Run Number and Date	Points Included in the Average		Average NOx Emission	
		Pressure Jet Atomizer	Twin Fluid Atomizer	Pressure Jet	Twin Fluid
0.95 ± 0.03	21, 6/28/79	253			
	21, 6/28/79	381			
	24, 7/26/79	306			
	24, 7/26/79	476			
	29, 8/20/79		217		
	29, 8/20/79		381		
	30, 8/21/79		288		
	30, 8/21/79		460		
				354	337
1.15 ± 0.05	18, 6/25/79		128		
	18, 6/25/79		198		
	19, 6/26/79		148		
	19, 6/26/79		196		
	25, 8/8/79	165			
	26, 8/9/79	170			
	27, 8/15/79	172			
	31, 8/22/79		89		
	31, 8/22/79		182		
				169	157
1.28 ± 0.03	26, 8/9/79	113			
	27, 8/15/79	95			
	31, 8/22/79		72		
				104	72
1.45 ± 0.05	26, 8/9/79	71			
	26, 8/9/79	80			
	26, 8/9/79	79			
	26, 8/9/79	77			
	26, 8/9/79	69			
	27, 8/15/79	75			
	31, 8/22/79		77		
				75	77
1.73 ± 0.04	19, 6/26/79		85		
	26, 8/9/79	80			
	27, 8/15/79	89			
	31/ 8/22/79		93		
	31, 8/22/79		100		
				85	93
1.95 ± 0.1	18, 6/25/79		93		
	25, 8/8/79	82			
	26, 8/9/79	87			
	27, 8/15/79	96			
	31, 8/22/79		91		
				88	92

TABLE C.2

EXPERIMENTAL DATA AVERAGING STUDY; EXAMINATION OF THE EFFECT OF INLET COMBUSTION AIR TEMPERATURE ON FLUE GAS NOx LEVELS (VARIATIONS DUE TO OTHER VARIABLES --ATOMIZER TYPE, DEGREE OF SWIRL--ARE AVERAGED); NOx IN THE FLUE GAS VERSUS FUEL EQUIVALENCE RATIO (NOx IN PPM AT 3% O_2)

Burner Fuel Equivalence Ratio	CRF Run Number and Date	Points Included in the Average		Average NOx Emissions	
		T_{air} = 730°K	T_{air} = 533°K	T_{air} = 730°K	T_{air} = 533°K
0.95 ± 0.03	21, 6/28/79		253		
	21, 6/28/79		381		
	24, 7/26/79	306			
	24, 7/26/79	476			
	30, 8/21/79	288			
	30, 8/21/79	460			
	29, 8/20/79		217		
	29, 8/20/79		381		
				383	308
1.15 ± 0.05	18, 6/25/79		128		
	18, 6/25/79		198		
	19, 6/26/79	148			
	19, 6/26/79	196			
	25, 8/8/79		165		
	26, 8/9/79		170		
	27, 8/15/79	172			
	31, 8/22/79		89		
	31, 8/22/79		182		
				172	155
1.28 ± 0.03	26, 8/9/79		113		
	27, 8/15/79	95			
	31, 8/22/79		72		
				95	93
1.45 ± 0.05	26, 8/9/79		80		
	26, 8/9/79		79		
	26, 8/9/79		77		
	26, 8/9/79		69		
	26, 8/9/79		71		
	27, 8/15/79	75			
	31, 8/22/79		77		
				75	76
1.75 ± 0.02	26, 8/9/79		80		
	27, 8/15/79	89			
	31, 8/22/79		100		
				89	90
1.69 ± 0.0	19, 6/26/79	85			
	31, 8/22/79		93		
				85	93
1.95 ± 0.1	18, 6/25/79		93		
	25, 8/8/79		82		
	26, 8/9/79		87		
	27, 8/15/79	96			
	31, 8/22/79		91		
				96	88

TABLE C.3

EXPERIMENTAL DATA AVERAGING STUDY; EXAMINATION OF THE EFFECT OF DEGREE OF SWIRL ON FLUE GAS NOx LEVELS (VARIATIONS DUE TO OTHER VARIABLES—INLET COMBUSTION AIR TEMPERATURE, ATOMIZER TYPE--ARE AVERAGED); NOx IN THE FLUE GAS VERSUS FUEL EQUIVALENCE RATIO (NOx IN PPM AT 3% O_2)

Burner Fuel Equivalence Ratio		CRF Run Number and Date	Points Included in the Average		Average NOx Emissions	
			Low Swirl S = 0.53	High Swirl S = 2.7	Low Swirl S = 0.53	High Swirl S = 2.7
0.95	0.03	21, 6/28/79	253			
		21, 6/28/79		381		
		24, 7/26/79	306			
		24, 7/26/79		476		
		30, 8/21/79	288			
		30, 8/21/79		460		
		29, 8/20/79	217			
		29, 8/20/79		381		
					266	424
1.15	0.05	18, 6/25/79	128			
		18, 6/25/79		198		
		19, 6/26/79	148			
		19, 6/26/79		196		
		25, 8/8/79	165			
		26, 8/9/79	170			
		27, 8/15/79	172			
		31, 8/22/79	89			
		31, 8/22/79		182		
					145	192
1.45	0.05	26, 8/9/79	79			
		26, 8/9/79		71		
					79	71
1.95	0.1	18, 6/25/79	93			
		25, 8/8/79	82			
		26, 8/9/79	87			
		27, 8/15/79	96			
		31, 8/22/79		91		
					90	91